STUDIES OF RADIOACTIVITY

MEASUREMENTS BY THE SUM-PEAK METHOD

1992

Takao Kawano

CONTENTS

ABSTRACT

The present thesis has been completed based on results of researches which have been carried out at University of Tsukuba. The author is a technical official at Radioisotope Center of the University and has investigated radioactivity measurements by developing the daily works of radiation monitoring and related activities. This thesis contains results of radioactivity measurements of ^{60}Co by the sum-peak method.

The sum-peak method was originally developed by G. A. Brinkman and collaborators. The method can be applied to determination of the disintegration rate of a radioisotope emitting two or more coincident γ-rays. With some limitations the sum-peak method can be applied regardless of the type of a detector, a source-to-detector geometry and an absorber between a radioactive source and a detector.

At the beginning of this thesis, the effects of "distance", "displacement" and "absorbers" between a source and a detector are studied on the disintegration rate determined by the sum-peak method using a ^{60}Co point source and lead absorber plates. Through these studies the distinguished properties of the sum-peak method are demonstrated.

It is known that the sum-peak method gives an underestimated disintegration rate when applied to an extended source such as a bulky liquid source. This underestimation seems to be caused by the negligence of "a tacit assumption" that a detector should be equally responsive to all parts of a source whenever the sum-peak method is

employed. At the second stage of the studies, the tacit assumption is investigated and the practical meaning of this assumption is inferred and proved by experiments using ^{60}Co bulky sources in bottles.

Following our inference of the practical meaning of the tacit assumption, Oderkerk and Brinkman derived equations of error and error upper bounds when the sum-peak method was used for an extended source. In the present studies, the equation of error is proved and the equation of error upper bound is corrected by an experiment with two ^{60}Co point sources which were used to simulate a simple extended source.

Furthermore, through a series of the present studies, the method of determination of the photopeak area of a ^{60}Co spectrum is developed. In this method a ^{22}Na spectrum is used to eliminate a part attributed to Compton scattering of 1332 keV γ-ray under the photopeak of 1173 keV γ-ray in the spectrum. The effect of ^{208}Tl, which is one of naturally occurring radionuclides, on the sum peak area of a ^{60}Co spectrum is also successfully investigated.

ACKNOWLEDGEMENTS

I would like to express my sincere appreciation to Professor Hiroshi Ebihara and Professor Shoichiro Tanigawa for their kind guidance, continued support and encouragement for the past fifteen years at University of Tsukuba, without which this thesis would not have been possible. I am grateful to Professor Shigeki Mori for his kind guidance to complete this thesis. I would also like to thank my supervisors including Professor Takayoshi Aoki and my colleagues at Radioisotope Center of the University of Tsukuba.

RADIOACTIVITY MEASUREMENTS

BY THE SUM-PEAK METHOD

§1. Introduction

The disintegration rate of a sample source emitting γ(X)-rays can be determined by using a radiation detector, the response of which is adequately known for γ(X)-rays. However, in many actual cases such a detector is not available and the disintegration rate is determined by comparing the γ-ray spectrum of the sample source with that of an adequate standard source, the disintegration rate of which is accurately known. That is, in the case of an ordinary method[1], the disintegration rate of the sample source is derived under the assumption that the photopeak areas of the γ-ray spectra are proportional to the disintegration rates. The sample source and the standard source should have the same or similar dimensions, compositions and nuclides, and both the γ-ray spectra must be obtained under the same measuring condition. Adopting the ordinary method, the measurement using a standard source usually occupies the important position of a radioactivity measurement. In the case of the sum-peak method, the disintegration rate can be determined by analyzing a γ-ray spectrum of a sample source without using a standard source.

G. A. Brinkman and collaborators successively published five articles with regard to the sum-peak method from 1963 to 1965[2-6]. In their articles the principle and fundamental problems of the sum-peak method were investigated from various view points. L. G. Sutherland and J. D. Buchanan also published an article[7] in which the sum-peak method was applied to bulky liquid sources of ^{60}Co and ^{125}I in

bottles. According to these previous investigations, the sum-peak method should give the absolute disintegration rate (Bq) of a radioactive source regardless of the type of a detector or the geometry between a radioactive source and a detector. However, the method can be used only when a radionuclide of a source emits two or more coincident γ-rays in a decay process and when a detector has an equal response to all parts of the source[7-10]. Furthermore, areas (numbers of counts) under the photopeaks, the sum peak and the whole spectrum of γ-rays emitted from a radionuclide of the source must be precisely determined. The first condition is fulfilled in the cases of ^{22}Na[4], ^{24}Na[5], ^{46}Sc[2,3], ^{60}Co[2,3], ^{110m}Ag[11], ^{123}I[12] and ^{125}I[13-19] sources which emit two or more γ-rays in cascade, and the second condition is satisfied when a point source or a very small source compared with dimensions of a detector is used in a measurement.

As mentioned above, Sutherland and Buchanan applied the sum-peak method to radioactivity determinations of bulky sources. They experimentally showed that the disintegration rates of the bulky sources determined by the sum-peak method decreased as the volumes of the sources increased[7], and suggested that the sum-peak method could be effective for the determination of a disintegration rate under "a tacit assumption" that a detector was equally responsive to all parts of a source. The present studies were started to clarify the practical meaning of the tacit assumption[8-10], and an equation to give an expression for the tacit assumption was proposed and

experimentally proved in the cases of bulky sources of ^{60}Co solutions (10 ~ 100 mℓ) in bottles. Based on our investigations, Oderkerk and Brinkman derived two formulas which can provide estimates of an error and the upper bound of the error when the sum peak method is applied to extended sources including bulky sources. Through the present studies, the distinct features of the sum-peak method expected from theoretical considerations were experimentally verified by using a ^{60}Co point source. The two formulas derived by Oderkerk and Brinkman were experimentally examined by using two ^{60}Co point sources. Finally, practical problems in radioactivity measurements of ^{60}Co sources by the sum-peak method were investigated and solutions to delineate these problems were found.

§2. Principle of the Sum-peak Method

(1) γ-ray spectrum and radioactivity measurement

Detection of all nuclear radiations is performed through interaction of radiations with a matter, because the radiations are not perceivable for persons. In the case of electromagnetic radiations as γ-rays, electrons energized by the radiations are detected instead of the primary radiations themselves. The energizing of electrons is mainly based on three types of processes[20-23], photoelectric effect, Compton scattering and pair production, and the detection of the energized electrons is based on the processes[24] of excitation or ionization of atoms in a detector.

Figure 1 shows a typical γ-ray spectrum of a nuclide emitting only one γ-ray at every disintegration measured by a NaI(Tl) detector[25]. The spectrum is composed of the peak of almost Gaussian-shape with a narrow energy range and the broad-spread part with a broad continuous energy range. The peak part corresponds to the entire energy absorption resulted from photoelectric interaction and multiple Compton interactions[24], and called a photopeak (or a full energy peak). The broad-spread part reflects recoil electrons when Compton scattered radiations escape out of the detector without any further interactions, and called a Compton continuum. The recoil electrons have a broad energy range, and Compton scattered radiations have also a broad energy range and an angular distribution. In Fig. 1, the pair production interaction is ignored, because the probability for this interaction is very small comparing

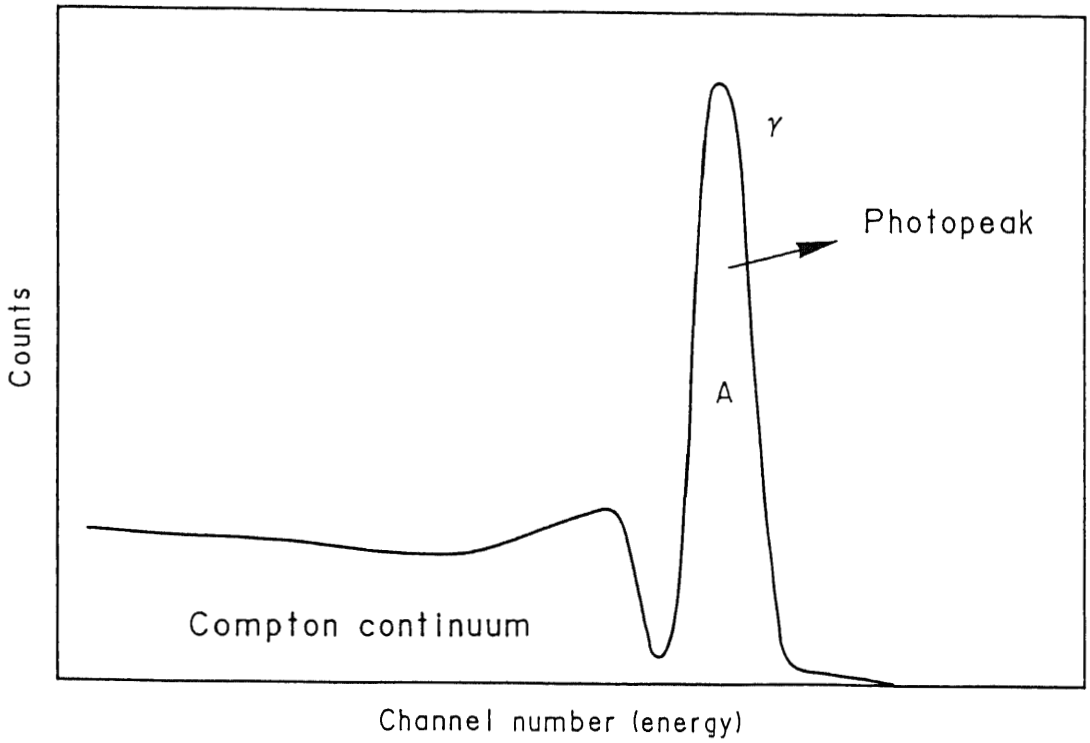

Fig. 1 Typical spectrum of a nuclide emitting only one γ-ray obtained by use of a NaI(Tl) detector.

with those for the other two interactions when the energy of a γ-ray is less than a few million electron volts[26-28].

(2) Radioactivity determination by an ordinary method

Assuming that the disintegration rate of a sample source emitting only one γ-ray is proportional to areas under the photopeak and the whole spectrum, the following equations can be obtained,

$$A = N \times p \times e, \qquad (1)$$

and

$$T = N \times p \times t, \tag{2}$$

where A and T stand for the areas represented in count rates under the photopeak and the entire spectrum, respectively. Symbols N and p are respectively the disintegration rate and the emission probability. Then (N × p) is the number of γ-rays emitted from the sample source. Symbol e is the photoelectric efficiency[29,30], namely the probability of the entire energy absorption of a γ-ray by a detector, and symbol t is the total efficiency[30], namely the probability that the detector detects at least a fraction of energy of a γ-ray through any interactions (photoelectric effect, Compton scattering or pair production). Therefore, e and t are dependent on the source-to-detector geometry and are independent of the radioactivity of the source.

Similarly for a standard source we define the following relations,

$$A^{[s]} = N^{[s]} \times p^{[s]} \times e^{[s]}, \tag{3}$$

and

$$T^{[s]} = N^{[s]} \times p^{[s]} \times t^{[s]}, \tag{4}$$

where $A^{[s]}$ and $T^{[s]}$ are the areas represented in count rates under the photopeak and the entire spectrum, respectively, $N^{[s]}$ and $p^{[s]}$ are respectively the known disintegration rate and the emission probability, and $e^{[s]}$ and $t^{[s]}$ are the photoelectric and total efficiencies, respectively. When the sample and the sources have the

same nuclide and the same source-to-detector geometry, then

$$e = e^{[s]}, \quad t = t^{[s]} \quad \text{and} \quad p = p^{[s]}. \tag{5}$$

Eliminating the efficiencies and the emission probability by using equations (1) ~ (5), we obtain the following relations

$$N = N^{[s]} \times \frac{A}{A^{[s]}}, \tag{6}$$

and

$$N = N^{[s]} \times \frac{T}{T^{[s]}}. \tag{7}$$

Since A, T, $A^{[s]}$ and $T^{[s]}$ can be obtained from the spectra of the sample and standard sources and since $N^{[s]}$ is known, the disintegration rate, N, of the sample source can be calculated by equation (6) or (7). The disintegration rate of the sample radioactive source can be determined through the above procedure in the ordinary method.

(3) Sum-peak method

Some radionuclides emit two or more coincident γ-rays and those γ-rays are incidentally detected at the same time by a detector. As a result, a sum peak will appear in a γ-ray spectrum[31-35]. Figure 2 shows schematically a spectrum[36,37] when the nuclide of a sample source emits two coincident γ-rays (γ_1 and γ_2). In Fig. 2, two photopeaks of γ_1 and γ_2 and the sum peak of (γ_1 + γ_2) are observed. Assuming that A_1, A_2, A_{12} and T are the areas

under the photopeak of γ_1, the photopeak of γ_2, the sum peak, and the entire spectrum, respectively, we have the following relations,

$$A_1 = N \times p \times e_1 \times (1-t_2), \tag{8}$$

$$A_2 = N \times p \times e_2 \times (1-t_1), \tag{9}$$

$$A_{12} = N \times p \times e_1 \times e_2, \tag{10}$$

and

$$T = N \times p \times (t_1 + t_2 - t_1 \times t_2), \tag{11}$$

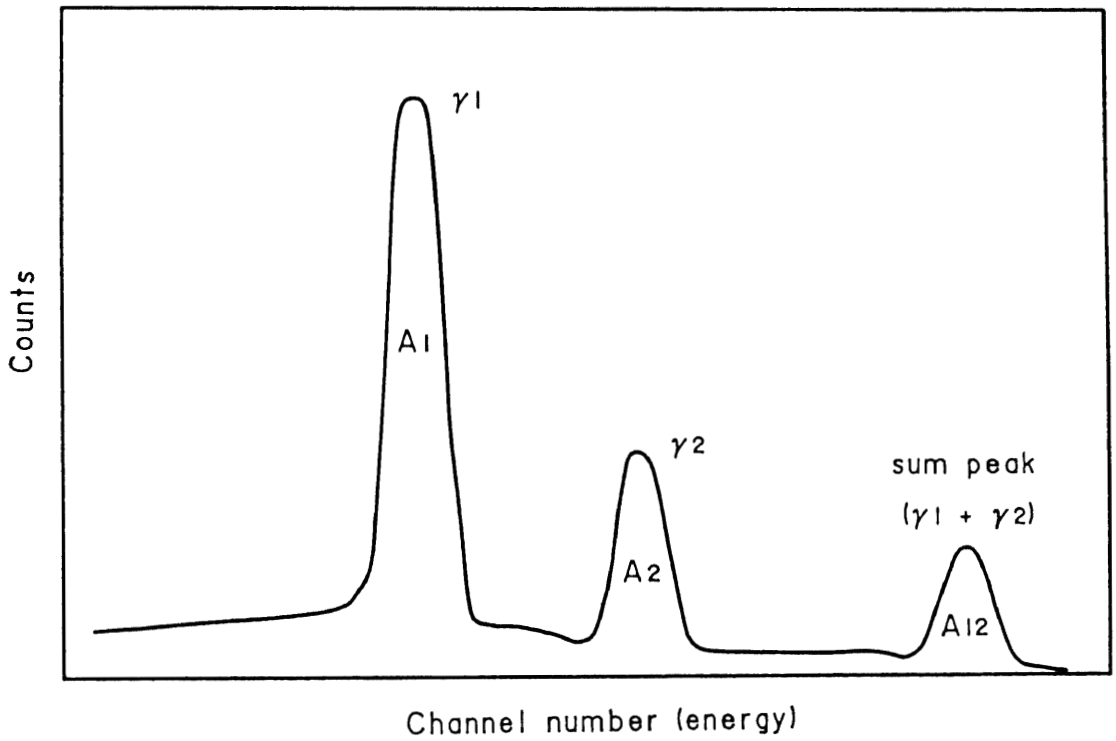

Fig. 2 Typical spectrum of a nuclide emitting two coincident γ-rays obtained by a NaI(Tl) detector.

where

p : the emission probability of γ_1 and γ_2 which are emitted in cascade,

N : the disintegration rate of the sample source,

e_1, e_2 : the photoelectric efficiencies of γ_1 and γ_2, respectively,

and

t_1, t_2 : the total efficiencies of γ_1 and γ_2, respectively.

Suppose we obtain a spectrum of a proper standard source, which has the same nuclide and the known disintegration rate of $N^{[s]}$, under the same measuring condition as the sample source. Then the photopeak area $A_1^{[s]}$ in the spectrum of the standard source can be calculated by the following equation

$$A_1^{[s]} = N^{[s]} \times p \times e_1 \times (1-t_2). \qquad (12)$$

Eliminating the photoelectric and total efficiencies e_1 and t_2, and the emission probability p by using equations (8) and (12), we obtain

$$N = N^{[s]} \times \frac{A_1}{A_1^{[s]}}. \qquad (13)$$

Equation (13) has the same form as equations (6) and (7). $N^{[s]}$ is known and the areas of A_1 and $A_1^{[s]}$ can be measured from the spectra of the sample and standard sources. Therefore, the disintegration rate, N, of the sample source can be determined by equation (13). In

the ordinary method the disintegration rate of the radioactive source, in which a nuclide emits two coincident γ-rays, can be determined by using one of the photopeak areas, A_1 or A_2, through the same process as that of a nuclide emitting only one γ-ray.

In the sum-peak method the disintegration rate can be determined by using all the areas, A_1, A_2, A_{12} and T, of the spectrum of the sample source instead of using the two spectra of the sample and standard sources. Equations (8) ~ (11) yield

$$\frac{(A_1 \times A_2)}{A_{12}} = N \times p \times (1-t_1)(1-t_2)$$

$$= N \times p - N \times p \times (t_1 + t_2 - t_1 \times t_2)$$

$$= N \times p - T.$$

Hence,

$$N = \frac{1}{p}\left[T + \frac{(A_1 \times A_2)}{A_{12}}\right], \qquad (14)$$

where p can be known from conventional data books[28),39)]. In the case of a ^{60}Co source used in the present studies p = 1, then

$$N = T + \frac{(A_1 \times A_2)}{A_{12}}. \qquad (15)$$

Equations (14) and (15) do not contain any efficiencies, and show that the disintegration rate can be determined by using only the four areas, A_1, A_2, A_{12} and T, which can be measured from the spectrum of the sample source. It must be emphasized that in the sum-peak method the disintegration rate is determined by a calculation of

a simple relation given by equation (14) or (15). The sum-peak method can give the disintegration rate of a radioactive source regardless of detector efficiencies and without requiring a standard source. In the present studies, equation (15) is examined using ^{60}Co sources and this equation is called the sum-peak formula.

The sum-peak formula (15) consists of two parts, T and $(A_1 \times A_2)/A_{12}$. In a usual pulse height spectrum, the second part composes of the majority of N, and the ratio of the second part to the first part increases very rapidly as the total efficiency (also the photoelectric efficiency) decreases. For instance, when the total efficiency is 5 % (see numerical data at the distance of 20 mm in Table 1 of §3), the second part is about ten times larger than the first part, whereas T is about 9 and 670 times larger than A_1 (or A_2) and A_{12}, respectively. In this case, errors of 10 % in A_1 (or A_2) and A_{12} cause an overall error of about 20 % in N, while an error of 10 % in T causes only 1 % error in N. Therefore, the uncertainty of N is dependent mainly on the accuracy of the photopeak and sum peak areas measured from a spectrum (see §5).

When an absorber is placed between a sample source and a detector, equations (8) ~ (11) are modified to the following equations

$$A_1 = N \times p \times (\alpha_1 \times e_1) \times (1 - \beta_2 \times t_2), \quad (16)$$

$$A_2 = N \times p \times (\alpha_2 \times e_2) \times (1 - \beta_1 \times t_1), \quad (17)$$

$$A_{12} = N \times p \times (\alpha_1 \times e_1) \times (\alpha_2 \times e_2), \quad (18)$$

and

$$T = N \times p \times (\beta_1 \times t_1 + \beta_2 \times t_2 - \beta_1 \times t_1 \times \beta_2 \times t_2), \quad (19)$$

where α_1 and β_1 are respectively the attenuation factors of areas under the photopeak and the whole spectrum attributed to γ_1, and α_2 and β_2 are those to γ_2. Rearranging the parameters by the following definitions

$$(\alpha_1 \times e_1) = \varepsilon_1, \quad (\alpha_2 \times e_2) = \varepsilon_2,$$

$$(\beta_1 \times t_1) = \tau_1 \quad \text{and} \quad (\beta_2 \times t_2) = \tau_2,$$

we have

$$A_1 = N \times p \times \varepsilon_1 \times (1 - \tau_2), \quad (20)$$

$$A_2 = N \times p \times \varepsilon_2 \times (1 - \tau_1), \quad (21)$$

$$A_{12} = N \times p \times \varepsilon_1 \times \varepsilon_2, \quad (22)$$

and

$$T = N \times p \times (\tau_1 + \tau_2 - \tau_1 \times \tau_2). \quad (23)$$

Equations (20) ~ (23) have the exactly same forms as equations (8) ~ (11). Therefore, formulas (14) and (15) can be obtained again through the same procedure. This result indicates that a disintegration rate determined by the sum-peak method is never affected by an absorber between a sample source and a detector[9,19,38]. From these results the sum-peak method might be expected to be the absolute determination method of the disintegration rate of a radioactive source regardless

of the geometry between the source and a detector, regardless of the photoelectric and total efficiencies, and regardless of the insertion of an absorber between the source and the detector.

(4) Determination of the areas under the photopeak, the sum peak and the whole spectrum of ^{60}Co

The present studies of the sum-peak method have been carried out through radioactivity measurements of ^{60}Co sources by using a NaI(Tl) detector. A representative measuring arrangement used is

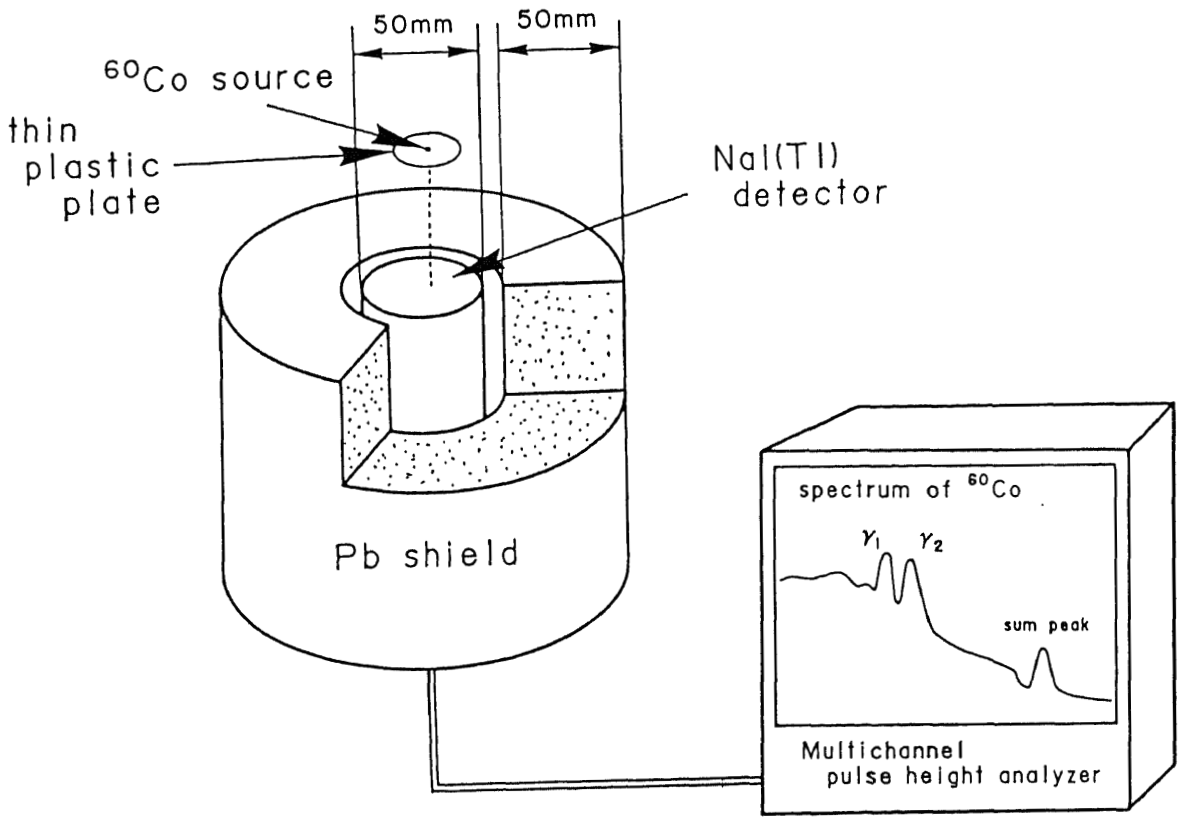

Fig. 3 Representative measuring arrangement used in a radioactivity measurement.

shown in Fig. 3. The NaI(Tl) detector was surrounded with a Pb shield of about 50 mm in thickness and was connected to a multichannel pulse height analyzer. Figure 4 shows the decay scheme of ^{60}Co [39,40] and a typical spectrum[37,41] of a ^{60}Co source obtained by the measuring arrangement shown in Fig. 3. Reading from the decay scheme shown in Fig. 4, the nuclide ^{60}Co emits two coincident γ-rays, γ_1 : 1173 keV and γ_2 : 1332 keV, with the emission probability of 100 % at every disintegration (p = 1). Two photopeaks for γ_1 and γ_2, and a sum peak for $\gamma_1 + \gamma_2$ (= 2505 keV) can be observed in the spectrum. Since the sum peak can be obtained clearly, (See Fig. 2.)

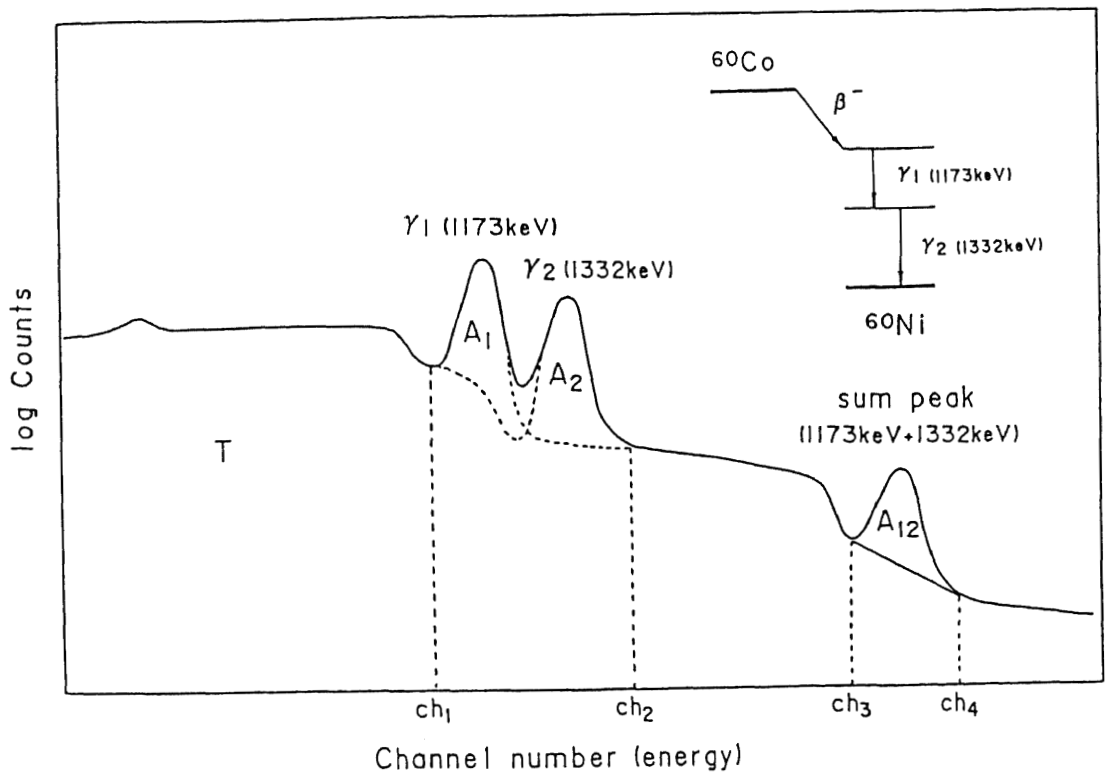

Fig. 4 Decay scheme and a typical spectrum of a ^{60}Co source obtained by a NaI(Tl) detector.

the disintegration rate of the ^{60}Co source can be basically calculated by the sum-peak formula (15). However, the two spectra shown in Figs. 2 and 4 are slightly different each other. In Fig. 4 the two photopeaks overlap noticeably and a part of the area under the Compton scattering of γ_2 also overlaps under the photopeak of γ_1. Accordingly, we determined the ratio of the area attributed to Compton scattering of γ_2 under the photopeak of γ_1 to the area of γ_2 by using the spectrum of a 1275 keV γ-ray emitted from a ^{22}Na source[42~45], which must have the same source-to-detector geometry as that of the ^{60}Co source. The spectrum measurement of the ^{22}Na source does not necessarily require any knowledge of the radioactivity level of the source. Furthermore, assuming that A_1 (area of γ_1) was equal to A_2 (area of γ_2) in each of the ^{60}Co spectra because the detector was responsive almost equally to the γ-rays of 1173 and 1332 keV, the areas, T (area under the whole spectrum), A_1, A_2 and A_{12} (area under the sum peak) were calculated by using the following relations

$$T = I_T - B_T, \tag{24}$$

$$A_1 = A_2 = \frac{(I_{1+2} - B_S)}{(2 + \alpha)}, \tag{25}$$

and

$$A_{12} = I_{12} - \frac{1}{2}(Ch_4 - Ch_3 + 1)(C_4 + C_3), \tag{26}$$

where

I_T and B_T : the area and the background area under the whole

spectrum, respectively,

I_{1+2} : the total area under the two photopeaks, γ_1 and γ_2,

B_S : the background area under the two photopeaks, γ_1 and γ_2,

α : the ratio of the area attributed to Compton scattering of γ_2 under the photopeak of γ_1 to A_2, as determined by using the spectrum of a ^{22}Na source,

I_{12} : the total area under the sum peak,

Ch_3 and Ch_4 : the starting channel and the last channel of the sum-peak, respectively,

and

C_3 and C_4 : the numbers of the counts in the channels of Ch_3 and Ch_4.

The background areas, B_T and B_S, were determined from a spectrum measured without radiation sources.

(5) A detector, a multichannel pulse height analyzer and radioactive sources

In the present studies all the measurements of γ-ray spectra were carried out by using a single NaI(Tl)[46] scintillation detector (Canberra 2007p) with a diameter of 50 mm and a height of 50 mm, and a multichannel pulse height analyzer (SEIKO EG & G Model 7800) which has a measurable energy range for γ-rays from about 10 keV to 3000 keV. Point sources and bulky sources of ^{60}Co and ^{22}Na were used in spectrum measurements. The spectra of ^{22}Na sources were available for

the estimation of the values of "α" in equation (25).

Sources of our own making were prepared together with standard sources. The point sources were made of grains of ion-exchange resin with diameters smaller than 0.5 mm, and the bulky sources, 10 $\mu\ell$-solutions of ^{60}Co and ^{22}Na, were prepared by diluting with water of from 10 to 100 mℓ in bottles with a volume of 100 mℓ. Disintegration rates of the point sources were determined according to the ordinary method described in §2.(*2*). A ^{60}Co standard source with a disintegration rate of 1.4×10^5 Bq (± 3 %) and a ^{22}Na standard source with a disintegration rate of 2.3×10^4 Bq (± 3 %) supplied from the LMRI (Laboratoire de Metrologie des Rayonnements Ionisants, France) were used. These standard sources had the shape of ellipses smaller than 2 mm in width on thin plastic plates, regarded as points when compared with the dimensions of the NaI(Tl) detector shown in Fig. 3. The disintegration rates of the bulky sources were indirectly determined through radioactivity calibrations of point sources made by drying 10 $\mu\ell$-solutions of ^{60}Co and ^{22}Na on thin plastic plates. The volume of the 10 $\mu\ell$-solutions was the same as those used to make the bulky sources. In the present radioactivity calibrations, all γ-ray spectra were measured by using a Ge(Li) semiconductor gamma detector (Princeton Gamma-Thech). Uncertainties of the radioactivity of these homemade sources were determined to be about 5 % or less.

Sources prepared by ourselves were used in all the experiments except for those of *Appendix-1* and §5.(*1*), in which the standard sources were used as point sources.

(6) Error Estimation

In the present studies, disintegration rates, entire areas under spectra, photopeak areas, sum peak areas and so forth were determined through various experiments and calculations, and errors associated with these rates and areas were estimated using standard deviations which could be determined based on the following formula[47,48,49];

$$(\sigma_F)^2 = (\sigma_x)^2 \left[\frac{\partial F}{\partial x}\right]^2 + (\sigma_y)^2 \left[\frac{\partial F}{\partial y}\right]^2 + (\sigma_z)^2 \left[\frac{\partial F}{\partial z}\right]^2 + \cdots\cdots , \quad (27)$$

in which "F" is a function with variables of x, y, z, ... (that is, $F = F(x,y,z,\cdots\cdots)$, and σ_F, σ_x, σ_y, σ_z, ... are standard deviations of F, x, y, z, ... , respectively. This formula shows how the errors (the standard deviations; σ_x, σ_y, σ_z, ...) of determinations of some parameters (x, y, z, ...) will be propagated to the final error (σ_F : the standard deviation of the final result of F).

In the case of the sum-peak formula (15) treated in the present studies, the disintegration rate is a function of count rates of the entire area under a spectrum, the photopeak areas of γ_1 and γ_2, and the sum peak area. That is,

$$N = T + \frac{A_1 \times A_2}{A_{12}} = \frac{t}{s} + \frac{\frac{a_1}{s} \times \frac{a_2}{s}}{\frac{a_{12}}{s}} = \frac{t}{s} + \frac{a^2}{s \times a_{12}}$$

$$= N(t, a, a_{12}),$$

in which

N : the disintegration rate determined by the sum-peak formula,

T : the count rate of the entire area under a spectrum,

A_1 : the count rate of the photopeak area of γ_1,

A_2 : the count rate of the photopeak area of γ_2,

A_{12} : the count rate of the sum peak area,

s : the measuring time of a spectrum,

t : the entire area under a whole spectrum (= T × s),

a_1 : the photopeak area of γ_1 (= A_1 × s),

a_2 : the photopeak area of γ_2 (= A_2 × s),

a : the photopeak area of γ_1 or γ_2 (= $a_1 = a_2$),

and

a_{12} : the sum peak area (= A_{12} × s).

Then formula (27) yields

$$(\sigma_N)^2 = (\sigma_t)^2 \left[\frac{\partial N}{\partial t}\right]^2 + (\sigma_a)^2 \left[\frac{\partial N}{\partial a}\right]^2 + (\sigma_{a12})^2 \left[\frac{\partial N}{\partial a_{12}}\right]^2$$

$$= (\sigma_t)^2 \left[\frac{1}{s}\right]^2 + (\sigma_a)^2 \left[\frac{2 \times a}{s \times a_{12}}\right]^2 + (\sigma_{a12})^2 \left[\frac{a^2}{s \times a_{12}^2}\right]^2$$

where

σ_N : the standard deviation of N,

σ_t : the standard deviation of t,

σ_a : the standard deviation of a (= $a_1 = a_2$),

and

σ_{a12} : the standard deviation of a_{12}.

Since

$$(\sigma_t)^2 = t = s \times T, \tag{28}$$

$$(\sigma_{a12})^2 = a_{12} = s \times A_{12}, \tag{29}$$

and

$$(\sigma_a)^2 = \frac{s \times A}{(2+\alpha)} + \left(\frac{C_n}{P_n^2} + \frac{C_n^2}{P_n^3} \right) \times \left(\frac{s \times A}{(2+\alpha)} \right)^2, \tag{30}$$

we have

$$(\sigma_N)^2 = \frac{T}{s} + (\sigma_a)^2 \left(\frac{2 \times A}{s \times A_{12}} \right)^2 + \left(\frac{A^4}{s \times A_{12}^3} \right) \tag{31}$$

where

A : the count rate of the photopeak area of γ_1 or γ_2, ($A = A_1 = A_2$)

α : the ratio of the area attributed to Compton scattering of γ_2 under the photopeak of γ_1 to A_2,

C_n : the area attributed to Compton scattering of γ_2 under the photopeak of γ_1, which was practically determined from the spectrum of a ^{22}Na source,

P_n : the photopeak area of γ_2, which was practically determined from the spectrum of a ^{22}Na source.

In the present studies, the errors of the areas and disintegration rates were estimated based on equations (28) ~ (31).

§3. Application to ^{60}Co Sources

The sum-peak formula is a simple function of areas represented in count rates which can be obtained from a γ-ray spectrum, and does not require measurements of the photoelectric and total efficiencies of a detector. Consequently, it is expected that a disintegration rate can be derived by a calculation of the sum-peak formula regardless of the source-to-detector geometry and an absorber between a source and the detector[8,9,19,38]. On the other hand, there is the tacit assumption in the application of the sum-peak method that the detector must have the same response for the entire part of the radioactive source. This assumption holds automatically for a point source but not for an extended source such as a bulky source. In the section *1* of this chapter, we ascertain experimentally the distinct advantages of independence of the geometry and of no effect due to absorbers by measurements with ^{60}Co point sources. In the section *2*, the sum-peak method is applied to bulky sources of ^{60}Co solutions in bottles which are typical examples of extended sources and errors caused are experimentally and analytically investigated.

1. Point source

(1) Experimental Procedure

Figure 5 shows schematically measuring arrangements used in three types of experiments. In the arrangement (A), a ^{60}Co point source with a disintegration rate of 3.2×10^4 Bq was used and the position of the source was varied upward from the surface of the

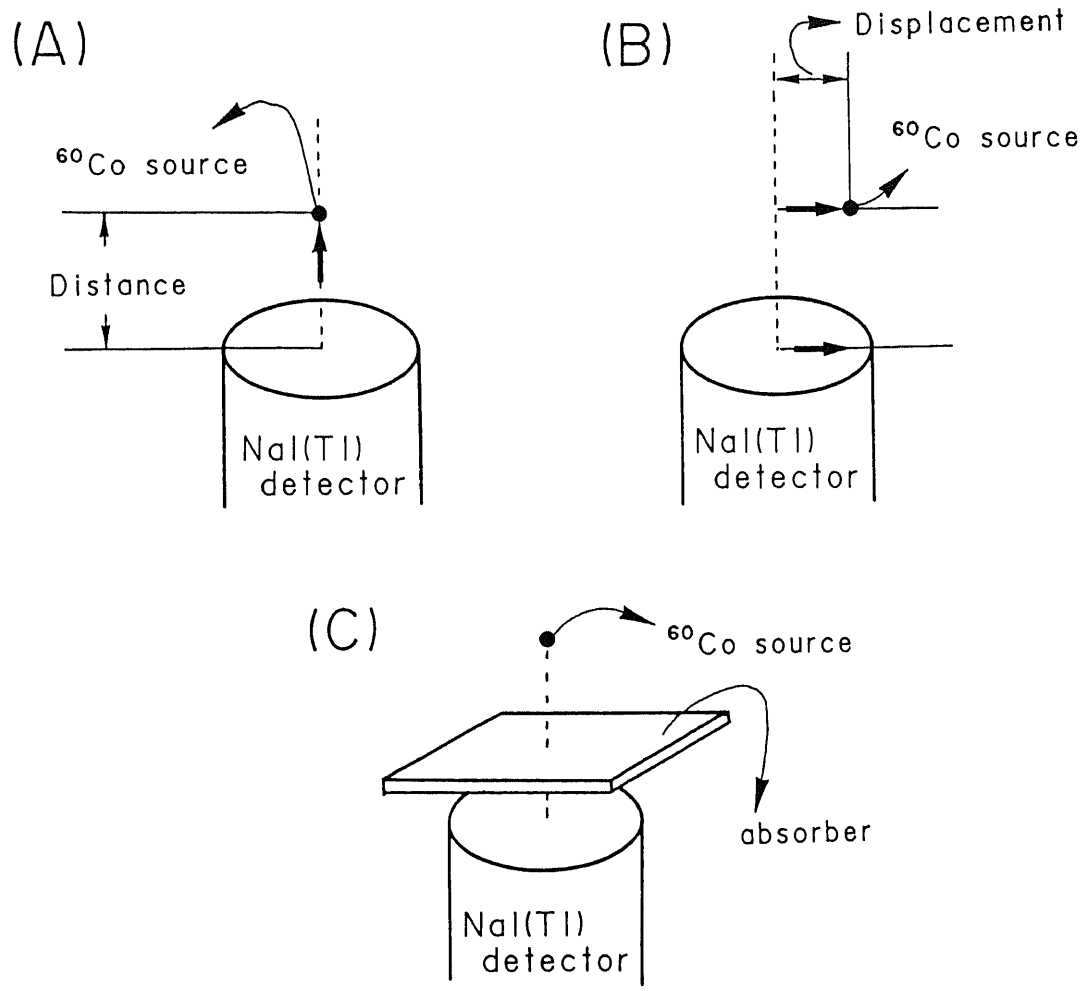

Fig. 5 Measuring arrangements of three types of experiments.

detector along the center axis of the detector at an interval of 5 mm. In this arrangement the disintegration rate calculated by the sum-peak formula could be inspected as a function of the vertical distance from the source to the detector surface. In (B), a ^{60}Co point source with a disintegration rate of 2.2×10^4 Bq was used and

the position of the source was varied at every 5 mm within 30 mm along either of the two lines parallel to the surface of the detector. One line was on the detector surface and the other was 50 mm above the detector. The calculated disintegration rate could be examined as a function of the horizontal displacement from the source to the center axis of the detector. In (C), a ^{60}Co point source of 3.2×10^4 Bq was placed at the fixed position, 20 mm from the detector surface at the center axis and lead absorbers with thicknesses of 3 ~ 12 mm were placed between the source and the detector. The calculated disintegration rate could be examined as a function of the absorber thickness. In each case, measurements of γ-ray spectra were carried out and the areas under the entire spectrum, the photopeaks and the sum peak were determined by using equations (24), (25) and (26), and the sum-peak method was applied to determine the disintegration rates of the point sources.

(2) Results

(a) Effect of distance

Table 1 gives the absolute values of areas under the entire spectrum (T), the photopeak of γ_1 or γ_2 (A_1 or A_2), and the sum peak (A_{12}) calculated by equations (24), (25), and (26), and the disintegration rates calculated by the sum-peak formula (15). In Table 1, the relative standard deviations of the entire areas (T), the photopeak areas (A_1 or A_2), the sum peak areas (A_{12}) and the disintegration rates are also shown in parentheses, which are

Table 1 Areas under the entire spectrum, the photopeak and the sum peak obtained from ^{60}Co spectra, and disintegration rate determined.

Distance(mm)	Areas (cps)			Disintegration rate	
	T	A_1 or A_2	A_{12}	$\frac{A_1 \times A_2}{A_{12}}$	$T + \frac{A_1 \times A_2}{A_{12}}$
0	7.8×10^3 (0.04)	8.8×10^2 (0.07)	3.5×10 (0.54)	2.2×10^4	3.0×10^4 (0.41)
5	6.0×10^3 (0.03)	6.9×10^2 (0.06)	1.9×10 (0.51)	2.5×10^4	3.1×10^4 (0.42)
10	4.6×10^3 (0.03)	5.4×10^2 (0.07)	1.1×10 (0.67)	2.6×10^4	3.0×10^4 (0.58)
15	3.7×10^3 (0.03)	4.3×10^2 (0.06)	7.2 (0.68)	2.6×10^4	3.0×10^4 (0.61)
20	3.0×10^3 (0.03)	3.5×10^2 (0.07)	4.5 (0.86)	2.7×10^4	3.0×10^4 (0.78)
25	2.5×10^3 (0.03)	2.9×10^2 (0.06)	3.1 (0.80)	2.7×10^4	2.9×10^4 (0.74)
30	2.1×10^3 (0.03)	2.4×10^2 (0.06)	2.1 (0.82)	2.7×10^4	2.9×10^4 (0.77)
40	1.5×10^3 (0.03)	1.8×10^2 (0.05)	1.2 (0.93)	2.6×10^4	2.8×10^4 (0.88)
50	1.2×10^3 (0.02)	1.4×10^2 (0.05)	7.0×10^{-1} (0.98)	2.6×10^4	2.7×10^4 (0.94)
60	9.4×10^2 (0.02)	1.1×10^2 (0.05)	4.6×10^{-1} (1.05)	2.4×10^4	2.5×10^4 (1.01)
70	7.6×10^2 (0.02)	8.4×10^1 (0.05)	3.2×10^{-1} (1.01)	2.2×10^4	2.3×10^4 (0.98)
80	6.3×10^2 (0.02)	7.0×10^1 (0.04)	2.5×10^{-1} (1.00)	1.9×10^4	2.0×10^4 (0.97)
90	5.3×10^2 (0.02)	5.8×10^1 (0.04)	2.0×10^{-1} (1.01)	1.7×10^4	1.8×10^4 (0.98)
100	4.6×10^2 (0.02)	4.9×10^1 (0.04)	1.6×10^{-1} (1.01)	1.5×10^4	1.5×10^4 (0.99)

True disintegration rate is 3.2×10^4 Bq,

T : the entire area of the spectrum,

A_1 or A_2 : the photopeak area of γ_1 or γ_2,

A_{12} : the sum peak area,

$T + \frac{(A_1 \times A_2)}{A_{12}}$: the sum-peak formula, and

(S.D. , %) : the relative standard deviation.

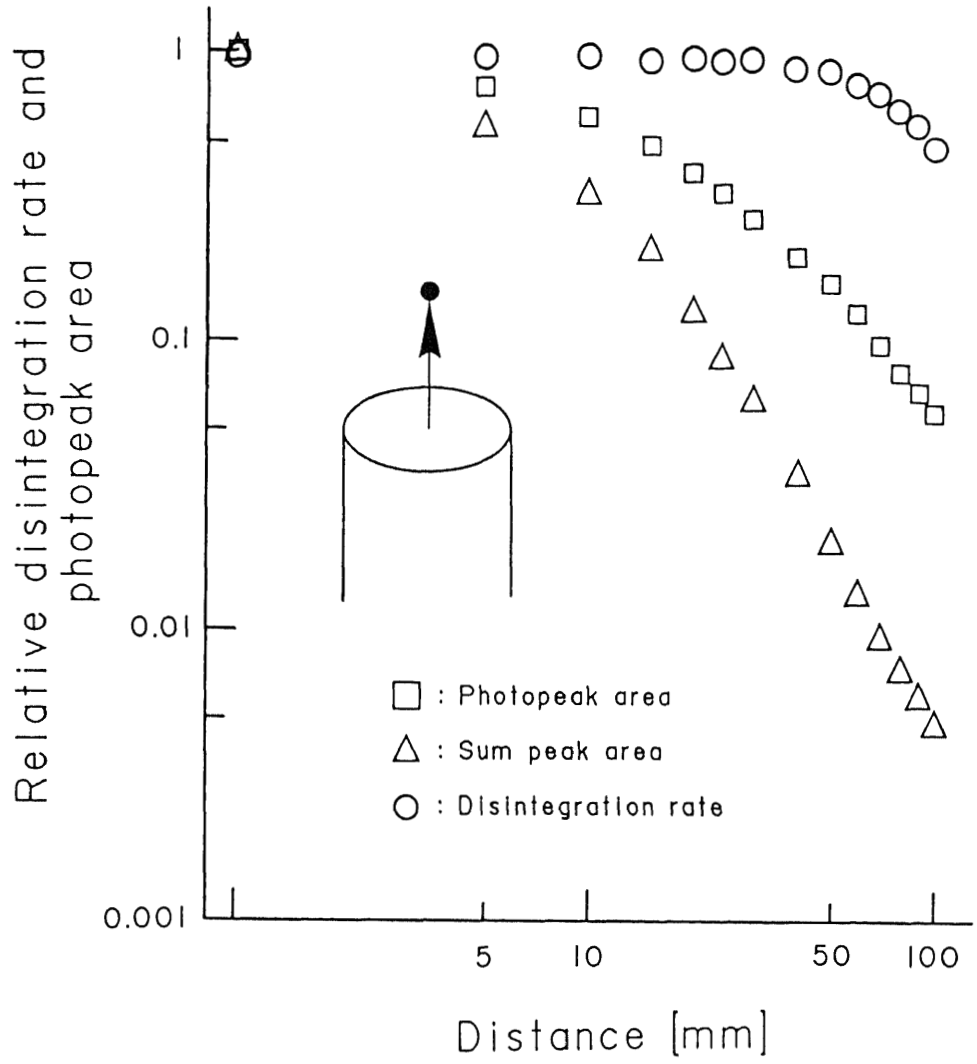

Fig. 6 Effect of the distance on the disintegration rate (calculated with the sum-peak formula) and on the peak areas, relative to the data at zero distance. Circle : relative disintegration rate, square : photopeak area A_1, triangle : sum peak area A_{12}.

less than 0.05 %, 0.1 %, 1.1 % and 1 %, respectively. Figure 6 shows these areas and the disintegration rates as a function of the distance between the source and the detector. The rates and areas

are normalized to 1 at the distance of 0 mm. Figure 6 shows that the relative disintegration rate calculated by the sum-peak formula (15) decreases slightly with increasing distance up to about 50 mm, and decreases rapidly, over 50 mm. The slight decrease at short distances can be related to γ_1-γ_2 directional (angular) correlation[50], and the rapid falloff is associated with a radionuclide of ^{208}Tl which is one of naturally occurring radionuclides and emits γ-rays of 2614 keV.

The angular distribution of γ-rays depends on the spin orientation of an exited nucleus. In a usual case, since the nuclear spin axis is randomly oriented in space, an isotropic emission of γ-rays is observed. In the case of ^{60}Co which emits two γ-rays in cascade, two γ-rays have the following angular correlation;

$$W(\theta) = 1 + 0.102 \times P_2(\cos\theta) + 0.0091 \times P_4(\cos\theta) + \cdots\cdots .$$

where θ is the angle between the two γ-rays and P_k's are Legendre polynomials[50], given by

$$P_2(x) = \frac{1}{2}(3x^2-1), \qquad P_4(x) = \frac{1}{8}(35x^4-30x^2+3), \cdots\cdots .$$

Thus we have

$$W(\theta) = 0.952 + 0.119 \times \cos^2\theta + 0.040 \times \cos^4\theta + \cdots\cdots .$$

Using this function $W(\theta)$, we make an estimate of errors caused by the angular correlation in the case of ^{60}Co when the sum-peak method is

applied in the measurement shown in Fig. 5 (A). The effective solid angle covered by the detector can be modeled as indicated in the figure. Then the angular correlation factor F is given by

$$F = \frac{\int_{\Delta\Omega} W(\theta)\,d\Omega}{\int_{\Delta\Omega} d\Omega} = \frac{\int_{\theta}^{\theta} W(\theta)\,2\pi(\sin\theta)\,d\theta}{\int_{\theta}^{\theta} 2\pi(\sin\theta)\,d\theta}$$

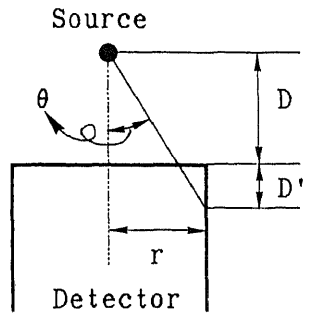

$$= 0.952 + \frac{0.040(1-\cos^3\theta) + 0.008(1-\cos^5\theta)}{(1-\cos\theta)} .$$

For the detector radius r = 25 mm the calculated correlation factor as a function of D + D' is given in the table. D is the distance from the source to the detector surface and D' the effective depth corresponding to the detector acceptance. It must be noted that the sum peak area can be overestimated as large as 10 % for D = 100 mm.

Distance D+D' (mm)	Angular correlation factor
0	1.000
10	1.025
25	1.062
50	1.091
75	1.101
100	1.105
125	1.107
...	.....
∞	1.111

Next, the effect of ^{208}Tl to the sum-peak method will become significant when the count rate of the sum peak is not so large as

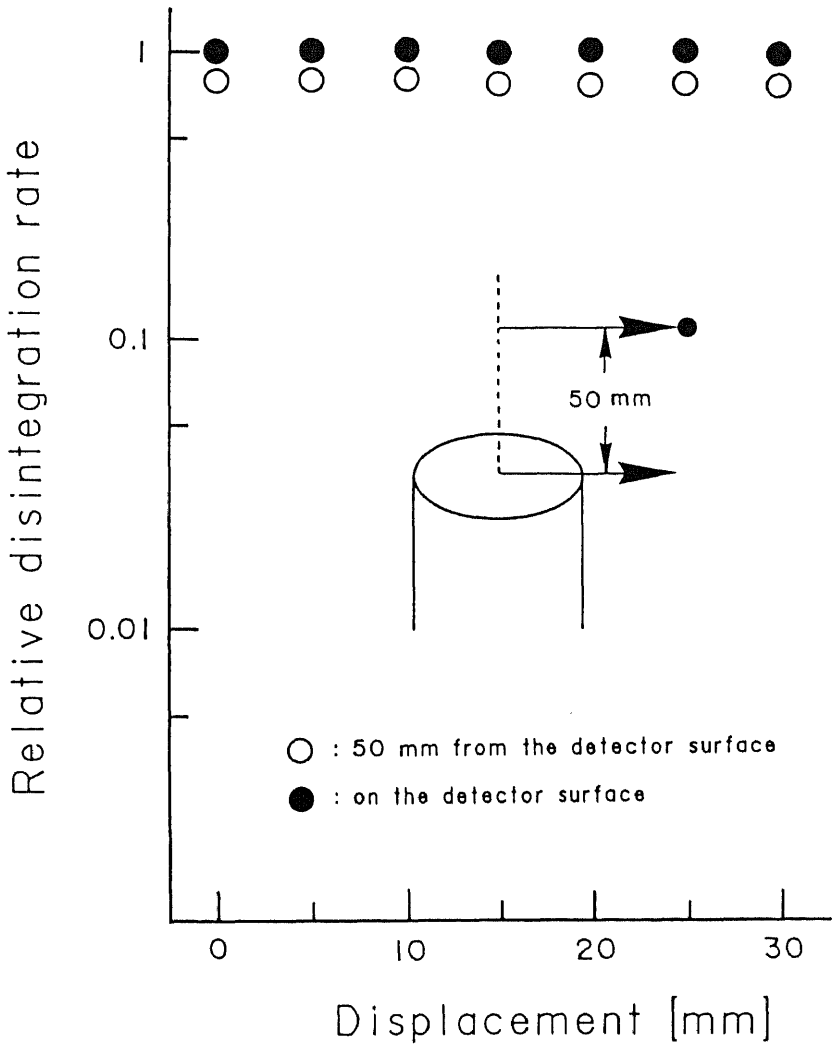

Fig. 7 Effect of the displacement on the disintegration rate (calculated with the sum-peak formula). Black circle : source placed on the detector surface, white circle : source placed at the high position of 50 mm from the detector surface.

compared with 0.1 cps as discussed in §5. 2. and 3..

In Fig. 6, deviations from the true disintegration rate (= 1 in

the relative value) are reasonably small up to the distance of about 50 mm. On the other hand, the photopeak and sum peak areas decrease significantly as the distance increases.

(b) Effect of displacement

Figure 7 shows the disintegration rate calculated by the sum-peak formula as a function of the horizontal displacement from the source to the center axis of the detector. Black circles correspond to the results when the ^{60}Co point source was on the detector surface and white circles to those at the higher position of 50 mm from the detector surface. The standard deviations of all the disintegration rates shown in Fig. 7 are less than 1.0 %, and the small differences between the black and white circles must be due to the directional correlation of two γ-rays, γ_1 and γ_2. The horizontal displacement within 30 mm along both lines affects very little. Deviations in the data obtained at 0, 5, 10, 15, 20, 25 and 30 mm in displacement from the center axis of the detector are within 5% tolerance.

These results shown in Figs. 6 and 7 prove that the sum-peak method can be a radioactivity standardization technique regardless of the source-to-detector geometry, because the source-to-detector geometry can be defined by the distance and displacement.

(c) Effect of absorbers

Figure 8 shows the relative disintegration rate determined

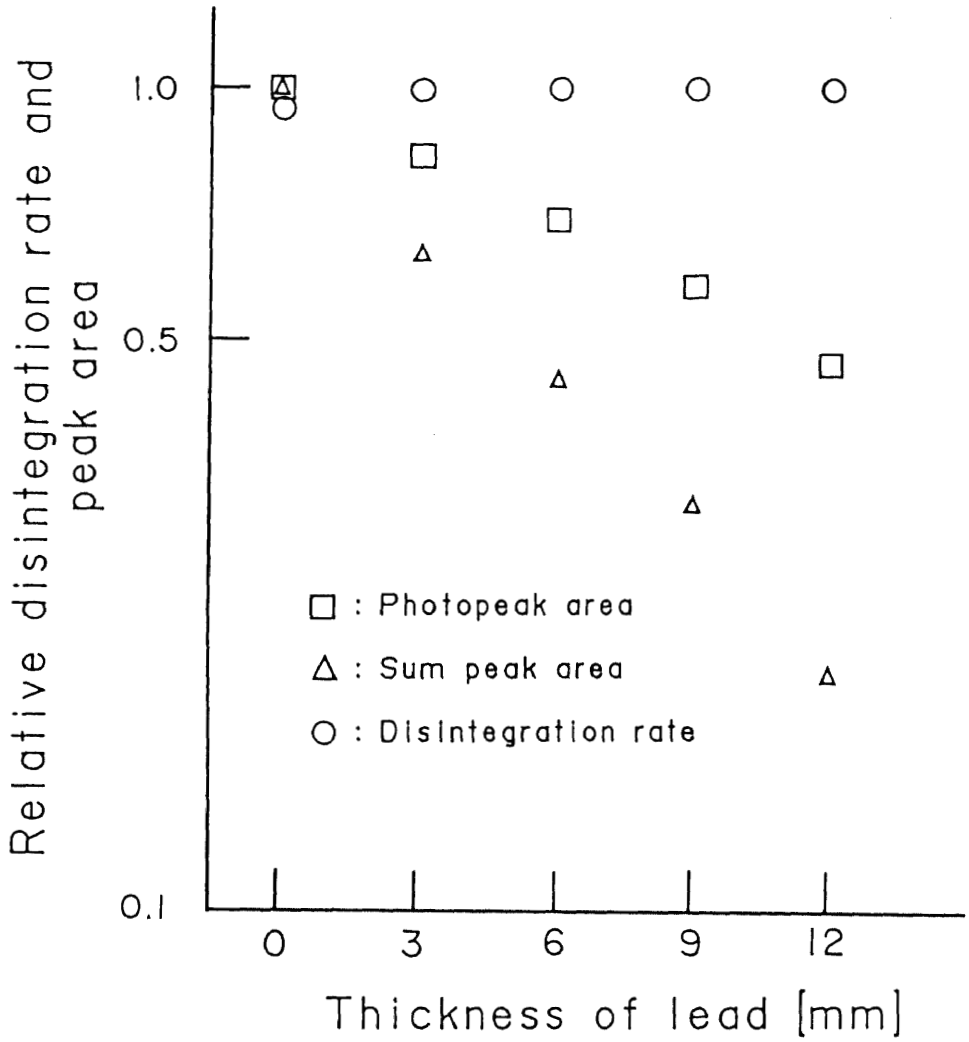

Fig. 8 Effect of the absorber on the disintegration rate (calculated with the sum-peak formula) and on the peak areas, relative to the data without the absorber. Circle : relative disintegration rate, square : photopeak area A_1, triangle : sum peak area A_{12}.

by the sum-peak method as a function of the thickness of lead absorbers. In Fig. 8, all the symbols are used in the same way as in Fig. 6. The relative disintegration rate shown is the ratios to the true disintegration rate of the ^{60}Co point source used, and the relative areas are normalized to those obtained without absorbers. The standard deviations of the photopeak areas, the sum peak areas and the disintegration rates shown in Fig. 8 are less than 0.1 %, 1.1 % and 1.0 %, respectively. We can see the results similar to those concerning the distance. The disintegration rate determined by the sum-peak method is essentially not affected by the absorbers, whereas the areas under the photopeak and the sum peak decrease significantly with increasing absorber thickness.

2. Bulky source

(1) Experimental Procedure and Results

The measuring arrangement used for bulky sources is shown schematically in Fig. 9. A polyethylene bottle used had a diameter of about 50 mm and a height of 55 mm (total volume ~ 100 mℓ). The volume of a ^{60}Co solution of 1.1×10^4 Bq was varied by successive dilution from 10 to 100 mℓ in the bottle. In Fig. 10, circles show the relative disintegration rate calculated by the sum-peak formula as a function of the volume of the ^{60}Co solution in the bottle. The relative disintegration rate is the ratio of the value determined by the sum-peak method to the true rate of the bulky source. The standard deviations of results shown by circles were less than 1 %. These data

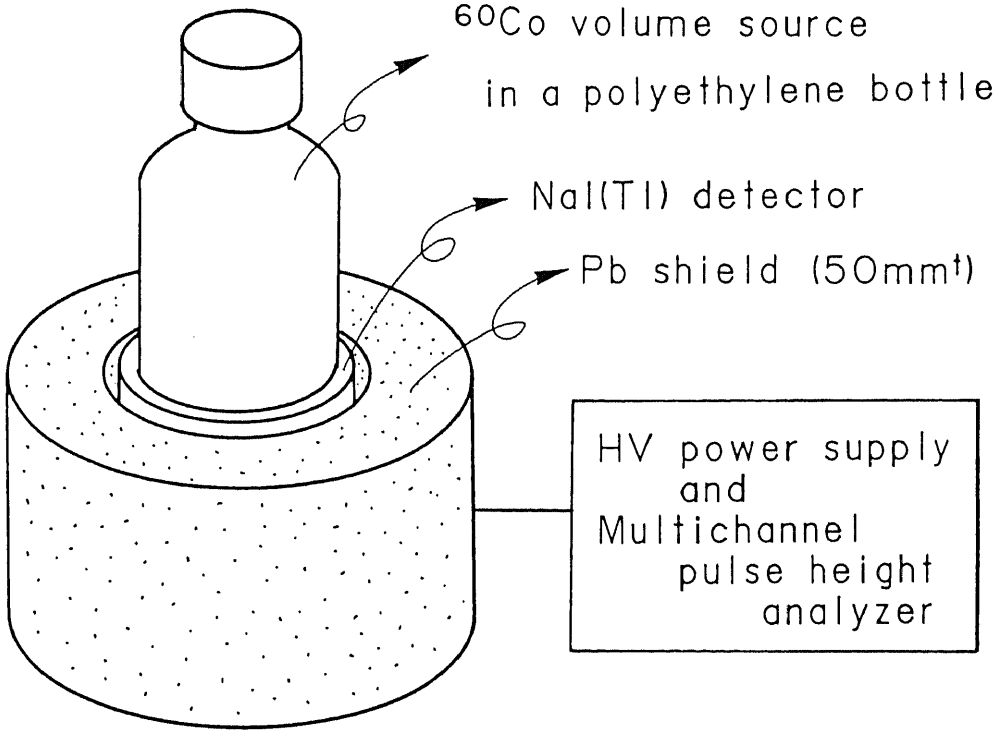

Fig. 9 Geometrical arrangement of a NaI(Tl) detector and a bulky source (a ^{60}Co volume source)

show that the calculated relative disintegration rate decreases proportionally with the volume. The reduction rate is about 30 % for 100 ml compared with that for 10 mℓ. This reduction was substantially larger even if taking account of the effect of the directional correlation of two γ-rays and the background radiations of

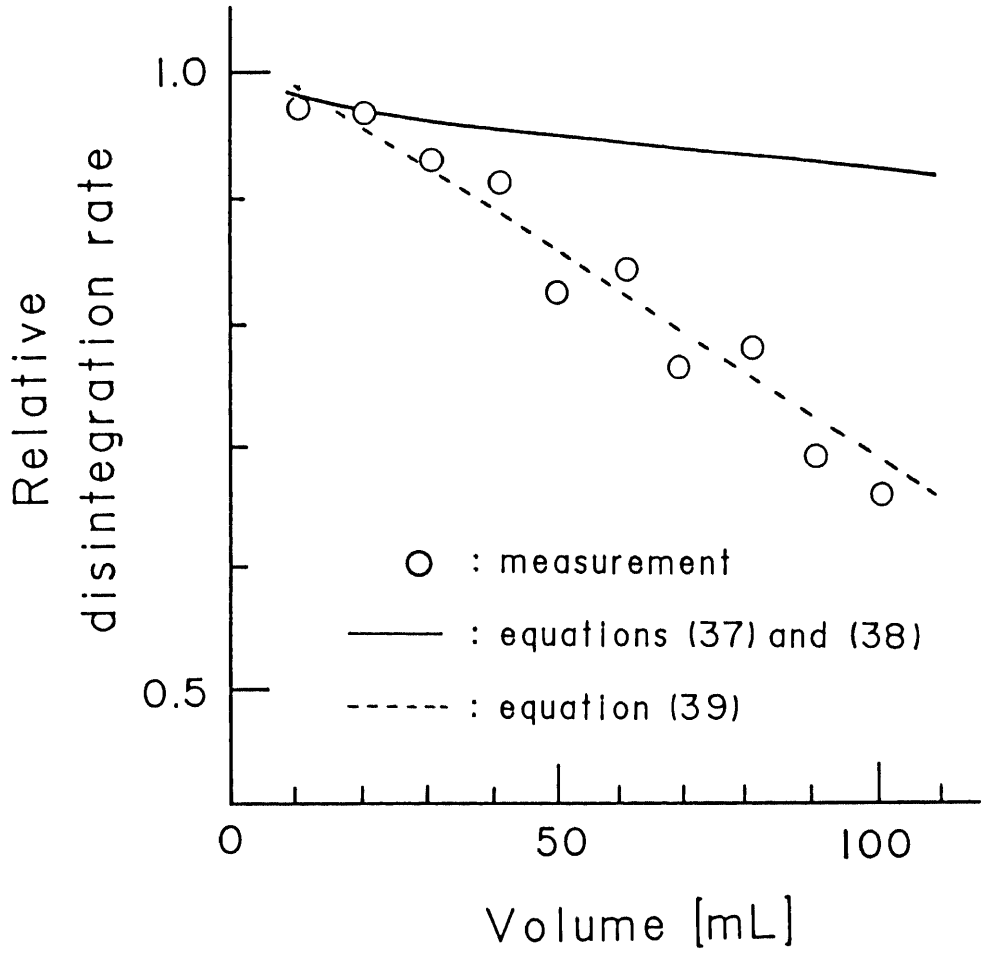

Fig. 10 Effect of the volume on the relative disintegration rate determined by the sum-peak method. Circle : experimental results, solid line : calculated from equations (37) and (38), dotted line : calculated from equation (39).

^{208}Tl. We concluded that the reduction must be associated with the sum-peak method itself. These results are similar to those obtained by Sutherland and Buchanan although the dimensions of the NaI(Tl) scintillation detectors and the bottles differ[7,8].

(2) Discussion

We define $A_1^{[e]}$, $A_2^{[e]}$, $A_{12}^{[e]}$ and $T^{[e]}$ to be the areas under the photopeak of γ_1, the photopeak of γ_2, the sum peak and the entire spectrum, respectively, obtained by a measurement of an extended source such as the bulky sources. We also define $N^{[e]}$, $e_1^{[e]}$, $t_1^{[e]}$, $e_2^{[e]}$ and $t_2^{[e]}$ being the disintegration rate of an extended source, the photoelectric and total efficiencies of γ_1 and γ_2, respectively. Since the emission probability of γ_1 and γ_2 of ^{60}Co is 1, we have the following four equations:

$$A_1^{[e]} = N^{[e]} \times e_1^{[e]} \times (1-t_2^{[e]}), \tag{32}$$

$$A_2^{[e]} = N^{[e]} \times e_2^{[e]} \times (1-t_1^{[e]}), \tag{33}$$

$$A_{12}^{[e]} = N^{[e]} \times e_1^{[e]} \times e_2^{[e]}, \tag{34}$$

and

$$T^{[e]} = N^{[e]} \times (t_1^{[e]} + t_2^{[e]} - t_1^{[e]} \times t_2^{[e]}), \tag{35}$$

where the superscript [e] indicates "extended source". Equations (32) ~ (35) have the exactly same forms as equations (8) ~ (11), respectively. Therefore, a sum-peak formula for an extended source can be obtained through the same procedure used in deriving the sum-peak formula (15). Namely

$$N^{[e]} = T^{[e]} + \frac{(A_1^{[e]} \times A_2^{[e]})}{A_{12}^{[e]}}. \tag{36}$$

Equation (36) seems to imply that the sum-peak method should give the

true disintegration rate of an extended source regardless of the source volume; nevertheless the experimental results shown in Fig. 10 indicate clearly strong volume dependence.

To evaluate the experimental results in Fig. 10 it is assumed that the solution in the bottle can be divided into n very small parts of an equal volume and that each contains an activity of N/n (N being the true disintegration rate of the primary bulky source). If all the parts are measured separately and all the individual results obtained by the sum-peak method are amalgamated, then the calculated value of $N^{[A]}$ ([A] meaning "amalgamation") is given by;

$$N^{[A]} = \sum_{i=1}^{n} N^{[i]}, \tag{37}$$

and

$$N^{[i]} = T^{[i]} + \frac{(A_1^{[i]} \times A_2^{[i]})}{A_{12}^{[i]}}, \tag{38}$$

where the superscript [i] indicates the i-th part, and $A_1^{[i]}$, $A_2^{[i]}$, $A_{12}^{[i]}$ and $T^{[i]}$ are the areas under the photopeak of γ_1, the photopeak of γ_2, the sum peak and the entire spectrum obtained by the measurement of the i-th part. As proved by the experiments with ^{60}Co point sources at different "distances" and "displacement" over the detector in §3.*1*, $N^{[i]}$ must be equal to the true disintegration rate, N/n, for i = 0 ~ n. Then $N^{[A]}$ = N, when the volume of the i-th part can be regarded as a point. However, in a practical measurement with a bulky source by using an apparatus such as a multichannel pulse

height analyzer, the areas, $A_1^{[i]}$, $A_2^{[i]}$, $A_{12}^{[i]}$ and $T^{[i]}$, attributed to the i-th part can not be obtained separately. Only the sums over the total area containing all the parts can be measured as follows;

$$\sum_{i=1}^{n} A_1^{[i]}, \qquad \sum_{i=1}^{n} A_2^{[i]}, \qquad \sum_{i=1}^{n} A_{12}^{[i]} \quad \text{and} \quad \sum_{i=1}^{n} T^{[i]},$$

which correspond to $A_1^{[e]}$, $A_2^{[e]}$, $A_{12}^{[e]}$ and $T^{[e]}$ of equation (36), respectively. Therefore, the actual value determined for the extended source through the measurement by the sum-peak method is given by

$$N^{[e]} = \sum_{i=1}^{n} T^{[i]} + \frac{\left(\sum_{i=1}^{n} A_1^{[i]}\right) \times \left(\sum_{i=1}^{n} A_2^{[i]}\right)}{\sum_{i=1}^{n} A_{12}^{[i]}}. \qquad (39)$$

We presume that equations (37) and (38) give the true disintegration rate, whereas equation (39) gives a practically determined rate when the sum-peak method is applied to an extended source.

(3) Experimental verification of the presumption

In order to demonstrate the above presumption, the areas, $A_1^{[i]}$, $A_2^{[i]}$, $A_{12}^{[i]}$ and $T^{[i]}$, attributed to the i-th part of a bulky source were obtained using a ^{60}Co point source of 1.4×10^5 Bq at 54 positions distributed throughout the whole volume of the bottle as shown in Fig. 11. The values of $N^{[a]}$ and $N^{[e]}$ were calculated based on equations (37) and (39) [*Appendix-1*]. The real disintegration

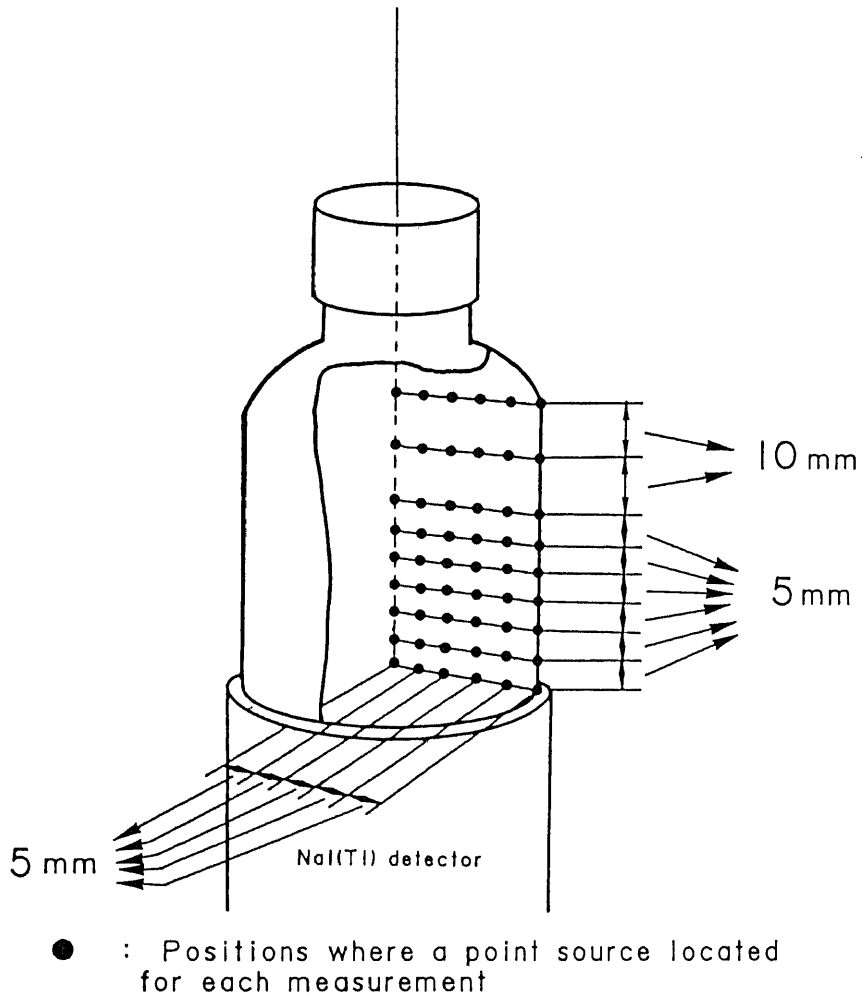

Fig. 11 Fifty four positions where a ^{60}Co point source is located for each measurement.

rate of each ^{60}Co source was taken as unity. The relative activity and the areas of the point source for the 54 positions were calculated with equations (15), (24), (25) and (26).

The solid line in Fig. 10 is the relative disintegration rate calculated by using equations (37) and (38), and the dotted line is that calculated by using equation (39). The solid line is almost

equal to unity and shows very small effects due to the source volume. On the other hand, the dotted line reproduces precisely the experimental results shown by the circles.

We determined two curves by means of the least squares fit to $Y = A \times e^{(B \times X)}$ (Y : disintegration rate, X : volume, A and B : constant values) using the experimental data shown by circles and the results from the calculation of equation (39), respectively. And the disintegration rates at 10 ~ 100 mℓ were determined again by respective two curves. Both disintegration rates thus obtained at the same volumes coincided with each other within the absolute difference of (1.3 ± 0.9) %. Therefore, we can conclude that our presumption represented by equations (37), (38) and (39) has been experimentally proved.

(4) Error estimation

Based on our presumption, when the sum-peak method is applied for the determination of the disintegration rate of an extended source, an error can be given by;

$$N - N^{[e]} = \sum_{i=1}^{n} \left(\frac{(A_1^{[i]} \times A_2^{[i]})}{A_{12}^{[i]}} \right) - \frac{(\sum_{i=1}^{n} A_1^{[i]}) \times (\sum_{i=1}^{n} A_2^{[i]})}{\sum_{i=1}^{n} A_{12}^{[i]}} . \quad (40)$$

If we take the continuum limit, equation (40) yields

$$D(v) = \int \left(\frac{(A_{p1} \times A_{p2})}{A_{p12}} \right) dv - \left(\frac{\int A_{p1} dv \times \int A_{p2} dv}{\int A_{p12} dv} \right).$$

According to Oderkerk and Brinkman[9], equation (40) can be transformed as follows [*Appendix-2*];

$$N - N_c = \frac{1}{2A_{12}} \sum_{k}^{n} \sum_{m}^{n} A_{12}{}^{k} \, A_{12}{}^{m} \, (\chi_1{}^{k} - \chi_1{}^{m}) \, (\chi_2{}^{k} - \chi_2{}^{m}), \qquad (41)$$

where

$$\chi_1{}^{k} = \frac{A_2{}^{k}}{A_{12}{}^{k}}, \qquad \chi_1{}^{m} = \frac{A_2{}^{m}}{A_{12}{}^{m}}, \qquad \chi_2{}^{k} = \frac{A_1{}^{k}}{A_{12}{}^{k}},$$

and

$$\chi_2{}^{m} = \frac{A_1{}^{m}}{A_{12}{}^{m}},$$

where an extended source is divided into 'n' parts, each of which is very small and can be regarded as a point, and

N : the real value of the absolute disintegration rate of an extended source,

N_c : measured disintegration rate by the sum-peak method,

$A_1{}^{k}$ and $A_2{}^{k}$: the areas under the photopeaks of γ_1 and γ_2 referring to the k-th part of an extended source ($k = 1, \ldots n$),

$A_1{}^{m}$ and $A_2{}^{m}$: the areas under the photopeaks of γ_1 and γ_2 referring to the m-th part of an extended source ($m = 1, \ldots n$),

$A_{12}{}^{k}$ and $A_{12}{}^{m}$: the areas under the sum peaks referring to the

k-th and the m-th parts of an extended source ($k, m = 1, \ldots n$),

and

$$A_{12} = \sum_{k}^{n} A_{12}{}^{k}, \quad (k = 1, \ldots n).$$

Assuming that the k-th and the m-th parts of an ^{60}Co extended source have disintegration rates of R^k Bq and R^m Bq, respectively, the following equations are obtained;

$$A_1{}^k = R^k \times e_1{}^k \times (1-t_2{}^k), \qquad A_1{}^m = R^m \times e_1{}^m \times (1-t_2{}^m),$$

$$A_2{}^k = R^k \times e_2{}^k \times (1-t_1{}^k), \qquad A_2{}^m = R^m \times e_2{}^m \times (1-t_1{}^m),$$

$$A_{12}{}^k = R^k \times e_1{}^k \times e_2{}^k, \quad \text{and} \quad A_{12}{}^m = R^m \times e_1{}^m \times e_2{}^m,$$

where $e_1{}^k$, $e_2{}^k$, $t_1{}^k$ and $t_2{}^k$ are the photoelectric and total efficiencies of both the γ-rays emitted from the k-th part, and $e_1{}^m$, $e_2{}^m$, $t_1{}^m$ and $t_2{}^m$ are those of the m-th part. By these equations, we obtain[10];

$$\chi_1{}^k = \frac{A_2{}^k}{A_{12}{}^k} = \frac{(1-t_1{}^k) \times e_1{}^m}{(1-t_1{}^m) \times e_1{}^k} \times \chi_1{}^m,$$

and

$$\chi_2{}^k = \frac{A_1{}^k}{A_{12}{}^k} = \frac{(1-t_2{}^k) \times e_2{}^m}{(1-t_2{}^m) \times e_2{}^k} \times \chi_2{}^m.$$

Consequently;

$$(\chi_1{}^k - \chi_1{}^m) = \left(\frac{(1-t_1{}^k) \times e_1{}^m}{(1-t_1{}^m) \times e_1{}^k} - 1 \right) \times \chi_1{}^m, \qquad (42)$$

and

$$(\chi_2{}^k - \chi_2{}^m) = \left(\frac{(1-t_2{}^k) \times e_2{}^m}{(1-t_2{}^m) \times e_2{}^k} - 1 \right) \times \chi_2{}^m . \qquad (43)$$

Equations (42) and (43) do not include the radioactivities of parts. Except for the only case in which the photoelectric and total efficiencies are equal at all the parts, all values of $(\chi_1{}^k - \chi_1{}^m)$ and $(\chi_2{}^k - \chi_2{}^m)$ for any combinations of 'k' and 'm' are not zero. Hence the values of $(N - N_c)$ are positive in general for the following reason. If $(\chi_1{}^k > \chi_1{}^m)$, then $(\chi_2{}^k > \chi_2{}^m)$, and if $(\chi_1{}^k < \chi_1{}^m)$, then $(\chi_2{}^k < \chi_2{}^m)$ owing to the practical and physical imaging as discussed by Oderkerk and Brinkman. Therefore, the sum-peak formula applied to an extended source gives a lower disintegration rate than the true rate.

In the only case in which that the detector has an equal efficiency for all parts, we have

$$(\chi_1{}^k - \chi_1{}^m) = (\chi_2{}^k - \chi_2{}^m) = 0,$$

for any combinations of 'k' and 'm' in equations (42) and (43). Then the value of $(N - N_c)$ must be identically zero regardless of the distribution of the radioactivity. This means that the sum-peak method can give the real value of the absolute disintegration rate.

Equation (41) will express theoretically the magnitude of the error caused when the sum-peak method is applied for the radioactivity measurement of an extended source. However, equation (41) is too complicated to be practically used to estimate the error, since equation (41) contains a double volume integration with respect to k

and m of individual parts of an extended source. For this reason, Oderkerk and Brinkman derived a simple inequality relation from equation (41) [*Appendix-2*] given by

$$N - N_c \leq \frac{1}{2} A_{12} (\chi_1^{max} - \chi_1^{min}) (\chi_2^{max} - \chi_2^{min}), \qquad (44)$$

where χ_1^{max} and χ_1^{min} are the maximum and minimum values of χ_1^k or χ_1^m, and χ_2^{max} and χ_2^{min} are the maximum and minimum values of χ_2^k or χ_2^m. Equation (44) can give the upper bounds of the error. According to calculations by Oderkerk and Brinkman, the upper bound determined based on equation (44) were 6, 8 and 10 times larger than the actual errors calculated based on equation (41) for line-segment, disk-shaped and solid-sphere sources, respectively.

§4. Model Studies of Two Point Sources of ^{60}Co

The sum-peak method gives sometimes an underestimated disintegration rate with a large error for an extended source when the tacit assumption is not fulfilled[7] as shown in §3.2. Oderkerk and Brinkman proposed equation (41) by which the magnitude of the error caused by applying the sum-peak method can be estimated[8,9]. In this chapter, the sum-peak method is applied to determine the disintegration rate of various extended sources composed of two ^{60}Co point sources[10]. It is verified that the absolute disintegration rates of the extended sources can be accurately determined when a detector has an equal efficiency for both point sources and otherwise they are underestimated. In other words it is confirmed that the sum-peak method is valid when the tacit assumption is strictly fulfilled, and not valid when not fulfilled. The magnitude of errors for the extended sources will be examined by comparing experimental results with calculated values based on equation (41).

(1) Experimental Procedure

Figure 12 shows schematically five measuring arrangements (A), (B), ... and (E), each of which consisted of two ^{60}Co point sources and a NaI(Tl) detector connected to a multichannel pulse height analyzer. In the cases of (A) and (B), two point sources had almost the same radioactivity (3.8×10^4 Bq and 3.6×10^4 Bq), and different radioactivities (3.8×10^4 Bq and 9.8×10^3 Bq),

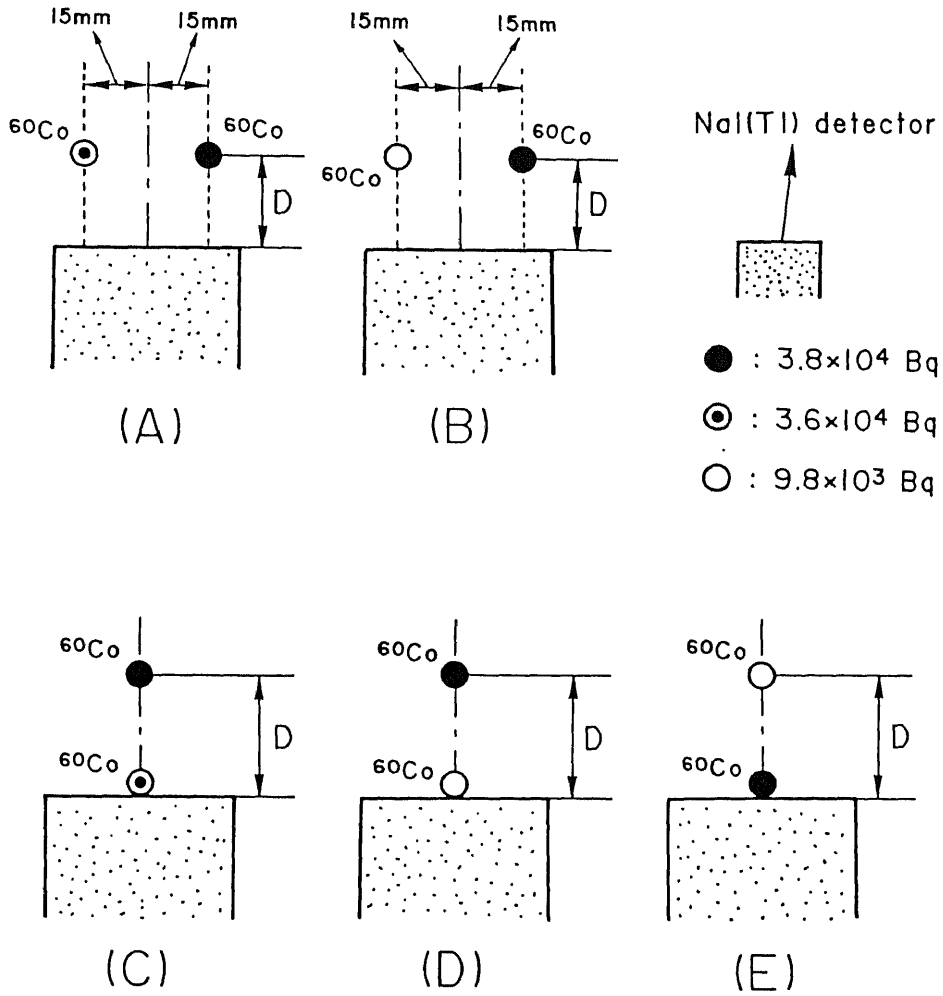

Fig. 12 Five geometrical (measuring) arrangements; black circle : 3.8×10^4 Bq source, double circle (white and small black circles) : 3.6×10^4 Bq source, white circle : 9.8×10^3 Bq, D : distance, dot-dash-line : center axis of a detector.

respectively. They were placed at several symmetrical positions with respect to the center axis (15 mm left and right from the axis). The distance from the detector surface was also varied from 0 to 50 mm. Hence the detector had an equal efficiency for the two sources in

these cases. In (C), (D) and (E), one source was placed at the center of the detector surface, and the second source was placed at several positions with distances from 5 to 50 mm along the center axis. Therefore, the detector had different efficiencies for the two sources, that is, the efficiency for the upper source decreases with increasing distance and is always less than that for the source placed at the detector surface (constant value).

(2) Results

Relative disintegration rates were derived respectively from the disintegration rate calculated by the sum-peak formula (15). The relative disintegration rate was defined as the ratio of the disintegration rate determined by the sum-peak method to the true rate.

Figure 13 shows the relative disintegration rates determined from measurements (A) and (C), and Fig. 14 shows those from (B), (D) and (E). In both figures, the standard deviations of results are less then 1.1 %. The disintegration rates shown by squares decrease very rapidly with increasing distances and the falloff rate is much too large even if taking account of the effect of the directional correlation of γ rays and background radiations owing to ^{208}Tl.

It can be concluded from Figs. 13 and 14 that the sum-peak method can give the true disintegration rate regardless of the radioactivity and efficiency when the detector is equally responsive for the two point sources, and otherwise it gives an underestimated

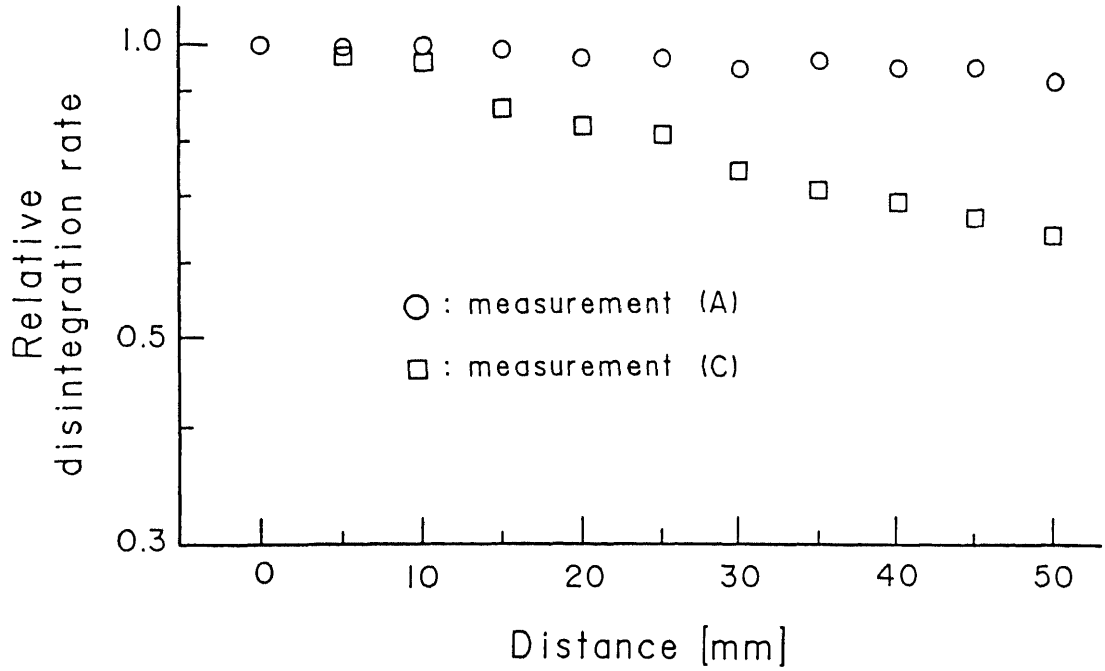

Fig. 13 Relative disintegration rate determined by the sum-peak method with the measurements (A) and (C). Circle and square : measurements (A) and (C), respectively.

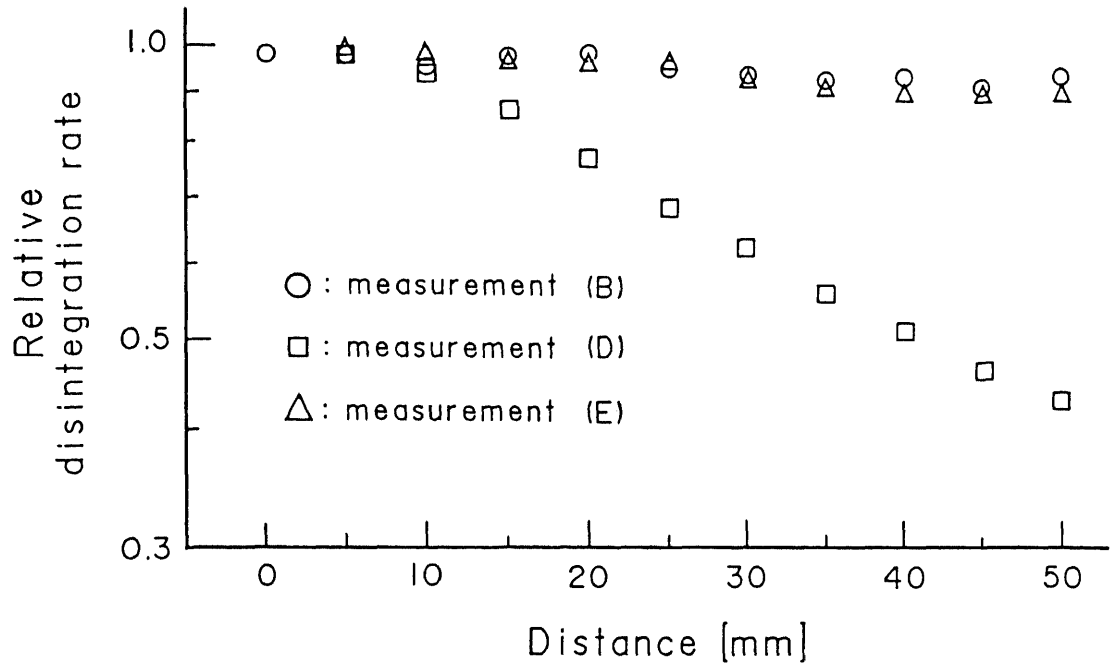

Fig. 14 Relative disintegration rate determined by the sum-peak method with the measurements (B), (D) and (E). Circle, square and triangle : measurements (B), (D) and (E), respectively.

rate. However, in (E) the relative disintegration rate is not appreciably underestimated because the strength of the source located at the detector surface is very large (about four times larger) compared with that of the other source.

(3) Discussion

The experimental results shown in §3. *1* proved that the sum-peak method was perfectly effective and that the disintegration rate obtained was not influenced by the efficiency of a detector to γ-rays for one point source. In the cases of the extended sources formed by the combination of the two point sources, the sum-peak method gives the true disintegration rate when a detector is equally responsive to both the point sources, but otherwise it gives an underestimated rate. We will theoretically explain these experimental facts below.

In the present measurements by using the two ^{60}Co point sources, we could assume that the two sources formed an extended source, which consisted of two very small parts, and the value of 'n' must be 2. Rearranging equations (41) and (44) by substituting '2' into 'n', and adopting superscripts [1] and [2] to specify both sources, we obtain the following equations [*Appendix-3*]:

$$N - N_c = \frac{A_{12}^{[1]} A_{12}^{[2]}}{A_{12}} (\chi_1^{[1]} - \chi_1^{[2]})^2, \qquad (45)$$

and

$$N - N_c \leq \frac{A_{12}}{2} (\chi_1^{[1]} - \chi_1^{[2]})^2 , \tag{46}$$

where

$$A_{12} = A_{12}^{[1]} + A_{12}^{[2]} .$$

Equations (45) and (46) were derived under the assumption that two areas under the photopeaks of the γ-rays of 1173 and 1332 keV emitted from each ^{60}Co point source, $A_1^{[k]}$ and $A_2^{[k]}$ (k = 1 or 2), were equal because the detector was almost equally sensitive to both γ-rays.

Next we define 'Max(N - N_c)' and 'F_R(N - N_c)', when a detector does not have an equal response for both parts of the extended source, as follows,

$$Max(N - N_c) = \frac{A_{12}}{2} (\chi_1^{[1]} - \chi_1^{[2]})^2 , \tag{47}$$

and

$$F_R(N - N_c) = \frac{Max(N - N_c)}{N - N_c}$$

$$= \frac{(\beta + 1)^2}{2\beta} , \tag{48}$$

where

$$\frac{A_{12}^{[1]}}{A_{12}^{[2]}} = \beta > 0. \tag{49}$$

Max(N - N_c) is the upper bound of (N - N_c), and F_R(N - N_c) is the ratio of the upper bound of (N - N_c) to (N - N_c). Equations (45) ~ (49) are effective for the extended source formed by the combination

of two ^{60}Co point sources.

(3.1) Disintegration rate determined by the sum-peak method

(3.1.1) Equally responsive detector

In the case of an extended source which consists of two ^{60}Co point sources, equations (42) and (43) can be replaced by the following equation;

$$\chi_i^{[1]} - \chi_i^{[2]} = \left[\frac{(1-t_i^{[1]}) \times e_i^{[2]}}{(1-t_i^{[2]}) \times e_i^{[1]}} - 1 \right] \times \chi_i^{[2]}, \qquad (50)$$

where the subscript 'i' is 1 or 2. When the detector is equally responsive to the two point sources,

$$(\chi_1^{[1]} - \chi_1^{[2]}) = (\chi_2^{[1]} - \chi_2^{[2]}) = 0.$$

In consequence, the value of $(N - N_c)$ given by equation (45) must be zero regardless of the distribution of radioactivity as expected from Figs. 13 and 14.

(3.1.2) Not equally responsive detector

If equation (45) based on equation (41) is exactly effective for the extended source formed by the combination of two ^{60}Co point sources, the disintegration rate determined by the sum-peak method can be expressed by

$$N_c = N - \frac{A_{12}^{[1]} A_{12}^{[2]}}{A_{12}} (\chi_1^{[1]} - \chi_1^{[2]})^2, \qquad (51)$$

where

$$N = R^{[1]} + R^{[2]}, \qquad A_{12} = A_{12}^{[1]} + A_{12}^{[2]},$$

$$\chi_1^{[1]} = \frac{A_2^{[1]}}{A_{12}^{[1]}}, \qquad \text{and} \qquad \chi_1^{[2]} = \frac{A_2^{[2]}}{A_{12}^{[2]}}.$$

Figure 15 shows the relative disintegration rates calculated by equation (51) in the measurements (C), (D) and (E), in which the

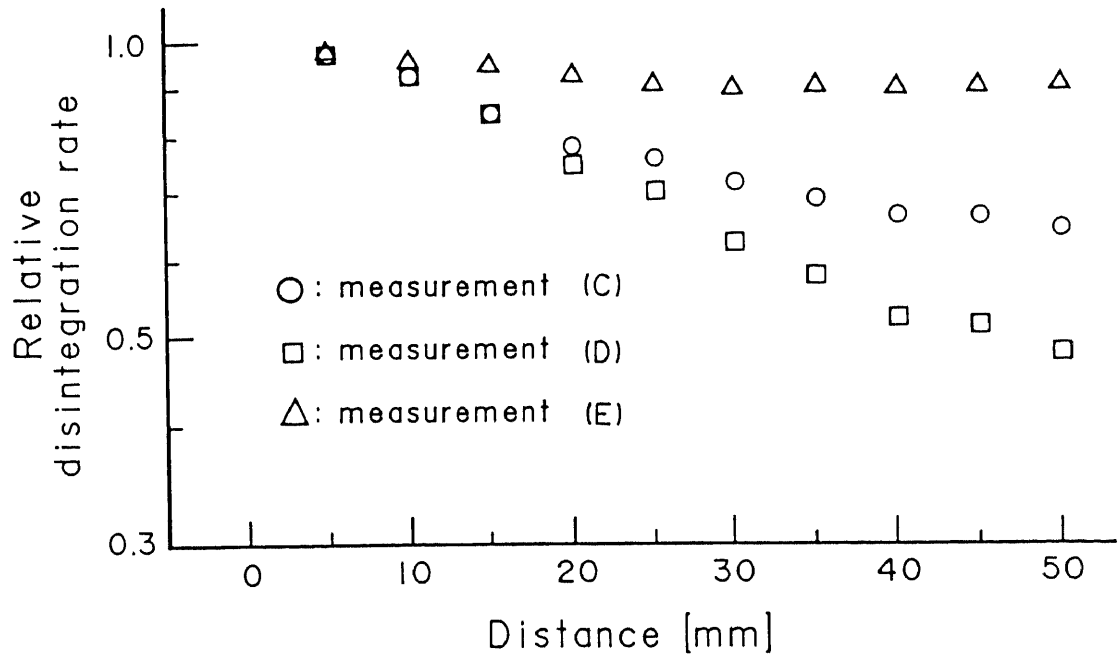

Fig. 15 Relative disintegration rate determined by the calculation of equation (51) with the measurements (C), (D) and (E). Circle, square and triangle : measurements (C), (D) and (E), respectively.

Table 2 Relative disintegration rates determined again by the least-squares fit to $Y = A \times e^{(B \times X)}$. exp. : based on the experiments of two point sources, and eq.(51) : based on the calculations of equation (51)

	Relative disintegration rate					
	(C)		(D)		(E)	
Distance(mm)	exp.	eq.(51)	exp.	eq.(51)	exp.	eq.(51)
5	0.97	0.94	1.03	0.98	1.03	0.96
10	0.93	0.90	0.93	0.90	1.01	0.95
15	0.88	0.86	0.84	0.83	0.99	0.95
20	0.84	0.82	0.76	0.76	0.97	0.94
25	0.80	0.78	0.69	0.70	0.95	0.93
30	0.76	0.75	0.63	0.64	0.94	0.93
35	0.72	0.71	0.57	0.59	0.92	0.92
40	0.69	0.68	0.52	0.54	0.90	0.91
45	0.66	0.65	0.47	0.50	0.89	0.91
50	0.63	0.62	0.42	0.46	0.87	0.90
Absolute difference	(1.8 ± 0.6) %		(2.2 ± 1.2) %		(2.7 ± 1.9) %	

detector has different efficiencies to the sources. We determined again the disintegration rates from two different data sets using the least-squares fit to $Y = A \times e^{(B \times X)}$ (Y : disintegration rate, X : distance, A and B : constant values). Then, one data set was based

on the experiments of two point sources (Figs. 13 and 14), and another set, the calculations of equation (51) (Fig. 15). Thus determined disintegration rates are given in Table 2, in which "exp." and "eq.(51)" correspond to the experiments of two point sources and the calculations of equation (51), respectively. Table 2 shows that the absolute differences between both disintegration rates determined based on "exp." and "eq.(51)" are (1.8 ± 0.6) %, (2.2 ± 1.2) % and (2.7 ± 1.9) % for the measurements (C), (D) and (E) in Fig. 12, respectively. These results indicate that the disintegration rates calculated by equation (51) (Fig. 15) are in good agreement with those determined by the sum-peak formula (15) (Figs. 13 and 14).

(3.2) Upper bound of error : Max($N - N_c$)

We have investigated the upper bound of the error estimated by Max($N - N_c$), by using $F_R(N - N_c)$, when the detector is not equally responsive for both point sources of the extended sources.

Differentiating equation (48), $F_R(N - N_c)$, with respect to β, we obtain;

$$\frac{dF_R(N - N_c)}{d\beta} = \frac{(\beta - 1)(\beta + 1)}{2\beta^2}, \tag{52}$$

and

$$\frac{d^2 F_R(N - N_c)}{d\beta^2} = \frac{1}{\beta^3} > 0.$$

Since the value of β is always positive, the $F_R(N - N_c)$ takes

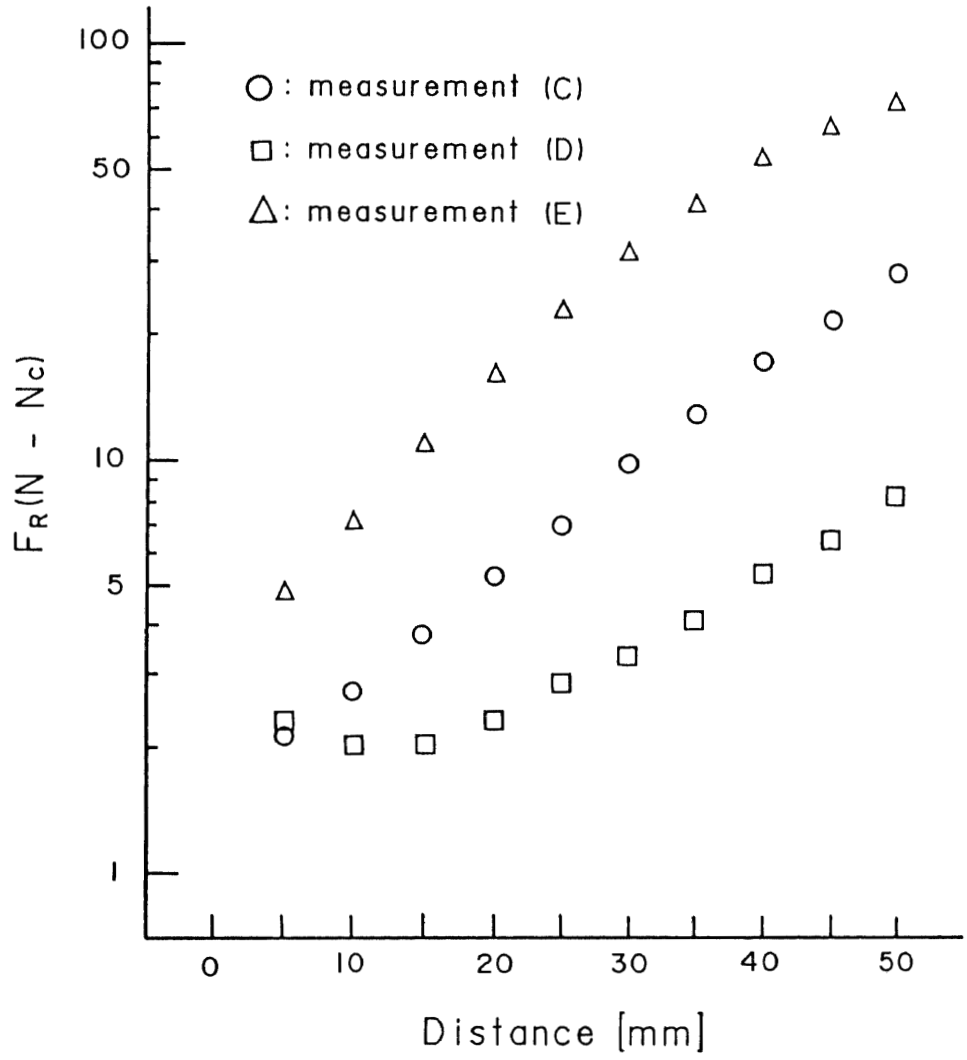

Fig. 16 Value of $F_R(N - N_c)$ when an extended source consists of two point sources. Circle, square and triangle : measurements (C), (D) and (E), respectively.

the minimum value of 2 when $\beta = 1$. In consequence, the error estimated by equation (47), $\mathrm{Max}(N - N_c)$, is at least twice as large as the true error, $(N - N_c)$. Figure 16 shows that the values of

$F_R(N - N_c)$ in the measurements (C), (D) and (E) as a function of the distance of the upper source from the detector surface. All the experimental values of $F_R(N - N_c)$ in Fig. 16 are larger than 2 as theoretically expected, although $F_R(N - N_c)$ has various values.

In an arbitrary extended source which can be divided into very small 'n' parts, noticing two very small parts, k-th and m-th, of all the parts and assuming an extended source composed of the k-th and m-th parts, equation (41) can be transformed as shown below;

$$N - N_c = \frac{1}{2A_{12}} \sum_i^{(k,m)} \sum_j A_{12}{}^i \, A_{12}{}^j \, (\chi_1{}^i - \chi_1{}^j)\,(\chi_2{}^i - \chi_2{}^j)$$

$$= \frac{A_{12}{}^{[k]} A_{12}{}^{[m]}}{A_{12}} (\chi_1{}^{[k]} - \chi_1{}^{[m]})(\chi_2{}^{[k]} - \chi_2{}^{[m]}).$$

In the above transformation of the equation, brackets are used to distinguish "k" and "m" standing for the definite two parts from "i" and "j". Removing those brackets and adopting a superscript of [k,m] meaning the extended source composed of the k-th and m-th parts, we have

$$(N - N_c)^{[k,m]} = \frac{A_{12}{}^k A_{12}{}^m}{A_{12}{}^k + A_{12}{}^m} (\chi_1{}^k - \chi_1{}^m)(\chi_2{}^k - \chi_2{}^m), \qquad (53)$$

and

$$\mathrm{Max}(N - N_c)^{[k,m]} = \frac{A_{12}{}^k + A_{12}{}^m}{2} (\chi_1{}^k - \chi_1{}^m)(\chi_2{}^k - \chi_2{}^m), \qquad (54)$$

where $(N - N_c)^{[k,m]}$ and $Max(N - N_c)^{[k,m]}$ are the error and the upper bound of the error when the sum-peak formula (15) is applied to an extended source composed of two very small parts (k-th and m-th parts) [*Appendix-4, 5*]. Defining $Max(N - N_c)^{arb}$ to be the upper bound of an error for the source formed by including all the 'n' parts, $A_{12}{}^{arb}$ is the total sum of $A_{12}{}^{j}$ (j=1 to n). The superscript 'arb' means an 'arbitrary' extended source. Thus

$$A_{12}{}^{k} + A_{12}{}^{m} \leq A_{12}{}^{arb},$$

and

$$(\chi_1{}^{k} - \chi_1{}^{m})(\chi_2{}^{k} - \chi_2{}^{m}) \leq (\chi_1{}^{max} - \chi_1{}^{min})(\chi_2{}^{max} - \chi_2{}^{min}).$$

Consequently,

$$Max(N - N_c)^{[k,m]} \leq \frac{A_{12}{}^{arb}}{2}(\chi_1{}^{max} - \chi_1{}^{min})(\chi_2{}^{max} - \chi_2{}^{min})$$

$$\leq Max(N - N_c)^{arb}.$$

Since $F_R(N - N_c) \geq 2$ when a source consists of two very small parts,

$$(N - N_c)^{[k,m]} \leq \frac{1}{2}Max(N - N_c)^{[k,m]} \leq \frac{1}{2}Max(N - N_c)^{arb}. \qquad (55)$$

By using equation (53) and inequality (55), we modify equation (41) as follows:

$$N - N_c = \frac{1}{2A_{12}{}^{arb}} \sum_{k}^{n} \sum_{m}^{n} A_{12}{}^{k} A_{12}{}^{m} (\chi_1{}^{k} - \chi_1{}^{m})(\chi_2{}^{k} - \chi_2{}^{m})$$

$$= \frac{1}{2A_{12}{}^{arb}} \sum_{k}^{n} \sum_{m}^{n} \frac{A_{12}{}^{k}\, A_{12}{}^{m}}{(A_{12}{}^{k}+A_{12}{}^{m})} (\chi_1{}^{k} - \chi_1{}^{m})(\chi_2{}^{k} - \chi_2{}^{m})(A_{12}{}^{k} + A_{12}{}^{m})$$

and substitute equation (53) into the above equation. Then we have

$$N - N_c = \frac{1}{2A_{12}{}^{arb}} \sum_{k}^{n} \sum_{m}^{n} (N - N_c)^{[k,m]} (A_{12}{}^{k} + A_{12}{}^{m}).$$

Substituting inequality (55), we have

$$N - N_c \leq \frac{1}{4A_{12}{}^{arb}} \mathrm{Max}(N - N_c)^{arb} \sum_{k}^{n} \sum_{m}^{n} (A_{12}{}^{k} + A_{12}{}^{m})$$

$$\leq \frac{\mathrm{Max}(N - N_c)^{arb}}{2}.$$

Hence

$$2(N - N_c) \leq \mathrm{Max}(N - N_c)^{arb}.$$

It can be concluded that the upper bound of the error, $\mathrm{Max}(N - N_c)^{arb}$, is at least twice larger than the true error, $(N - N_c)$, in an arbitrary extended source. Consequently, equation (44) must be corrected to following relation

$$N - N_c \leq \frac{1}{4} A_{12} (\chi_1{}^{max} - \chi_1{}^{min})(\chi_2{}^{max} - \chi_2{}^{min}). \qquad (56)$$

This relation can be effective for any arbitrary extended source of ^{60}Co.

(3.3) Upper bound of error in the general case

Relation (56) was proved by using inequality $F_R(N - N_c) \geq 2$.

However, this inequality was derived when the areas under the photopeaks of both γ-rays of 1173 and 1332 keV were equal. In this section, it will be proved that equation (56) is effective in the case in which both photopeak areas are not equal.

Supposing that an extended source is composed of two point sources noted k and m, equations (53) and (54) are effective in general. Consequently [*Appendix-6*],

$$F_R(N - N_c)^{[k,m]} = \frac{Max(N - N_c)^{[k,m]}}{(N - N_c)^{[k,m]}}$$

$$= \frac{[A_{12}{}^k + A_{12}{}^m]^2}{2A_{12}{}^k A_{12}{}^m}$$

$$= 2 + \frac{[A_{12}{}^k - A_{12}{}^m]^2}{2A_{12}{}^k A_{12}{}^m}.$$

Hence,

$$F_R(N - N_c)^{[k,m]} > 2,$$

and

$$Max(N - N_c)^{[k,m]} > 2(N - N_c)^{[k,m]}.$$

In consequence

$$N - N_c < \frac{1}{4} A_{12}(\chi_1{}^{max} - \chi_1{}^{min})(\chi_2{}^{max} - \chi_2{}^{min}). \quad (57)$$

Equation (57) coincides with equation (56) except for the case of β = 1 (meaning $A_{12}{}^{[k]} = A_{12}{}^{[m]}$). When $A_{12}{}^{[k]}$ is not equal to $A_{12}{}^{[m]}$ under the condition that the photoelectric efficiencies of the two

coincident γ-rays (γ_1 and γ_2) are different, equation (56) must be replaced by equation (57).

§5. Studies of Various Practical Effects in the Sum-peak Methods

Based on the theory of the sum-peak method, the disintegration rate of a ^{60}Co point source including a very small source can be determined with a direct calculation of the sum-peak formula (15) and an error caused when the sum-peak method is applied to an extended source such as a bulky source can be estimated by using equation (41). Nevertheless, there are many cases in which the sum-peak method gives an underestimated disintegration rate with a large error even for a point source and also there are cases in which the error caused in an extended source can not be estimated by using equation (41). Such inconsistency seems to be due to some practical causes on measurements[38,51].

In the sum-peak method, the disintegration rate of a source is determined by the sum-peak formula using only areas under the photopeaks, the sum peak and the entire spectrum measured from a pulse height spectrum. The accuracy of a determined disintegration rate depends on the precise measurements of these areas. In the case of ^{60}Co, the sum-peak formula is given by

$$N = T + \frac{A_1 \times A_2}{A_{12}}, \qquad (15)$$

where N, T, A_1, A_2 and A_{12} stand for a disintegration rate, the entire area of a spectrum, the photopeak area of γ_1 (1173 keV), the photopeak area of γ_2 (1332 keV) and the sum peak area (2505 keV),

respectively. Since the contribution of T to N is relatively small as discussed in §2.(3) (see p.19) and as given in Table 1, the accuracy of N calculated by formula (15) is dependent dominantly on errors associated with A_1, A_2 and A_{12}. It is desirable to measure these areas as accurately as possible when the sum-peak method is applied for radioactivity determination.

In an actual ^{60}Co spectrum obtained using a NaI(Tl) detector, it is not easy to determine exact photopeak areas because of partial overlapping of two photopeaks. This overlapping causes an underestimate of the photopeak areas when they are determined based on the total peak area method. As a result the sum-peak formula gives an underestimated disintegration rate. In section *1* of this chapter, this problem is investigated and a precise method to determine the photopeak areas is proposed and verified through experiments using a ^{60}Co point source.

Another problem investigated in this chapter is concerned with the sum peak area. In a ^{60}Co spectrum, the sum peak appears at 2505 keV. Unfortunately, a photopeak due to ^{208}Tl appears at 2614 keV because ^{208}Tl is one of naturally occurring radionuclides in the thorium series[52] and becomes a background source. Therefore, a part of the area attributed to Compton scattering of the γ-ray emitted from ^{208}Tl superposes on the sum peak area of ^{60}Co. This superposition causes the underestimation of a disintegration rate calculated by formula (15) due to an overestimate of the sum peak area. We note, however, that the effect due to superposition can be negligible when

a count rate of the sum peak is reasonably large. In sections 2 and 3 of this chapter, using bulky sources and point sources of various radioactivity levels, we will examine the cases in which the effect due to superposition can not be negligible.

1. Photopeak counting rates

(1) Experimental Procedure

The sum-peak method used for a point source can not be affected by a source-to-detector geometry. The source-to-detector geometry is varied by changing the distance between a source and a detector and the displacement between the source and the center axis of the detector. Therefore, if the sum-peak method is effective, the true disintegration rate can be determined independent of the distance and displacement. In this section, the effects of the distance and displacement on the disintegration rate of a ^{60}Co point source determined by the sum-peak method are investigated. It can be shown that the sum-peak method is perfectly effective for the determination of the disintegration rate of a ^{60}Co point source when the photopeak areas under the two photopeaks are determined by the precise method. In this method the area attributed to Compton scattering of γ_2 under that of γ_1 is eliminated by using a spectrum of a ^{22}Na point source.

(a) Measuring arrangement

The arrangement of a measuring system is shown in Fig. 17. Measurements of spectra were performed for a ^{60}Co point source of

1.4 $\times 10^5$ Bq. With the source located at several positions over the NaI(Tl) detector, measurements of γ-ray spectra were carried out. Those positions of the source are schematically shown in Figs. 18(A) and (B). In the case of (A), the position of the source was varied upward from the surface of the NaI(Tl) detector along the center axis

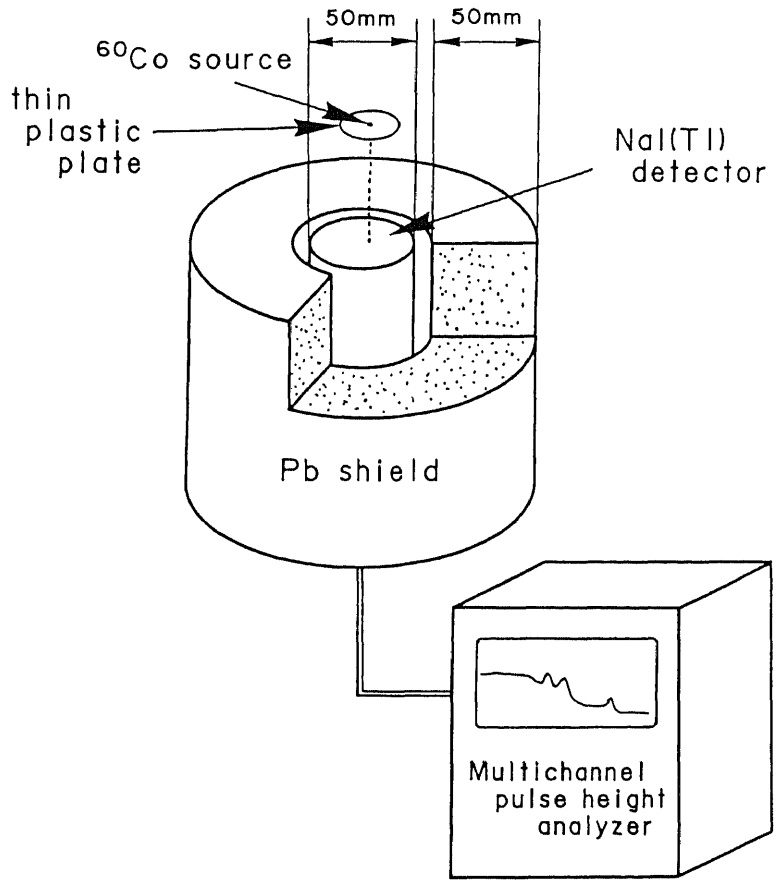

Fig. 17 Arrangement of γ-ray measuring system with a NaI(Tl) detector and a ^{60}Co point source.

of the detector at an interval of 5 mm. In this arrangement the effect of the disintegration rate calculated by the sum-peak formula

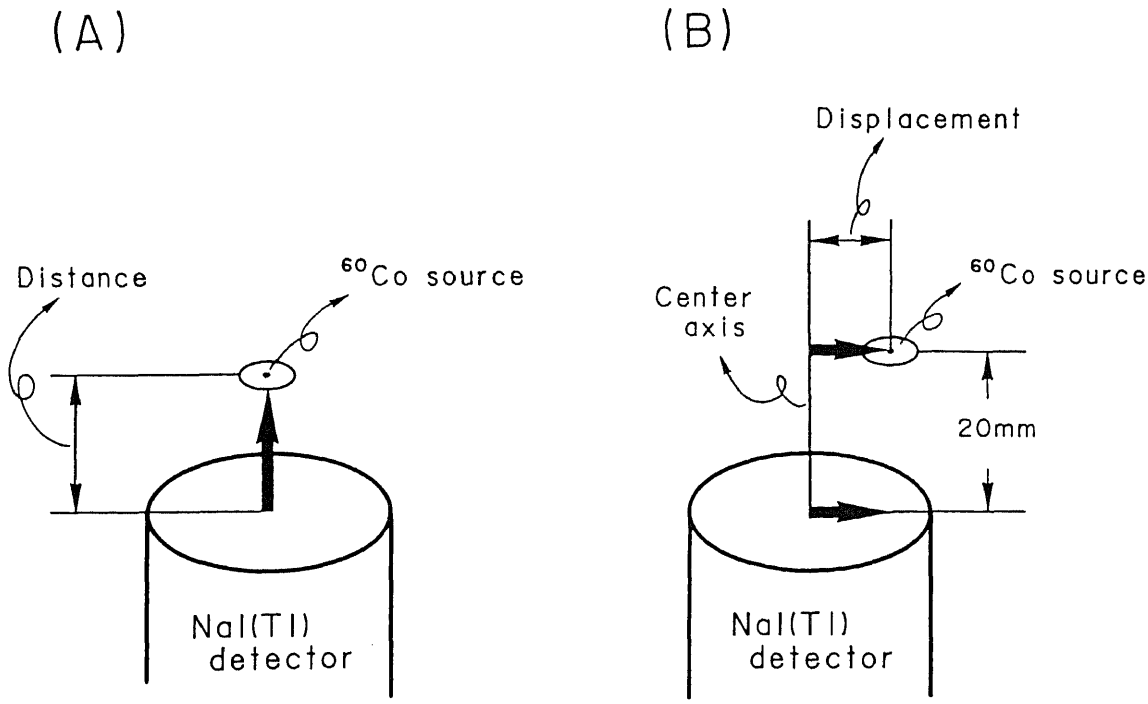

Fig. 18 Situation between a NaI(Tl) detector and a ^{60}Co point source in measurements.

could be studied as a function of the vertical "distance" from the source to the surface of the NaI(Tl) detector. In the case of (B), the source position was varied at every 5 mm within 20 mm along either of the two lines parallel to the surface of the detector. One line was on the surface of the detector and the other was at a height of 20 mm. In this case the calculated disintegration rate could be examined as a function of the horizontal displacement from the source to the center axis of the detector.

(b) Sum-peak method for a ^{60}Co source

A typical spectrum of the ^{60}Co point source is shown in Fig. 19. In the spectrum, two photopeaks of 1173 and 1332 keV γ-rays from the source, and their sum peaks (1173 + 1332 = 2505 keV) can be observed[39,40,41]. If one can measure the exact areas under the whole spectrum (T), the photopeaks (A_1 and A_2) and the sum peak (A_{12}) by a

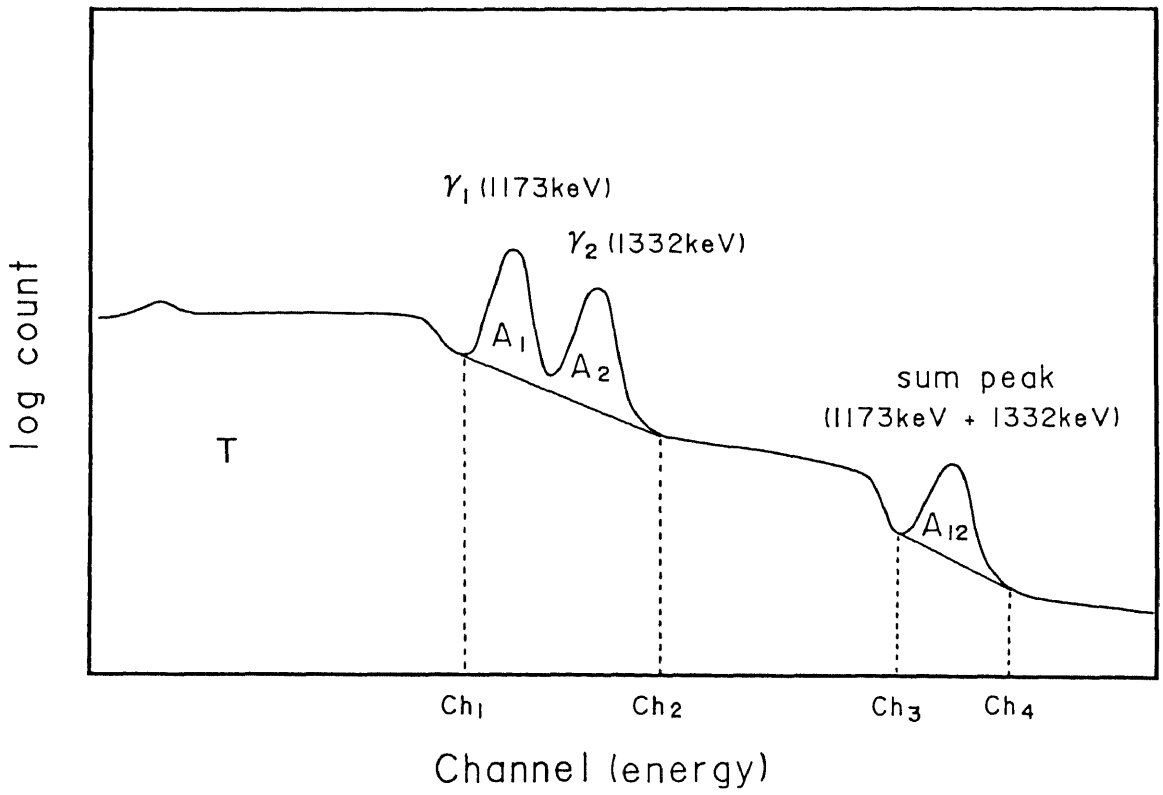

Fig. 19 Typical γ-ray spectrum of ^{60}Co as measured with a NaI(Tl) detector. A_1 : the area under the photopeak of γ_1, A_2 : the area under the photopeak of γ_2, A_{12} : the area under the sum peak, and T : the area under the whole spectrum.

proper method, the disintegration rate N of the source can be calculated by the sum-peak formula (15)[53]. In the present experiment, T was calculated by the following equation

$$T = I_T - B_T, \tag{58}$$

where I_T and B_T are the entire area and the background area under the whole spectrum, respectively. Then, assuming that A_1 was equal to A_2 because the detector was considered to be almost equally sensitive to γ-rays of both 1173 keV and 1332 keV, the areas of A_1, A_2 and A_{12} were calculated by the following equations based on the total peak area method[54,55]:

$$A_1 = A_2 = \frac{1}{2}\left\{ I_{1+2} - \frac{1}{2}(Ch_2 - Ch_1 + 1)(C_2 + C_1) \right\}, \tag{59}$$

and

$$A_{12} = I_{12} - \frac{1}{2}(Ch_4 - Ch_3 + 1)(C_4 + C_3), \tag{60}$$

where

I_{1+2} : the total area under the two photopeaks, γ_1 and γ_2 (between Ch_1 and Ch_2 in Fig. 19),

Ch_1 and Ch_2 : the starting channel of γ_1 and the last channel of γ_2,

C_1 and C_2 : the numbers of counts in channels Ch_1 and Ch_2,

I_{12} : the total area under the sum peak (between Ch_3 and Ch_4 in Fig. 19),

Ch_3 and Ch_4 : the starting channel and the last channel of the sum peak,

and

C_3 and C_4 : the numbers of counts in channels Ch_3 and Ch_4.

(2) Results and Discussion

Figure 20 shows the relative disintegration rate calculated by the sum-peak formula as a function of the distance between the source and the NaI(Tl) detector as denoted by white circles. The relative disintegration rate is defined by the ratio of the calculated disintegration rate to the true disintegration rate. The photopeak area was obtained by using equation (59). The standard deviations of the results were all less than 1 %. White square points will be explained later. The true disintegration rate can be described by a horizontal line with a value of 1, as shown by the dotted line in Fig. 20. Figure 20 shows that the relative disintegration rate calculated by the sum-peak formula decreased slightly with increasing distance. This seems to be owing to the directional correlation of two γ-rays. However, ignoring the change within 0.05 in the relative value, it was considered that the disintegration rate was underestimated by about 0.3 in the relative value when compared with the true disintegration rate. The distance dependence of the disintegration rates calculated by the sum-peak formula was rather small. Figure 21 shows the disintegration rates

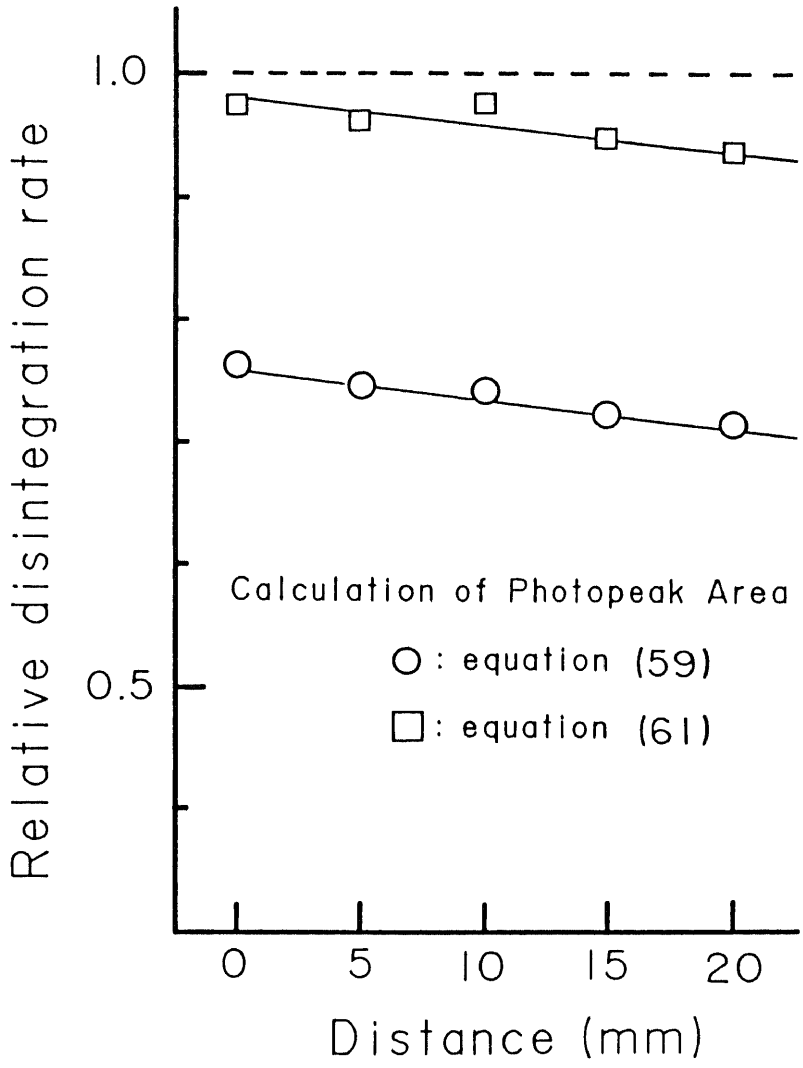

Fig. 20 Effect of the distance on the disintegration rate determined by the sum-peak method. Circle : in the case that the areas under the photopeaks were derived by equation (59), and square : in the case that the areas under the photopeaks were derived by equation (61) instead of (59).

as a function of the displacement, indicated by white and black circles just the same as in Fig. 20. The photopeak area was obtained by using equation (59). The standard deviations of these results were

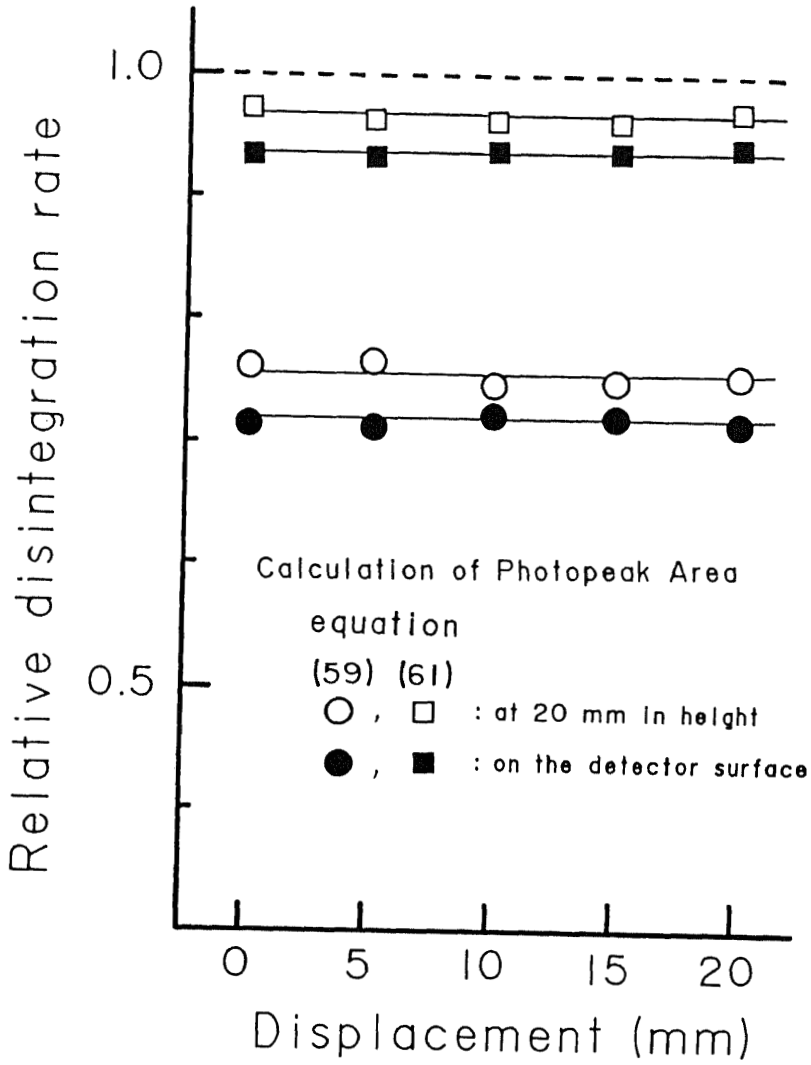

Fig. 21 Effect of the displacement on the disintegration rates determined by the sum-peak method. White and black circles : in the case that the areas under the photopeaks were derived by equation (59) for a ^{60}Co point source on the detector surface and at high position of 20 mm from the surface, white and black squares : in the case that the areas under the photopeaks were derived by formula (61) instead of (59) for a ^{60}Co point source on the detector surface and at high position of 20 mm from the surface.

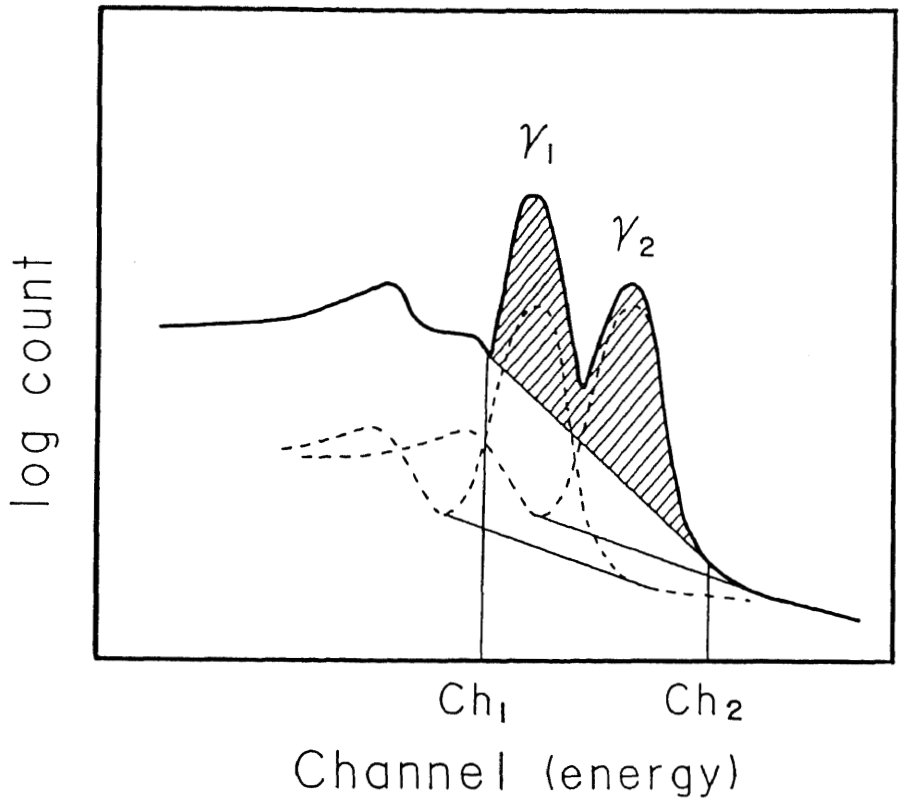

Fig. 22 Overlap of both the areas under the photopeaks of γ_1 and γ_2, and that of those under photopeak γ_1 and Compton scattering of γ_2 in a spectrum of ^{60}Co.

all less than 1 %. White and black square points will be explained later. Figure 21 shows that the relative disintegration rates calculated by the sum-peak formula are essentially constant independently of the displacement within 20 mm along the two lines, but were underestimated by about 0.3, as in the case of Fig. 20. These three lines of the disintegration rates calculated by the sum-peak formula shown in Figs. 20 and 21 were quite different from the true disintegration rate.

We presumed that these underestimates of the disintegration

rates were caused by the underestimation of the areas under the photopeaks, A_1 and A_2. Figure 22 shows schematically the two expanded photopeaks in the ^{60}Co spectrum. In Fig. 22, the shaded part is the area under two photopeaks calculated by equation (59), which is definitely smaller than the true area because the area calculated by equation (59) does not contain the lower parts of the true areas under the photopeaks, γ_1 and γ_2. Consequently, we proposed a precise method of the derivation of the areas under the photopeaks from the spectra of ^{60}Co.

In a ^{60}Co spectrum obtained by a NaI(Tl) detector, the two photopeaks overlap somewhat and a part of the area under Compton scattering of γ_2 also overlaps under the photopeak of γ_1, as shown in Fig. 22. We determined the ratio of the area attributed to Compton scattering of γ_2 under the photopeak of γ_1 to A_2 by using the spectrum of a γ-ray (1275 keV) emitted from a ^{22}Na point source[42,43] with a radioactivity of 1.6×10^4 Bq. And in this connection, spectra of ^{22}Na were obtained under the same measuring conditions as those of ^{60}Co [*Appendix*-7]. In the precise method, the areas under photopeaks A_1 and A_2 can be calculated by the following equation[45] instead of equation (59). That is,

$$I_{1+2} = A_1 + A_2(1 + \alpha) + B_s,$$

where

I_{1+2} : the total area under the two photopeaks, γ_1 and γ_2,

B_s : the background area under the two photopeaks, γ_1 and γ_2,

α : the ratio of the area attributed to Compton scattering of γ_2 under the photopeak of γ_1 to A_2.

Assuming that A_1 is equal to A_2, we have

$$I_{1+2} = A_1(2 + \alpha) + B_s$$

or

$$= A_2(2 + \alpha) + B_s .$$

By rearranging either of these equations, we get the following equation[45]:

$$A_1 = A_2 = \frac{(I_{1+2} - B_s)}{(2 + \alpha)} . \qquad (61)$$

The disintegration rates determined by the sum-peak formula (15) with the areas derived by equations (58), (61) and (60) are shown by the white squares in Fig. 20, and the white and black squares in Fig. 21. The standard deviations of these results were all less than 1 %. These squares are found near the bold dotted lines corresponding to the true disintegration rate, and show the relative disintegration rates of more than 0.9. These results suggest that we can obtain more exact areas under the photopeaks by equation (61) instead of equation (59) and that the sum-peak method is perfectly effective for the determination of the disintegration rate of a ^{60}Co point source when the areas under the whole spectrum, the photopeaks and the sum peak are determined by equations (58), (61) and (60), respectively.

2. Source intensity

(1) Experimental Procedure

The arrangement of a measuring system is shown in Fig. 23. Polyethylene bottles used were just the same as those used as bulky sources in §3.2. Three bulky sources with different radioactivities were prepared by pouring solutions of ^{60}Co of 1.1×10^4 Bq, 1.1×10^3

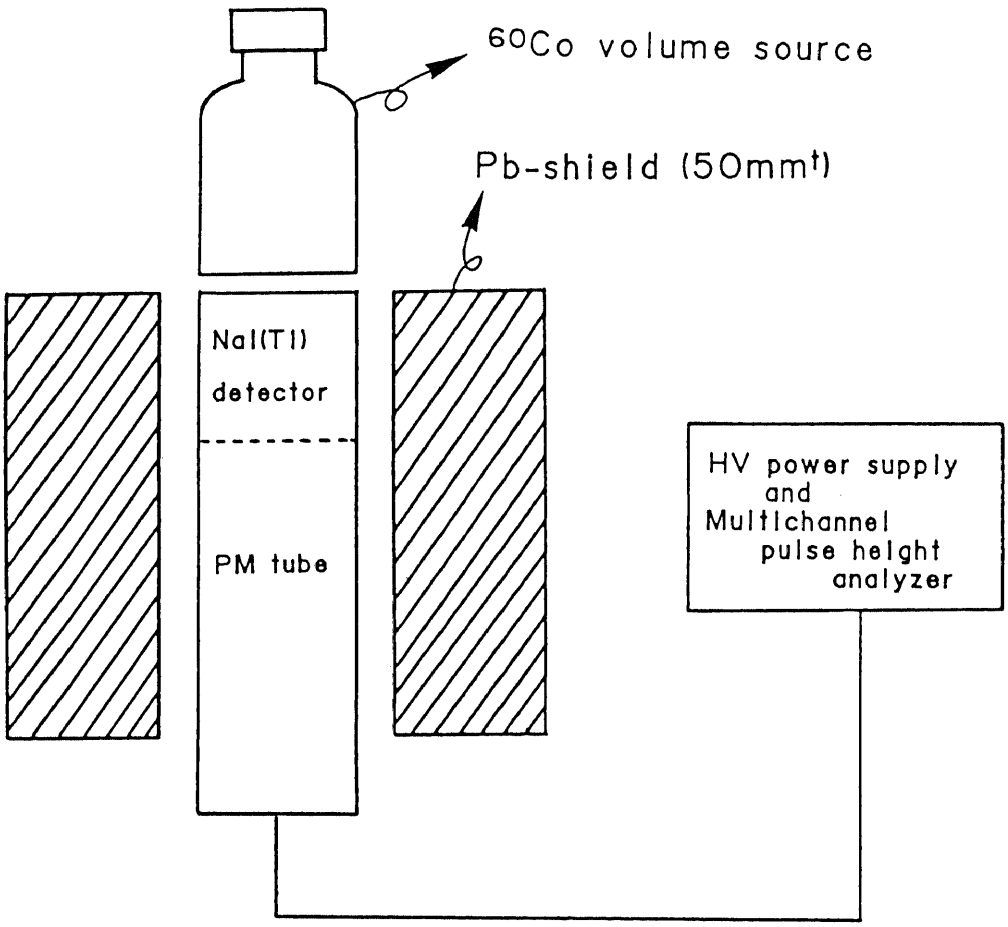

Fig. 23 Arrangement of a γ-ray measuring system and a bulky source (a ^{60}Co volume source).

Bq and 1.1×10^2 Bq into three bottles. The volume of the solution in each bottle was varied by successive dilution from 10 to 100 mℓ. The disintegration rates of these bulky sources were determined based on the sum-peak method by using the photopeak areas, the sum peak area and the entire area obtained by equations (24), (25) and (26) given in §2.(4).

(2) Results

Figure 24 shows the relative disintegration rate calculated by the sum-peak formula (15) as a function of the volume of the ^{60}Co solution in the bottle. The relative disintegration rate is defined by the ratio of the disintegration rate calculated by the sum-peak formula to the true disintegration rate. The standard deviations of these results were all smaller than 2 %. The relative disintegration rate decreases as the volume of the ^{60}Co solution in the bottle increases. The lower the true disintegration rates, the smaller the relative disintegration rates calculated by the sum-peak formula. These experimental results show that the increase of the volume of the bulky source and the decrease of the true disintegration rate make deviations larger between the calculated and true disintegration rates. In the case of the 1.1×10^4 Bq source the relative disintegration rate is nearly equal to 1 at 10 mℓ, and decreases to about 0.7 at 100 mℓ. In the cases of the 1.1×10^3 Bq and 1.1×10^2 Bq sources the relative disintegration rates are respectively about 0.8 and 0.4 for the volume of 10 mℓ and they are substantially lower

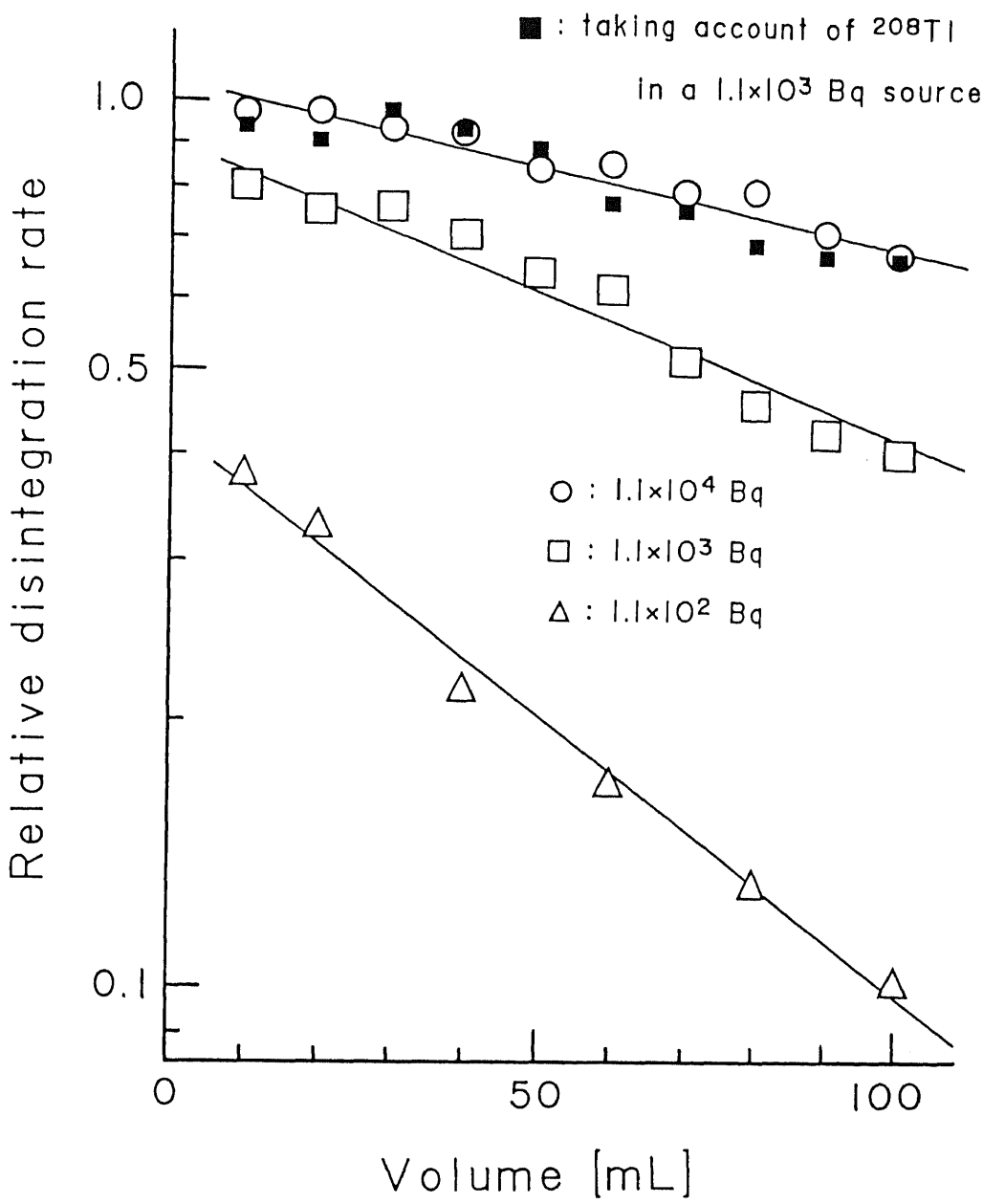

Fig. 24 Effect of volume and radioactivity on the disintegration rate of the bulky sources determined by the sum-peak method; circle : 1.1×10^4 Bq source, square : 1.1×10^3 Bq source, triangle : 1.1×10^2 Bq source, black square : results taking account of the effect of Compton scattering of ^{208}Tl.

than 1. The reduction rate of the calculated disintegration rate with the volume seems to be noticeably higher compared with that of the 1.1 × 10^4 Bq source. We think the larger reduction in the calculated rate for the weaker sources seems to be due to the fact that the exact areas could not be obtained when the count rates decreased.

(3) Discussion

If the disintegration rates of extended sources of ^{60}Co were exactly determined by the sum-peak method, the relative disintegration rates determined in the present experiment must be unity (=1) independent of the volume. However, the practically determined disintegration rates of the ^{60}Co bulky sources, except for the 1.1 × 10^4 Bq source with a smaller volume (~10 mℓ), deviate largely from the true disintegration rates as shown in Fig. 24. One of the causes of deviations was already demonstrated in §3 and §4. The disintegration rates of point or very small sources are precisely determined by the sum-peak method. On the other hand those of extended sources which could not be regarded as points are not precisely determined and deviations from the true rates were calculated from equations (40) or (41). The bold line running through circles in Fig. 24 was determined based on equation (39) (corresponding to the second term of equation (40)) which is the same curve shown in Fig. 10 (dotted curve). It is very consistent with the data point of the 1.1 × 10^4 Bq source, but not with those of the two other sources. It is concluded that equations (40) and (41) can explain the deviation of

the determined disintegration rates by the sum-peak method from the true disintegration rate for the 1.1×10^4 Bq source, but not for the other weaker sources. This experimental fact suggests that equations (40) and (41) are not sufficient to explain the underestimation of the disintegration rates determined by the sum-peak method in the cases of the 1.1×10^3 Bq and the 1.1×10^2 Bq sources. Apparently there exist some other reasons. To clarify the cause, we made a detailed investigation of the spectra obtained by the present measurements.

Figure 25 shows the variation of the areas per 1 Bq under the photopeak (1173 keV or 1332 keV) and that under the sum peak as a function of the true disintegration rate at each volume. The areas are normalized to those of the 1.1×10^4 Bq source with the volume of 10 mℓ, in which the relative disintegration rate calculated by the sum-peak formula (15) was almost equal to unity as shown in Fig. 24. We define the normalized areas under the photopeak and sum peak, A_{pn} and A_{sn}, respectively by the following relations;

$$A_{pn} = \frac{(A_p / A_r)}{(A_{p0} / A_{r0})}, \tag{62}$$

and

$$A_{sn} = \frac{(A_s / A_r)}{(A_{s0} / A_{r0})}, \tag{63}$$

where, A_p (A_s) and A_r are respectively the areas under the photopeak (sum peak) and the true disintegration rate of the ^{60}Co bulky source, A_{p0} (A_{s0}) is the area under the photopeak (sum peak) of the 1.1×10^4

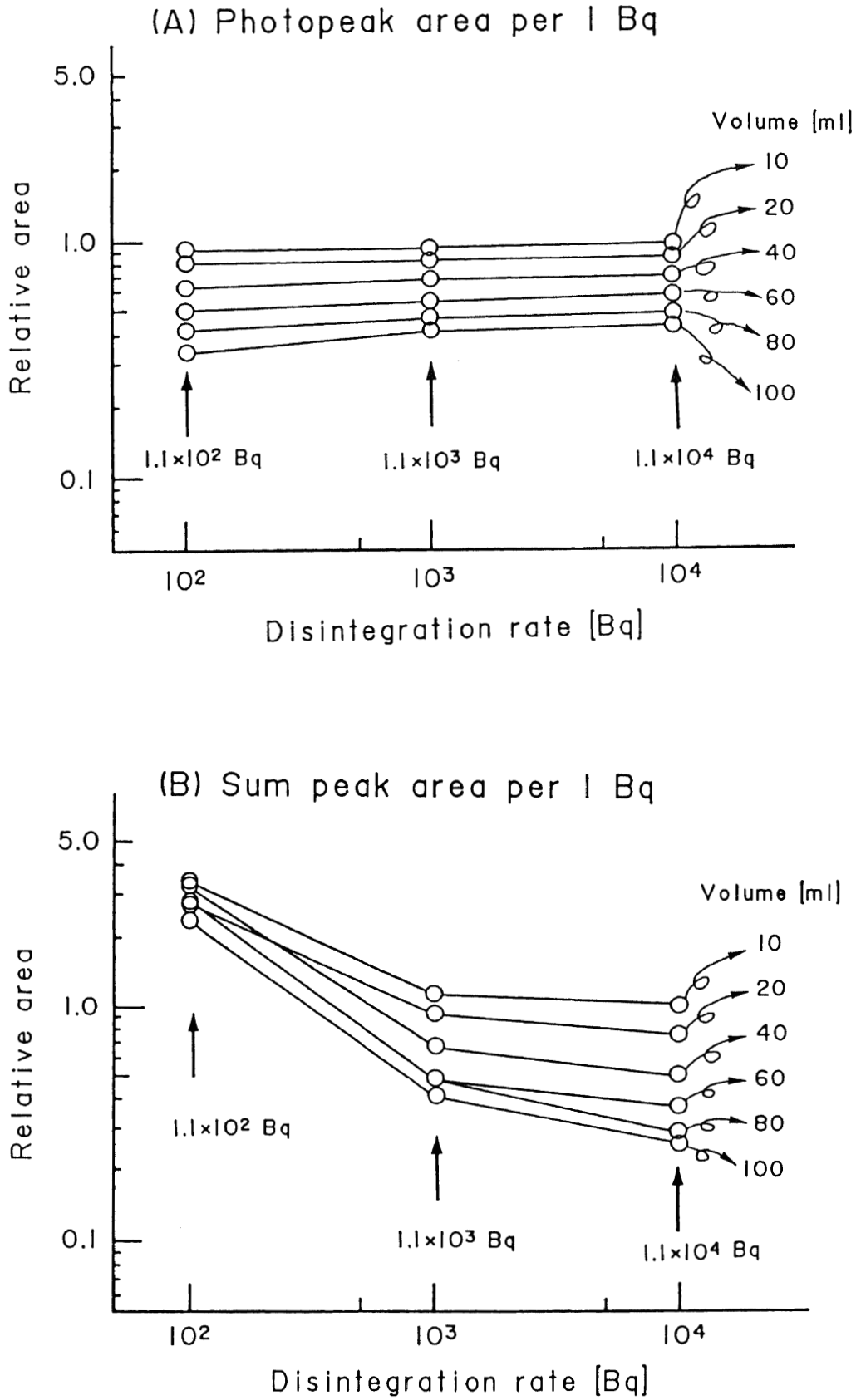

Fig. 25 Effect of volume and radioactivity on the areas under the photopeak and the sum peak.

Bq source with the volume of 10 mℓ, and A_{r0} is 1.1×10^4 Bq. The standard deviations of the photopeak and sum peak areas per 1Bq thus determined were smaller than 2 % and 3 %, respectively.

In Fig. 25(A), six curves are shown for the ^{60}Co bulky sources with different volumes of 10, 20, 40, 60, 80 and 100 mℓ. The slope does not vary appreciably as a function of the true disintegration rate. The curves for larger volumes give smaller relative areas. At the respective volume, the standard deviation of three areas per 1 Bq for three sources were about 10 % or less. These results indicate that the areas per 1 Bq under the photopeaks, A_{pn}'s, are not significantly affected by the source radioactivity, and hence the areas under the photopeaks are almost proportional to the magnitudes of the true disintegration rates if the volumes are fixed.

Figure 25(B) shows the areas per 1 Bq under the sum peaks, A_{sn}'s. The areas are smaller for the larger volume sources as are those under the photopeaks. On the other hand, unlike the case of the photopeak the areas under the sum peaks depend strongly upon the radioactivity level. They are estimated to be very large at the lower disintegration rates. In fact, Fig. 25(B) shows that the areas per 1 Bq under the sum peaks for the 1.1×10^2 Bq source are more than three times larger when compared with those for the 1.1×10^4 Bq source for each volume.

We presumed that the overestimation of the areas per 1 Bq under the sum peaks might be caused by ^{208}Tl which is one of naturally occurring radionuclides in the thorium series[52]. The

nuclide of ^{208}Tl emits γ-rays of 2614 keV, which is a little larger than the sum peak energy (1173 keV + 1332 keV = 2505 keV). The area attributed to Compton scattering of the γ-ray (2614 keV) from ^{208}Tl must creep into under the sum peak in the ^{60}Co spectrum. We assumed that taking account of the effect of ^{208}Tl on the sum peaks in the ^{60}Co spectra, the area per 1 Bq under the sum peak for the 1.1×10^4 Bq source should be equal to that for the 1.1×10^3 Bq and 1.1×10^2 Bq sources at a given volume. Namely,

$$\frac{(A_{s1,v} - \xi)}{A_{r1}} = \frac{(A_{s2,v} - \xi)}{A_{r2}}, \qquad (64)$$

where,

$$A_{r1} = 1.1 \times 10^4 \text{ Bq},$$

and

$$A_{r2} = 1.1 \times 10^3 \text{ Bq} \quad \text{or} \quad 1.1 \times 10^2 \text{ Bq},$$

where $A_{s1,v}$ is the area per 1 Bq under the sum peak for the 1.1×10^4 Bq source with the volume 'v', and $A_{s2,v}$ is that of either the 1.1×10^3 Bq or the 1.1×10^2 Bq source with the same volume 'v'. ξ is the area attributed to Compton scattering from ^{208}Tl under the sum peak. Substituting the numerical values of A_{r1} and A_{r2} into equation (64), and rearranging it, the following equations can be obtained. In the case of the 1.1×10^3 Bq source,

$$\xi = \frac{10}{9} \times A_{s2,v} - \frac{1}{9} \times A_{s1,v}, \qquad (65)$$

and in the case of the 1.1×10^2 Bq source,

$$\xi = \frac{100}{99} \times A_{s2,v} - \frac{1}{99} \times A_{s1,v}. \qquad (66)$$

The area attributed to the Compton scattering of ^{208}Tl under the sum peak was determined to be (0.097 ± 0.024) cps by calculations of equations (65) and (66) by taking into account all of the areas under the sum peaks obtained in the present measurements. This count rate is a few percent of those under the sum peaks of the 1.1×10^4 Bq source, whereas in the cases of the 1.1×10^3 Bq and 1.1×10^2 Bq sources, it is from 17 % to 45 % and from 57 % to 81 %, respectively.

Taking into account the background contribution from ^{208}Tl, equation (26) can be modified to the following equation,

$$A_{12} = I_{12} - \frac{1}{2} \times (Ch_4 - Ch_3 + 1)(C_4 + C_3) - \xi. \qquad (67)$$

The small black squares shown in Fig. 24 are the results for the 1.1×10^3 Bq source obtained by using equation (67). They are very consistent with the data points of the 1.1×10^4 Bq source and also with the solid curve calculated by equation (39). Applying the least-squares fit to $Y = A \times e^{(B \times X)}$ (X : volume, Y : disintegration rate, A and B : constant values), we determined again the relative disintegration rates from two different data sets shown by circles and black squares in Fig. 24. Two relative disintegration rates thus determined at the same volumes (10, 20, ... 100 mℓ) were consistent within the absolute difference of (2.6 ± 0.8) %.

We conclude as follows. If the count rates under the sum peaks of ^{60}Co sources are substantially larger than 0.1 cps as in the case of the 1.1×10^4 Bq source, the effect of the Compton scattering of the 2614 keV γ-ray from ^{208}Tl on the sum peak of ^{60}Co can be ignored. On the other hand, in the cases such as the 1.1×10^3 Bq and 1.1×10^2 Bq sources, the count rates under the sum peaks are not so large in comparison with 0.1 cps and the disintegration rates determined by the sum-peak method are underestimated without the correction for the effect of ^{208}Tl. Due to this effect of ^{208}Tl, the data points of the 1.1×10^3 Bq and 1.1×10^2 Bq sources in Fig. 24 are substantially reduced compared with those of the 1.1×10^4 Bq source.

3. Absorber thickness

(1) Experimental Procedure

The arrangement of a measuring system is shown in Fig. 26. In the arrangement, a ^{60}Co point source was kept in a lead container. We used two ^{60}Co point sources with radioactivities of 3.0×10^4 Bq and 3.5×10^5 Bq. Lead containers with several thicknesses (3, 6, 9, 15, 21, 27 and 33 mm) were adopted in the experiment; these were made by rolling a lead sheet of 3 mm in thickness, 1 to 11 times around a source holder in order to simulate solid lead containers. A NaI(Tl) detector was placed close to the outside surface of the

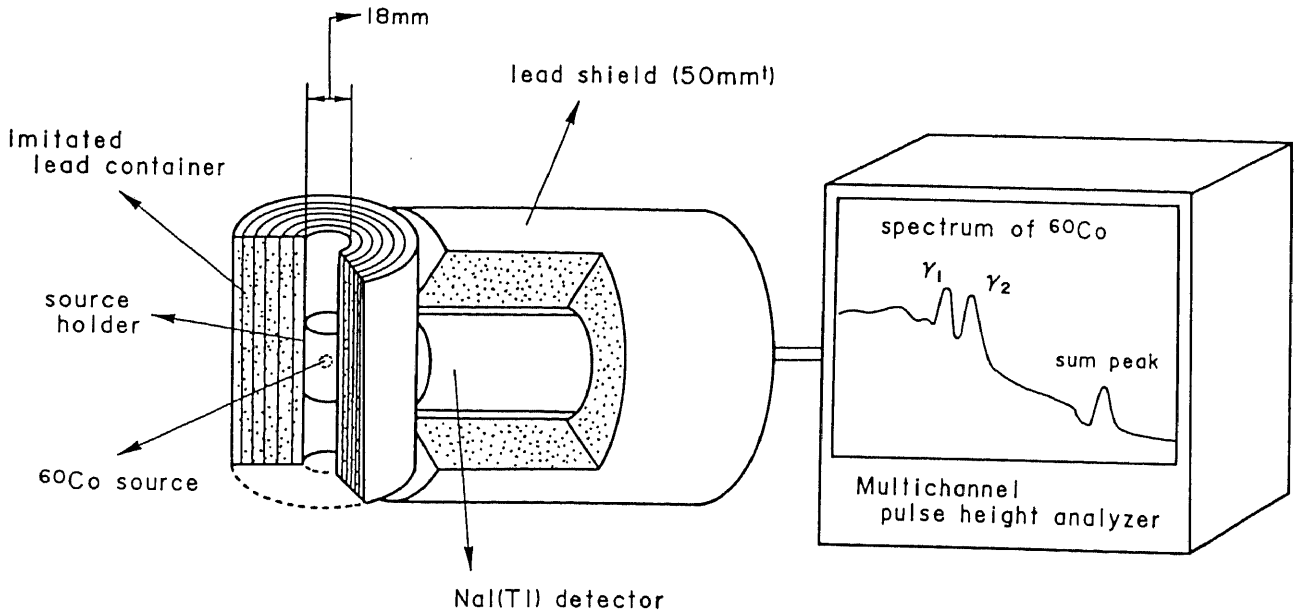

Fig. 26 Arrangement of γ-ray measuring system; a ^{60}Co point source, a lead shielding container, a NaI(Tl) detector and a multichannel pulse height analyzer.

container as shown in Fig. 26. Therefore, the distance between the source and the detector was obtained by adding 9 mm (the radius of a central hole of the container) to the thickness of the lead container. The disintegration rates of these sources were calculated by the sum-peak formula with the areas derived from the spectra by equations (24), (25) and (26) in §2.(4).

(2) Results

The disintegration rates and the photopeak areas were calculated by the sum-peak formula (15) and equation (25), respectively. Figure 27 shows results for the two ^{60}Co point sources as a function of the thickness of the lead container. In Fig. 27 the relative disintegration rates are the ratios of the disintegration rates calculated by the sum-peak formula to the true disintegration rates, and the relative areas are the ratios of the areas under the photopeak calculated by equation (25) to those measured without the lead container. When the disintegration rates determined by the sum-peak method were exactly equal to the true disintegration rates, the relative disintegration rates were unity, as indicated by the solid line in Fig. 27. The standard deviations of the disintegration rates and the photopeak areas shown in Fig. 27 were less than 2 % and less than 0.1 %, respectively.

For the 3.5×10^5 Bq source, Fig. 27 shows that the relative disintegration rates calculated by the sum-peak formula were almost equal to unity and did not significantly change with the thickness

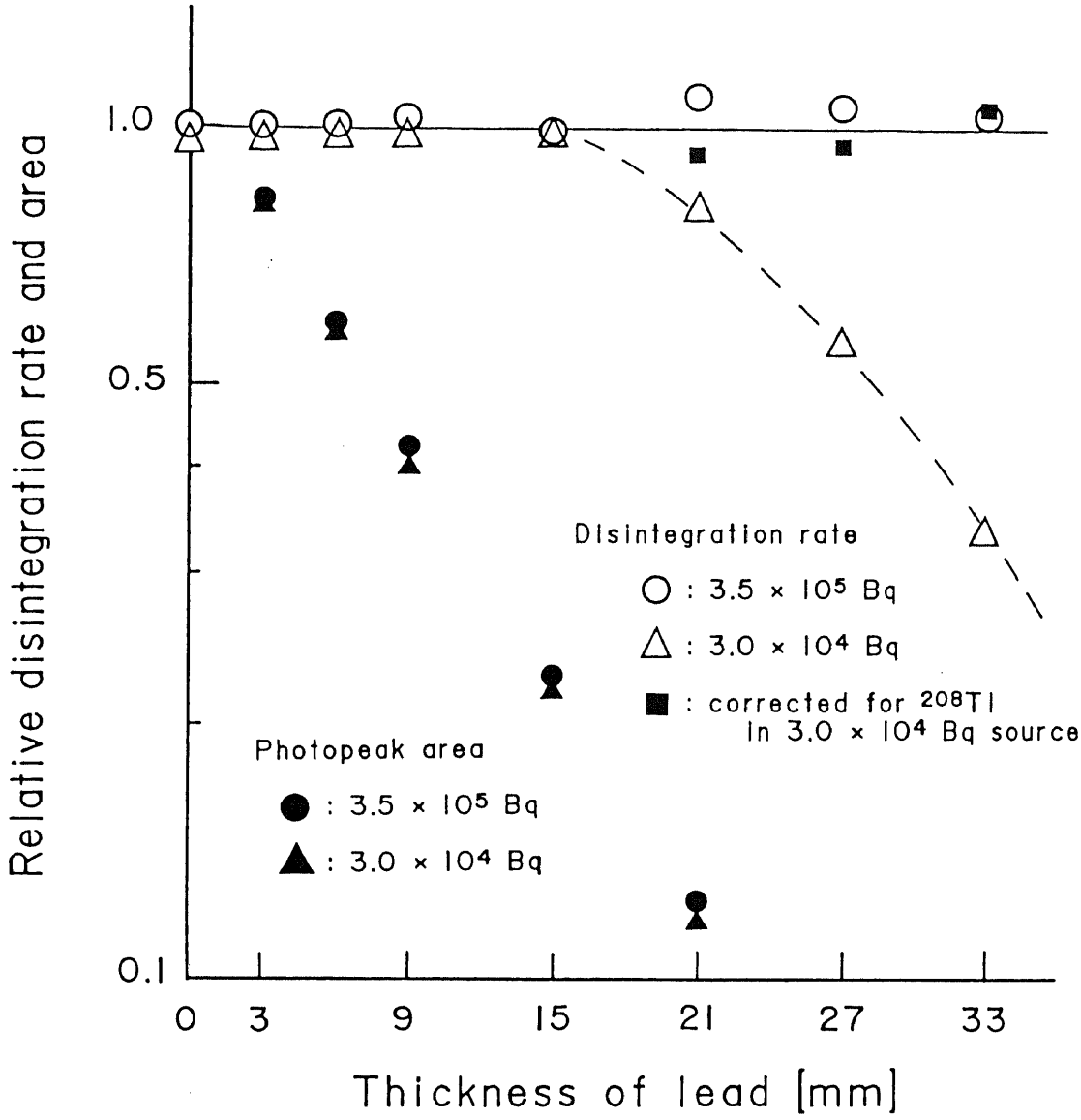

Fig. 27 Effect of the thickness of lead of the imitated container on the area under the photopeak and the disintegration rates determined by the sum-peak method. Black triangle and circle : the areas under the photopeaks of the ^{60}Co point sources with radioactivities of 3.0×10^4 Bq and 3.5×10^5 Bq as calculated by equation (25), white triangle and circle : the disintegration rates of the ^{60}Co point sources with radioactivities of 3.0×10^4 Bq and 3.5×10^5 Bq as calculated by the sum-peak formula (15), black square : the disintegration rates of the ^{60}Co point source with radioactivity of 3.0×10^4 Bq corrected for the contribution from ^{208}Tl.

of lead, although the relative areas under the photopeaks decreased strongly with increasing lead thickness.

For the 3.0×10^4 Bq source, Fig. 27 shows that the areas under the photopeaks also decreased with increasing lead thickness similarly as those for the 3.5×10^5 Bq source. The relative disintegration rates calculated by the sum-peak formula were almost equal to unity and did not significantly change within up to the thickness of 15 mm, but at thicknesses of 21, 27 and 33 mm, the relative disintegration rates were smaller than unity, and the deviations from the true disintegration rate increased with increasing thickness. It was concluded that the sum-peak method was effective for the point source of 3.0×10^4 Bq only with lead thicknesses of 15 mm or less.

(3) Discussion

If the disintegration rate of a ^{60}Co point source kept in the lead container was exactly determined by using the sum-peak method, the relative disintegration rate obtained in the present experiment must be unity irrespective of the source strength and the absorber thickness. However, the disintegration rate for the 3.0×10^4 Bq source deviated largely from the true disintegration rate in the cases of the thicknesses of 21, 27 and 33 mm as shown in Fig. 27. To explore why the sum-peak method sometimes underestimated the disintegration rate for the point source of 3.0×10^4 Bq, we compared the areas per 1 Bq under the photopeak and the sum peak.

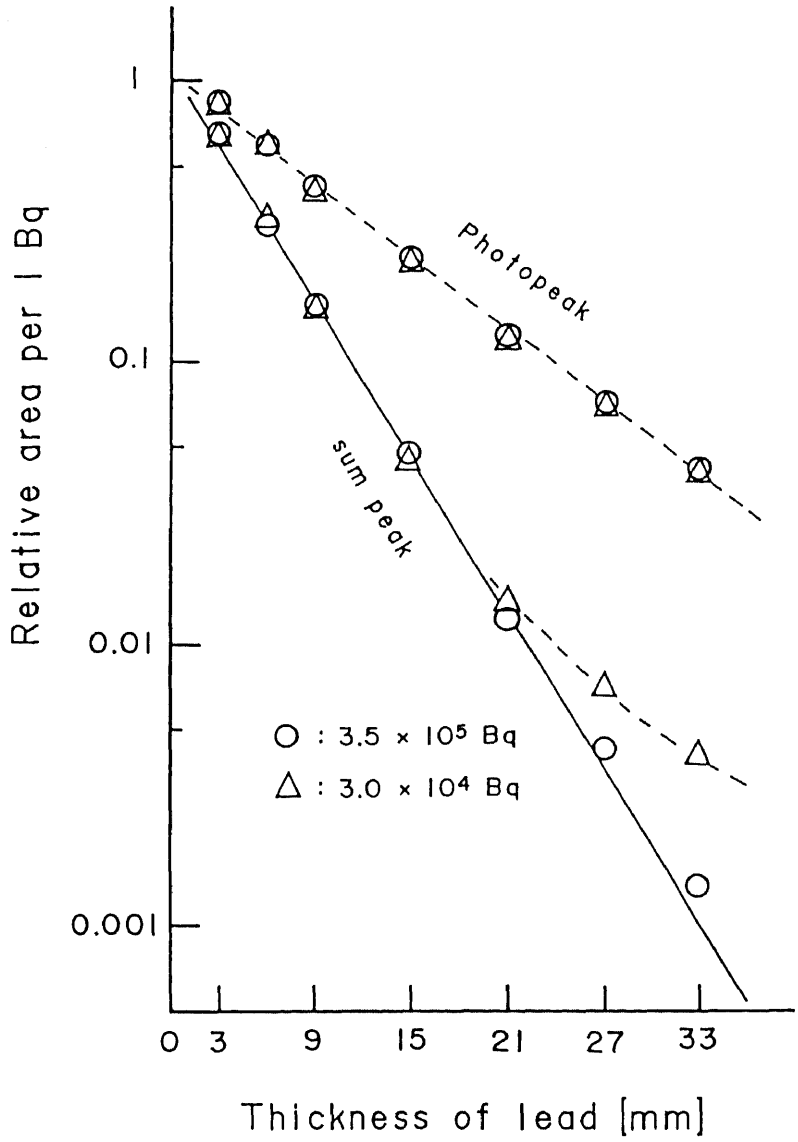

Fig. 28 Effect of thickness of imitated lead containers on the areas per 1 Bq under the photopeak and the sum peak.

Figure 28 shows the areas per 1 Bq under the photopeak and the sum peak which are normalized to those obtained for the 3.5×10^5 Bq source without lead container. The standard deviations of the

photopeak and the sum peak areas per 1 Bq shown in Fig. 28 were less than 0.1 % and 2 %, respectively. The areas for both the photopeak and the sum peak decrease with increasing thickness. In the case of the photopeak, the thickness dependence of the peak area is totally independent of the disintegration rate of sources in the thickness range of 0 to 33 mm used in the present experiment. On the other hand, the sum peak distribution shows that the thickness dependence of the area is also independent of the disintegration rate in the thickness range below 21 mm, but not above 21 mm. The relative areas per 1 Bq under the sum peaks for the 3.0×10^4 Bq source are 1.7 and 2.8 times larger than those of the 3.5×10^5 Bq source in the cases of 27 and 33 mm in thickness, respectively.

We presume that the overestimation of the areas under the sum peaks determined for the 3.0×10^4 Bq source in the lead containers with the thicknesses over 21mm might be caused by ^{208}Tl, which is one of naturally occurring radionuclides in the thorium series[52]. Taking account of the effect of ^{208}Tl on the sum-peak of ^{60}Co, the area per 1 Bq under the sum-peak for the 3.0×10^4 Bq source should be equal to that of the 3.5×10^5 Bq source at a fixed thickness of the lead container in Fig. 28. Therefore,

$$\frac{(A_{s1,t} - \xi_t)}{R_1} = \frac{(A_{s2,t} - \xi_t)}{R_2}, \qquad (68)$$

where $R_1 = 3.5 \times 10^5$ Bq, $R_2 = 3.0 \times 10^4$ Bq, and $A_{s1,t}$ and $A_{s2,t}$ are the areas under the sum peaks of the 3.5×10^5 Bq and 3.0×10^4

Bq sources, respectively, kept in a container of thickness 't'. ξ_t is the contribution under the sum-peak due to the 2614 keV γ-ray from ^{208}Tl. Substituting the numerical values of R_1 and R_2 into equation (68), and rearranging it, the following relation can be obtained,

$$\xi_t = \frac{35}{35 - 3} \times A_{s2,t} - \frac{3}{35 - 3} \times A_{s1,t}. \qquad (69)$$

Using equation (69), the γ-ray contribution from ^{208}Tl was determined to be 14 %, 42 % and 69 % of the area under the sum peak when the 3.0×10^4 Bq source was kept in the lead container with thicknesses of 21, 27 and 33 mm, respectively. Taking into account the background contribution from ^{208}Tl the sum peak area is given by

$$A_{12} = I_{12} - \frac{1}{2} \times (Ch_4 - Ch_3 + 1)(C_4 + C_3) - \xi_t. \qquad (70)$$

Black squares shown in Fig. 27 represent the corrected disintegration rate for the 3.0×10^4 Bq source using equation (70) (in which the area due to ^{208}Tl is subtracted from the sum peak area). The corrected rate is very consistent with the true disintegration rate of the source as seen in Fig. 27. Using the least-squares method, we determined again the relative disintegration rates from two different data sets of the 3.0×10^4 Bq and the 3.5×10^5 Bq sources (corrected data were used at 21, 27, 33 mm for the 3.0×10^4 Bq source) shown in Fig. 27. As results, the absolute differences between both relative disintegration rates at the same

thicknesses (3, 6, 9, 15, 21, 27 and 33 mm) were (5.9 ± 0.6) %. It showed that the sum-peak method can be effectively used for the determination of the disintegration rates of both the 3.0×10^4 Bq and the 3.5×10^5 Bq sources when taking account of the effect of ^{208}Tl.

§6. Results and Discussion

A γ-ray spectrum reflects characteristics of a radionuclide and the radioactivity of a radioactive source. The disintegration rate of the source can be determined by using information obtained from the spectrum. In an ordinary method, the magnitude of radioactivity of a sample source can be determined using a photopeak area provided that the detector response is known or a proper standard source with a known radioactivity is available. Therefore, the ordinary method is not applicable without a detector whose response to γ-rays is adequately known or without a standard source which has the dimension, composition and nuclide identical or closely similar to those of the sample source. In the case of a sample source of a radionuclide emitting two or more coincident γ-rays the sum-peak method can be applicable to determine the radioactivity. It does not require any standard source nor the information of detector response. The sum-peak method is not affected by a source-to-detector geometry nor by an absorber between a source and a detector according to theoretical considerations. These are the advantageous features of the sum-peak method which are distinguished from others.

In the present studies, the distinguished features of the sum-peak method were examined by experiments using ^{60}Co point sources and ^{60}Co bulky sources. As results, these features were confirmed for the point sources, but not for the bulky sources. Sutherland and Buchanan had pointed out already that the sum-peak method were not effective for extended sources such as bulky sources and suggested that the

sum-peak method should be applied for the determination of a disintegration rate keeping in mind "a tacit assumption" that a detector must be equally responsive to all parts of a radioactive source. This assumption is strictly fulfilled in the case of point sources.

We proposed an equation which explained why the sum-peak method could not retain its validity for bulky sources, and proved it by experiments using the bulky sources of ^{60}Co solutions in bottles and the ^{60}Co point source located at 54 different positions. Those positions were distributed throughout the whole volume of the source bottle on the detector. Transforming our equation, Oderkerk and Brinkman derived two equations; one to be used for estimation of an exact error (the equation of error) and the other for the upper bound of the error caused by the sum-peak method in an extended source (the equation of upper bound). Analyzing the error equation, it could be understood that the sum-peak formula should give an underestimated disintegration rate except for the only case in which the photoelectric and total efficiencies were independent of parts of a radioactive source. The implication of this result is nothing but that of the tacit assumption.

Subsequently, the model studies using two point sources of ^{60}Co were performed to examine the above two equations, the equation of error and the equation of upper bound. In the model studies, various simple extended sources were composed of two point sources. The disintegration rates of the simple extended sources were

experimentally determined by the sum-peak method, and compared with theoretical rates based on the equation of error. As results, both the disintegration rates obtained experimentally and theoretically were consistent with each other. These results indicated that the disintegration rates determined by the sum-peak method were approximately accurate without appreciable errors when a detector was equally responsive to two point sources. However, the sum-peak method gave significantly underestimated disintegration rates when a detector was not equally responsive, and the magnitude of error could be estimated theoretically by using the equation of error. Subsequently, the upper bound of the error was examined, and it was found that the error estimated by the equation of upper bound was at least twice as large as the true error, which was decisively verified by experimental data. Owing to these results, the equation of upper bound was corrected. The corrected equation was twice more precise than that of Oderkerk and Brinkman. The results were applied for an arbitrary extended source and were found to be effective in general. We conclude that all the results in the model studies basically support equations offered by Oderkerk and Brinkman, although the equation of upper bound must be corrected.

According to the results shown above, the true disintegration rate of a point source can be obtained by the sum-peak method, and an error caused when the sum-peak method is applied for an extended source can be estimated by calculation of the equation of error. Nevertheless there are many cases in which the sum-peak method gives

underestimated disintegration rates for point sources, and also the cases in which errors actually caused for extended sources are evidently larger than those expected from the equation of error. These problems seem to be caused with some practical situations associated with measurements. In the present studies practical effects in the sum-peak method were examined in three cases.

In the first case, the sum-peak method was applied to the determination of disintegration rate of a ^{60}Co point source for several source-to-detector geometries. In these measurements, the areas under the photopeaks and the sum peak were derived based on "the total peak area method" from each spectrum, and the disintegration rates thus determined were underestimated by about 0.3 in relative disintegration rate. We presumed that underestimates were caused by the underestimation of photopeak areas, and proposed the precise method of determination of the photopeak areas. In the proposed method, spectra of a ^{22}Na point source were used to subtract the area attributed to Compton scattering of γ_2 (1332 keV) from the area under the photopeak of γ_1 (1173 keV) in each spectrum of ^{60}Co. The disintegration rates determined using the photopeak areas derived by the proposed method instead of the total peak area method were more than 0.9 in relative disintegration rate. These results proved the effectiveness of the proposed method for the derivation of the areas under the photopeaks (γ_1 and γ_2) from the ^{60}Co spectrum.

In the second case, the sum-peak method was applied to determine the disintegration rates of ^{60}Co bulky sources with disintegration

rates of 1.1×10^4 Bq, 1.1×10^3 Bq and 1.1×10^2 Bq. The data obtained in the measurements of the 1.1×10^3 Bq and 1.1×10^2 Bq sources were substantially deviated from those estimated based on the equation of error, whereas those of the 1.1×10^4 Bq source were not significantly different from the calculated ones. By investigating the reason why the equation of error was not effective for the 1.1×10^3 Bq and 1.1×10^2 Bq bulky sources, it was presumed and proved experimentally that Compton scattering of γ-rays (2614 keV) emitted from a naturally occurring radionuclide ^{208}Tl caused overestimates of the areas under the sum peaks. Thus the disintegration rates determined by the sum-peak method were underestimated.

In the third case, the disintegration rates of ^{60}Co point sources with 3.0×10^4 Bq and 3.5×10^5 Bq kept in lead containers with several thicknesses (3 ~ 33 mm) were determined by the sum-peak method. As results, the disintegration rates obtained were almost equal to the true rate for the 3.5×10^5 Bq source regardless of the container thickness, but underestimated for the 3.0×10^4 Bq source in the containers with lead thicknesses of 21 mm or larger. This experimental fact contradicted the theoretical expectation on the effect of absorbers between a source and a detector. It was presumed and verified experimentally that overestimates of the sum peak areas caused by ^{208}Tl were the main reason of the underestimation of radioactivity for the 3.0×10^4 Bq source in the lead container with the thickness of 21 mm or larger just the same as in the second case.

From the results of the second and third cases it is concluded

that the area attributed to Compton scattering of ^{208}Tl must be subtracted from the sum-peak region in a ^{60}Co spectrum when the sum-peak method is applied to the determination of the disintegration rates of ^{60}Co sources with lower radioactivities.

§7. Conclusion

The conclusions of the present studies can be summarized as follows;

(1) Based on theoretical investigations, the sum-peak method should give the true disintegration rate of a point source regardless of the source-to-detector geometry and also irrespective of absorbers between a source and a detector. These distinguished features of the sum-peak method was confirmed by experiments using ^{60}Co point sources. These experimental facts are the evidence that the sum-peak method is effective for radioactivity standardization of radioisotopes which emit two or more coincident γ-rays.

(2) The sum-peak method underestimated the disintegration rates of ^{60}Co bulky sources with comparatively larger volumes. This result showed that the sum-peak method should be applied keeping in mind the tacit assumption that a detector must have an equal response for all parts of a sample source.

(3) We proposed an equation formulated from the practical meaning of the tacit assumption. The equation could be proved by experiments using a ^{60}Co point source located at 54 different positions. Subsequently, Oderkerk and Brinkman derived the equation of error and the equation of upper bound which could estimate the error caused when the sum-peak method was applied to an extended source.

(4) Through model studies using two ^{60}Co point sources, the equation

of error was verified and the equation of upper bound was corrected. The corrected equation could estimate the upper bound with a lower limit by a factor of 2 compared with that without the correction.

(5) Various practical effects in the radioactivity measurement of ^{60}Co sources by the sum-peak method were investigated. Two problems associated with the determination of the areas under the two photopeaks and the sum peak from a ^{60}Co spectrum were identified.

(a) One problem related to the estimation of photopeak areas was caused by the overlapping of the photopeak of γ_1 (1173 keV) and Compton scattering of γ_2 (1332 keV). This problem could be alleviated by the precise method of determination of the photopeak areas by using a ^{22}Na spectrum.

(b) The other problem was caused by Compton scattering of γ-ray (2614 keV) emitted from a naturally occurring radionuclide ^{208}Tl, which brought about the significant overestimation of the sum peak area for a ^{60}Co source with lower radioactivity. It was found that the sum-peak method could be effective by elimination of the area attributed to Compton scattering of ^{208}Tl from the sum-peak region in a ^{60}Co spectrum.

References

1)M. Noguchi : "γ-ray spectrometry" p.50 Nikkankogyo Shinbunsha(Tokyo 1980).

2)G. A. Brinkman, A. H. W. Aten, Jr. and J. Th. Veenboer : Int. J. Appl. Radiat. Isot. 14, 153(1963).

3)G. A. Brinkman, A. H. W. Aten, Jr. and J. Th. Veenboer : Int. J. Appl. Radiat. Isot. 14, 433(1963).

4)G. A. Brinkman and A. H. W. Aten, Jr. : Int. J. Appl. Radiat. Isot. 14, 503(1963).

5)G. A. Brinkman, A. H. W. Aten, Jr. and J. Th. Veenboer : Int. J. Appl. Radiat. Isot. 16, 15(1965).

6)G. A. Brinkman, and A. H. W. Aten, Jr. : Int. J. Appl. Radiat. Isot. 16, 177(1965).

7)L. G. Sutherland and J. D. Buchanan : Int. J. Appl. Radiat. Isot. 18, 786(1967).

8)T. Kawano and H. Ebihara : Appl. Radiat. Isot. 41, 163(1990).

9)R. P. Oderkerk and G. A. Brinkman : Appl. Radiat. Isot. 41, 169(1990).

10)T. Kawano and H. Ebihara : Appl. Radiat. Isot. 43, 705(1992).

11)G. A. Brinkman : Int. J. Appl. Radiat. Isot. 24, 649(1973).

12)G. A. Brinkman, L. Lindner and J. Th. Veenboer : Int. J. Appl. Radiat. Isot. 28, 271(1977).

13)J. S. Eldridge and P. Crowther : Nucleonics 22, 56(1964).

14)D. L. Horrocks and P. R. Klein : Nucl. Instrum. and Methods. 124,

585(1975).

15)D. L. Horrocks : Clin. Chem. 21, 370(1975).

16)K. Nishizawa, N. Hamada and S. Sakuma : Radioisotopes 32, 364(1983).

17)K. Nishizawa : Radioisotopes 34, 78(1985).

18)K. Nishizawa : Health Phys. 50, 415(1986).

19)T. Kawano : Technical report of the University of Tsukuba 8, 35(1988).

20)K. Siegbahn, Ed. : "Alpha-, Beta-, Gamma-ray spectroscopy" p.37 North Holland Pub. Co., (Amsterdam 1974).

21)F. Adams and R. Dams : "Applied gamma-ray spectrometry 2nd Edition and revision of original publication by C. E. Crouthamel" p.14 Pergamon Press,(Oxford 1975).

22)G. F. Knoll (translated by I. Kimura and E. Sakai) : "Radiation detection and measurement 2nd Edition." p.53 Nikkankogyo Shinbunsha (Tokyo 1991).

23)N. Tsoulfanidis(transleted by E. Sakai) : "Measurement and detection of radiation" p.153 Gendaikogakusha(Tokyo 1983).

24)F. Adams and R. Dams : "Applied gamma-ray spectrometry 2nd Edition and revision of original publication by C. E. Crouthamel" p.27 Pergamon Press,(Oxford 1975).

25)F. Adams and R. Dams : "Applied gamma-ray spectrometry 2nd Edition and revision of original publication by C. E. Crouthamel" p.341 Pergamon Press,(Oxford 1975).

26)K. Siegbahn Ed. : "Alpha-, Beta-, Gamma-ray spectroscopy"

p.287(Fig.29) North Holland Pub. Co., (Amsterdam 1974).

27)T. Hyodo : "Introduction to radiation shield" p.39(Fig. 4.4) and p.40(Fig.4.5) Sangyo tosho (Tokyo 1974).

28)Y. Murakami, H. Danno and M. Kobayashi : "Radiation data book" p.333 Chihou syokan (Tokyo 1982).

29)M. Noguchi : "γ-ray spectrometry" p.117 Nikkankogyo Shinbunsha (Tokyo 1980).

30)N. Tsoulfanidis(transleted by E. Sakai) : "Measurement and detection of radiation" p.417 Gendaikogakusha(Tokyo 1983).

31)K. Siegbahn Ed. : "Alpha-, Beta-, Gamma-ray spectroscopy" p.515 North Holland Pub. Co., (Amsterdam 1974).

32)M. Noguchi : "γ-ray spectrometry" p.139 Nikkankogyo Shinbunsha (Tokyo 1980).

33)F. Adams and R. Dams : "Applied gamma-ray spectrometry 2nd Edition and revision of original publication by C. E. Crouthamel" p.215 Pergamon Press,(Oxford 1975).

34)T. J. Kennett, W. V. Prestwich and G. L. Keech : Nucl. Instrum. and Methods. 29, 325(1964).

35)G. F. Knoll(translated by I. Kimura and E. Sakai) : "Radiation detection and measurement 2nd Edition." p.323 Nikkankogyo Shinbunsha (Tokyo 1991).

36)F. Adams and R. Dams : "Applied gamma-ray spectrometry 2nd Edition and revision of original publication by C. E. Crouthamel" p.363 Pergamon Press,(Oxford 1975).

37)R. K. Gupta and S. Jha : Nucl. Phys. 1, 2(1956).

38)T. Kawano and H. Ebihara : Appl. Radiat. Isot. 42, 1165(1991).

39)C. M. Lederer and V. S. Shirley Ed. : "Table of Isotopes 7th edition" p.179 J. Wiley & Sons. Inc. (New York 1978).

40)Y. Murakami, H. Danno and M. Kobayashi : "Radiation data book" p.64 Chihou syokan (Tokyo 1982).

41)F. Adams and R. Dams : "Applied gamma-ray spectrometry 2nd Edition and revision of original publication by C. E. Crouthamel" p.344 Pergamon Press,(Oxford 1975).

42)C. M. Lederer and V. S. Shirley Ed. : "Table of Isotopes 7th edition" p.36 J. Wiley & Sons. Inc. (New York 1978).

43)Y. Murakami H. Danno and M. Kobayashi "Radiation data book" p.38 Chihou syokan (Tokyo 1982).

44)F. Adams and R. Dams : "Applied gamma-ray spectrometry 2nd Edition and revision of original publication by C. E. Crouthamel" p.330 Pergamon Press (Oxford 1975).

45)T. Kawano and H. Ebihara : Jpn. J. Appl. Phys. 30, 3545(1991).

46)J. M. R. Hutchinson, W. B. Mann and P. A. Mullen : Nucl. Instrum. and Methods. 112, 187(1973).

47) P. R. Bevington : "Data reduction and analysis for the physical sciences" p.56 McGraw-Hill (New York 1969).

48)G. F. Knoll (translated by I. Kimura and E. Sakai) : "Radiation detection and measurement 2nd Edition." p.93 Nikkankogyo Shinbunsha (Tokyo 1991).

49)N. Tsoulfanidis(transleted by E. Sakai) : "Measurement and detection of radiation" p.62 Gendaikogakusha(Tokyo 1983).

50)K. Siegbahn Ed. : "Alpha-, Beta-, Gamma-ray spectroscopy" p.997, 1032 and 1687 North Holland Pub. Co., (Amsterdam 1974).

51)T. Kawano and H. Ebihara : Jpn. J. Appl. Phys. 30, 414(1991).

52)Y. Murakami, H. Danno and M. Kobayashi : "Radiation data book" p.309 Chihou syokan (Tokyo 1982).

53)M. Noguchi : "γ-ray spectrometry" p.61 Nikkankogyo Shinbunsha (Tokyo 1980).

54)D. F. Covell : Anal. Chem. 31, 1785(1959).

55)L. Kokta : Nucl. Instrum. and Methods. 112, 245(1973).

[Appendix]

[Appendix-1]

To illustrate the method of the practical calculations based on equations (37) and (39), we will describe only the division of the first 10 mm layer of the bottle (50 mm in diameter), with a volume

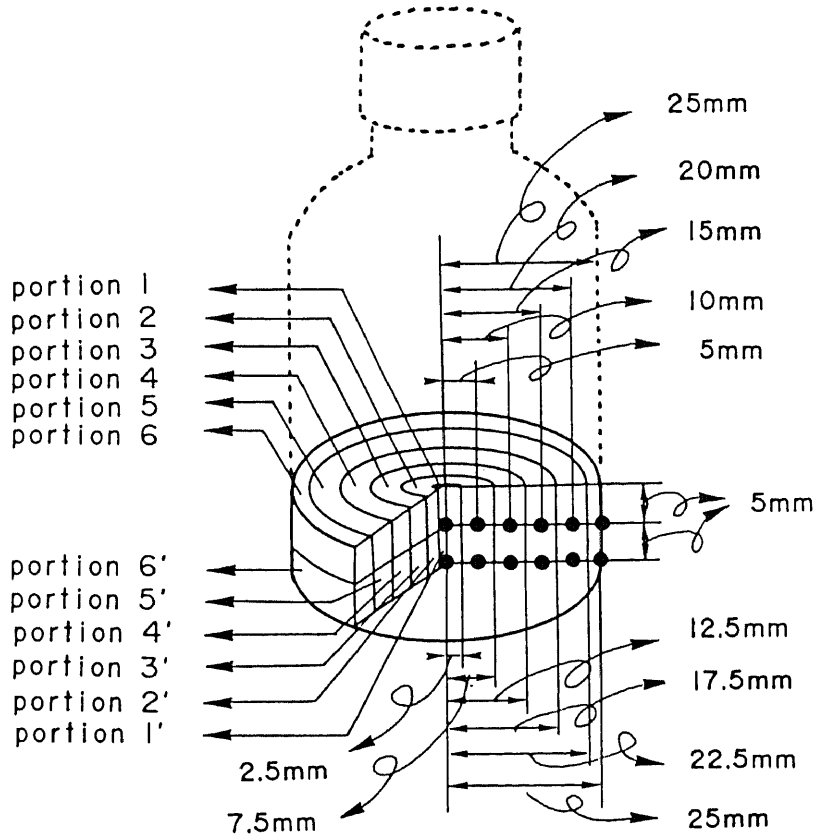

Fig. 29 Twelve positions (first 10 mm layer of the bottle) where a ^{60}Co point source located for each measurement.

V_0 = 19.6 mℓ. This layer is divided into 12 sub-layers (portions in Fig. 29), each with a depth of 5 mm: 2 disk were numbered 1 and 1' and 10 rings numbered 2, 2' through 6, 6', as shown in Fig. 29. The disks and the rings have the following volumes that are proportional to the disintegration rate of the ^{60}Co source:

disk 1 (portion 1) : $\pi \times (2.5 \times 2.5) \times 5 = v^1$

disk 1' (portion 1') : $\pi \times (2.5 \times 2.5) \times 5 = v^{1'}$

ring 2 (portion 2) : $\pi \times (7.5 \times 7.5 - 2.5 \times 2.5) \times 5 = v^2$

ring 2' (portion 2') : $\pi \times (7.5 \times 7.5 - 2.5 \times 2.5) \times 5 = v^{2'}$

.....

.....

ring 6 (portion 6) : $\pi \times (25 \times 25 - 22.5 \times 22.5) \times 5 = v^6$

ring 6' (portion 6') : $\pi \times (25 \times 25 - 22.5 \times 22.5) \times 5 = v^{6'}$

Because of the relatively small volumes of the portions it was assumed that the detector had an identical sensitivity to all the regions of each disk or ring.

A value of $N^{[A]}$ for the disintegration rate can be calculated by summing all the individual disintegration rates of parts calculated with the sum-peak method:

$$N^{[A]} = \sum_{i=1}^{n} N^{[i]} = \sum_{r=1}^{12} \sum_{p}^{n'} D^{[r,p]},$$

where,

n : the number of parts in the volume source,

12 : the number of portions in the volume source,

n' : the number of parts in portions,

i : parts of the volume source,

r : one of the disks or rings (portion r),

p : parts in a portion r,

$[r,p]$: a part p in a portion r,

$N^{[i]}$: a disintegration rate of a part i (proportional to that of the point source used in experiment),

and

$D^{[r,p]}$: a disintegration rate of a part p of a portion r.

Since the detector has the same sensitivity to all parts of a portion r, it can be stated that :

$$\sum_{p}^{n'} D^{[r,p]} = D^{r} \times v^{r},$$

in which D^{r} is the disintegration rate of a representative part of a portion r ($D^{[r,p]} = D^{r}$) and v^{r} is the number of parts in a portion r (proportional to the volume of portion r). The values of D^{r} were obtained by measurements. Finally:

$$N^{[A]} = \sum_{r=1}^{12} (D^{r} \times v^{r}). \qquad (71)$$

Equation (37) was taken the place of equation (71) at practical calculation.

A value of $N^{[e]}$ for the disintegration rate of the volume source can be calculation via another method. Following the precedent

notations:

$$\sum_{i=1}^{n} A_1[i] = \sum_{r=1}^{12} \sum_{p}^{n'} A_1[r,p], \qquad \sum_{i=1}^{n} A_2[i] = \sum_{r=1}^{12} \sum_{p}^{n'} A_2[r,p],$$

$$\sum_{i=1}^{n} A_{12}[i] = \sum_{r=1}^{12} \sum_{p}^{n'} A_{12}[r,p], \quad \text{and} \quad \sum_{i=1}^{n} T[i] = \sum_{r=1}^{12} \sum_{p}^{n'} T[r,p].$$

Assuming again that the detector has the same sensitivity to all parts of the portion r, it can be stated that:

$$\sum_{p}^{n'} A_1[r,p] = A_1^r \times v^r, \qquad \sum_{p}^{n'} A_2[r,p] = A_2^r \times v^r,$$

$$\sum_{p}^{n'} A_{12}[r,p] = A_{12}^r \times v^r, \quad \text{and} \quad \sum_{p}^{n'} T[r,p] = T_1^r \times v^r,$$

therefore,

$$\sum_{i=1}^{n} A_1[i] = \sum_{r=1}^{12} (A_1^r \times v^r), \qquad \sum_{i=1}^{n} A_2[i] = \sum_{r=1}^{12} (A_2^r \times v^r),$$

$$\sum_{i=1}^{n} A_{12}[i] = \sum_{r=1}^{12} (A_{12}^r \times v^r), \quad \text{and} \quad \sum_{i=1}^{n} T[i] = \sum_{r=1}^{12} (T_1^r \times v^r).$$

Consequently, equation (39) can be rewritten as follows;

$$N[e] = \sum_{r=1}^{12} (T_1^r \times v^r) + \frac{\sum_{r=1}^{12} (A_1^r \times v^r) \times \sum_{r=1}^{12} (A_2^r \times v^r)}{\sum_{r=1}^{12} (A_{12}^r \times v^r)}. \qquad (72)$$

The values of A_1^r, A_2^r, A_{12}^r and T_1^r were obtained by experiments, in which a ^{60}Co point source of 1.4×10^5 Bq and a ^{22}Na point source of

2.3×10^4 Bq were used for the spectrum measurements and the estimation of the values of "α", and practical calculations were performed by use of equation (72) instead of (39).

[Appendix-2]

According to Oderkerk and Brinkman, equation (41) can be obtained as shown under. Defining a function, E_n, as follows;

$$E_n = (N - N_c) \times \sum_i^n A_{12}{}^i$$

$$= \left(\sum_i^n \frac{A_1{}^i \times A_2{}^i}{A_{12}{}^i} - \frac{\sum_i^n A_1{}^i \times \sum_i^n A_2{}^i}{\sum_i^n A_{12}{}^i} \right) \times \sum_i^n A_{12}{}^i$$

$$= \sum_i^n A_{12}{}^i \times \sum_i^n \frac{A_1{}^i \times A_2{}^i}{A_{12}{}^i} - \sum_i^n A_1{}^i \times \sum_i^n A_2{}^i$$

$$= (A_{12}{}^n + \sum_i^{n-1} A_{12}{}^i) \times \left(\frac{A_1{}^n \times A_2{}^n}{A_{12}{}^n} + \sum_i^{n-1} \frac{A_1{}^i \times A_2{}^i}{A_{12}{}^i} \right)$$

$$- (A_1{}^n + \sum_i^{n-1} A_1{}^i) \times (A_2{}^n + \sum_i^{n-1} A_2{}^i)$$

$$= \underline{A_{12}{}^n \times \frac{A_1{}^n \times A_2{}^n}{A_{12}{}^n}} + A_{12}{}^n \times \sum_i^{n-1} \frac{A_1{}^i \times A_2{}^i}{A_{12}{}^i}$$

$$+ \sum_i^{n-1} A_{12}{}^i \times \frac{A_1{}^n \times A_2{}^n}{A_{12}{}^n} + \sum_i^{n-1} A_{12}{}^i \times \sum_i^{n-1} \frac{A_1{}^i \times A_2{}^i}{A_{12}{}^i}$$

$$- \underline{A_1{}^n \times A_2{}^n} - A_1{}^n \times \sum_i^{n-1} A_2{}^i - \sum_i^{n-1} A_1{}^i \times A_2{}^n - \sum_i^{n-1} A_1{}^i \times \sum_i^{n-1} A_2{}^i$$

$$= A_{12}{}^n \times \sum_i^{n-1} \frac{A_1{}^i \times A_2{}^i}{A_{12}{}^i} + \sum_i^{n-1} A_{12}{}^i \times \frac{A_1{}^n \times A_2{}^n}{A_{12}{}^n}$$

$$- A_1{}^n \times \sum_i^{n-1} A_2{}^i - \sum_i^{n-1} A_1{}^i \times A_2{}^n$$

$$+ \underbrace{\sum_i^{n-1} A_{12}{}^i \times \sum_i^{n-1} \frac{A_1{}^i \times A_2{}^i}{A_{12}{}^i} - \sum_i^{n-1} A_1{}^i \times \sum_i^{n-1} A_2{}^i}_{(= E_{n-1})},$$

hence

$$E_n - E_{n-1} = A_{12}^n \times \sum_i^{n-1} \frac{A_1^i \times A_2^i}{A_{12}^i} + \sum_i^{n-1} A_{12}^i \times \frac{A_1^n \times A_2^n}{A_{12}^n}$$

$$- A_1^n \times \sum_i^{n-1} A_2^i - \sum_i^{n-1} A_1^i \times A_2^n$$

$$= \sum_i^{n-1} \left(A_{12}^n \times \frac{A_1^i \times A_2^i}{A_{12}^i} + A_{12}^i \times \frac{A_1^n \times A_2^n}{A_{12}^n} \right.$$

$$\left. - A_1^n \times A_2^i - A_1^i \times A_2^n \right)$$

$$= \sum_i^{n-1} A_{12}^n \, A_{12}^i \left(\frac{A_1^i \, A_2^i}{A_{12}^i \, A_{12}^i} + \frac{A_1^n \, A_2^n}{A_{12}^n \, A_{12}^n} \right.$$

$$\left. - \frac{A_1^n \, A_2^i}{A_{12}^n \, A_{12}^i} - \frac{A_1^i \, A_2^n}{A_{12}^n \, A_{12}^i} \right)$$

$$= \sum_i^{n-1} A_{12}^n \, A_{12}^i \left(\chi_2^i \, \chi_1^i + \chi_2^n \, \chi_1^n - \chi_2^n \, \chi_1^i - \chi_1^n \, \chi_2^i \right),$$

where

$$\chi_1^i = \frac{A_2^i}{A_{12}^i}, \qquad \chi_2^i = \frac{A_1^i}{A_{12}^i},$$

$$\chi_1^n = \frac{A_2^n}{A_{12}^n}, \quad \text{and} \quad \chi_2^n = \frac{A_1^n}{A_{12}^n}.$$

Consequently,

$$E_n - E_{n-1} = \sum_i^{n-1} A_{12}^n \, A_{12}^i \, (\chi_2^i - \chi_2^n)(\chi_1^i - \chi_1^n).$$

Then,

$$\sum_{m=2}^{n} (E_m - E_{m-1}) = (E_2 - E_1) + (E_3 - E_2) + \cdots\cdots + (E_n - E_{n-1})$$

$$= - E_1 + E_n .$$

Since E_1 means an error when the sum-peak method was applied to an extended source composed of only one point source, $E_1 = 0$, hence;

$$\sum_{m=2}^{n} (E_m - E_{m-1}) = E_n ,$$

therefore

$$E_n = \sum_{m=2}^{n} (E_m - E_{m-1})$$

$$= \sum_{m=2}^{n} \sum_{i}^{m-1} A_{12}{}^m \; A_{12}{}^i \; (\chi_2{}^i - \chi_2{}^m)(\chi_1{}^i - \chi_1{}^m).$$

Assuming

$$F(m,i) = A_{12}{}^m \; A_{12}{}^i \; (\chi_2{}^i - \chi_2{}^m)(\chi_1{}^i - \chi_1{}^m),$$

then

$$F(m,m) = F(i,i) = 0, \quad \text{and} \quad F(m,i) = F(i,m),$$

hence,

$$E_n = \sum_{m=2}^{n} \sum_{i}^{m-1} F(m,i)$$

$$= \sum_{m=2}^{n} \left(\sum_{i}^{m-1} F(m,i) \right)$$

$$= \sum_{i}^{1} F(2,i) + \sum_{i}^{2} F(3,i) + \sum_{i}^{3} F(4,i) + \ldots + \sum_{i}^{n-1} F(n,i)$$

$$= F(2,1) +$$

$$F(3,1) + F(3,2) +$$

$$F(4,1) + F(4,2) + F(4,3) +$$

$$\ldots\ldots\ldots\ldots\ldots\ldots\ldots\ldots\ldots\ldots +$$

$$F(n,1) + F(n,2) + F(n,3) + \ldots\ldots + F(n,n-1)$$

Since $F(1,1) = F(2,2) = F(3,3) = \ldots\ldots = F(n,n) = 0$,

$$E_n = \Big\{ F(1,1) +$$

$$F(2,1) + F(2,2) +$$

$$F(3,1) + F(3,2) + F(3,3) +$$

$$F(4,1) + F(4,2) + F(4,3) + F(4,4) +$$

$$\ldots\ldots\ldots\ldots\ldots\ldots\ldots\ldots\ldots\ldots\ldots\ldots +$$

$$F(n,1) + F(n,2) + \ldots\ldots\ldots\ldots + F(n,n-1) + F(n,n) \Big\}$$

$$= \frac{1}{2} \Big\{ F(1,1) + F(2,1) + F(3,1) + F(4,1) + \ldots\ldots + F(n,1)$$

$$F(2,1) + F(2,2) + F(3,2) + F(4,2) + \ldots\ldots + F(n,2)$$

$$F(3,1) + F(3,2) + F(3,3) + F(4,3) + \ldots\ldots + F(n,3)$$

$$F(4,1) + F(4,2) + F(4,3) + F(4,4) + \ldots\ldots + F(n,4)$$

$$\ldots\ldots\ldots\ldots\ldots\ldots\ldots\ldots\ldots\ldots\ldots\ldots\ldots\ldots\ldots\ldots\ldots\ldots$$

$$F(n,1) + F(n,2) + \ldots\ldots\ldots\ldots + F(n,n-1) + F(n,n) \Big\}$$

Since $F(m,i) = F(i,m)$,

$$E_n = \frac{1}{2}\Big\{ F(1,1) + F(1,2) + F(1,3) + F(1,4) + \ldots + F(1,n)$$

$$F(2,1) + F(2,2) + F(2,3) + F(2,4) + \ldots + F(2,n)$$

$$F(3,1) + F(3,2) + F(3,3) + F(3,4) + \ldots + F(3,n)$$

$$F(4,1) + F(4,2) + F(4,3) + F(4,4) + \ldots + F(4,n)$$

$$\ldots\ldots\ldots\ldots\ldots\ldots\ldots\ldots\ldots\ldots\ldots\ldots\ldots\ldots$$

$$F(n,1) + F(n,2) + \ldots\ldots\ldots + F(n,n-1) + F(n,n)\Big\}$$

$$= \frac{1}{2}\Big\{ \sum_i^n F(1,i) + \sum_i^n F(2,i) + \sum_i^n F(3,i) + \ldots\ldots + \sum_i^n F(n,i)\Big\}$$

$$= \frac{1}{2} \sum_m^n \sum_i^n F(m,i)$$

$$= \frac{1}{2} \sum_m^n \sum_i^n A_{12}{}^m \; A_{12}{}^i \; (\chi_2{}^i - \chi_2{}^m)(\chi_1{}^i - \chi_1{}^m).$$

Consequently, the error made when the sum-peak method is applied to an extended source is given by:

$$N - N_c = \frac{1}{2A_{12}} \sum_m^n \sum_i^n A_{12}{}^m \; A_{12}{}^i \; (\chi_2{}^i - \chi_2{}^m)(\chi_1{}^i - \chi_1{}^m),$$

and

$$A_{12} = \sum_i^n A_{12}{}^i$$

This is equation (41).

And since

$$(\chi_2^i - \chi_2^m)(\chi_1^i - \chi_1^m) < (\chi_2^{max} - \chi_2^{min})(\chi_1^{max} - \chi_1^{min}),$$

χ_1^{max} and χ_1^{min} : the maximum and minimum values of χ_1^k or χ_1^m, and

χ_2^{max} and χ_2^{min} : the maximum and minimum values of χ_2^k or χ_2^m.

then

$$N - N_c \leq \frac{1}{2A_{12}} \sum_m^n \sum_i^n A_{12}^m A_{12}^i (\chi_2^{max} - \chi_2^{min})(\chi_1^{max} - \chi_1^{min})$$

$$\leq \frac{1}{2A_{12}} \sum_m^n A_{12}^m \sum_i^n A_{12}^i (\chi_2^{max} - \chi_2^{min})(\chi_1^{max} - \chi_1^{min})$$

$$\leq \frac{1}{2} A_{12} (\chi_2^{max} - \chi_2^{min})(\chi_1^{max} - \chi_1^{min}).$$

This is inequality (44).

[*Appendix-3*]

In the case of an extended source composed of two point sources, equation (45) can be derived from both equations (41) and (40) as follows;

(1) By using equation (41)

$$N - N_c = \frac{1}{2A_{12}} \sum_i^2 \sum_j^2 A_{12}{}^i A_{12}{}^j (\chi_1{}^i - \chi_1{}^j)(\chi_2{}^i - \chi_2{}^j)$$

$$= \frac{1}{2A_{12}} \sum_i^2 A_{12}{}^i \Big\{ A_{12}{}^{[1]} (\chi_1{}^i - \chi_1{}^{[1]})(\chi_2{}^i - \chi_2{}^{[1]}) + A_{12}{}^{[2]} (\chi_1{}^i - \chi_1{}^{[2]})(\chi_2{}^i - \chi_2{}^{[2]}) \Big\}$$

$$= \frac{1}{2A_{12}} \Big\{ A_{12}{}^{[1]} A_{12}{}^{[1]} \underbrace{(\chi_1{}^{[1]} - \chi_1{}^{[1]})}_{=0} \underbrace{(\chi_2{}^{[1]} - \chi_2{}^{[1]})}_{=0} + A_{12}{}^{[1]} A_{12}{}^{[2]} (\chi_1{}^{[1]} - \chi_1{}^{[2]})(\chi_2{}^{[1]} - \chi_2{}^{[2]}) + A_{12}{}^{[2]} A_{12}{}^{[1]} (\chi_1{}^{[2]} - \chi_1{}^{[1]})(\chi_2{}^{[2]} - \chi_2{}^{[1]}) + A_{12}{}^{[2]} A_{12}{}^{[2]} \underbrace{(\chi_1{}^{[2]} - \chi_1{}^{[2]})}_{=0} \underbrace{(\chi_2{}^{[2]} - \chi_2{}^{[2]})}_{=0} \Big\}$$

$$= \frac{A_{12}{}^{[1]} A_{12}{}^{[2]}}{A_{12}} (\chi_1{}^{[1]} - \chi_1{}^{[2]})(\chi_2{}^{[1]} - \chi_2{}^{[2]}).$$

Concerning ^{60}Co source,

$$A_1{}^{[1]} = A_2{}^{[1]} \quad \text{and} \quad A_1{}^{[2]} = A_2{}^{[2]},$$

then,

$$\chi_1^{[1]} = \chi_2^{[1]} \quad \text{and} \quad \chi_1^{[2]} = \chi_2^{[2]},$$

therefore,

$$= \frac{A_{12}^{[1]} A_{12}^{[2]}}{A_{12}} (\chi_1^{[1]} - \chi_1^{[2]})^2.$$

This is equation (45).

(2) By using equation (40)

We assume that $N^{[1]}$ and $N^{[2]}$ are disintegration rate of two point sources, respectively. Since the sum-peak method is effective for each point source,

$$N^{[1]} = T^{[1]} + \frac{A_1^{[1]} \times A_2^{[1]}}{A_{12}^{[1]}} \quad \text{and} \quad N^{[2]} = T^{[2]} + \frac{A_1^{[2]} \times A_2^{[2]}}{A_{12}^{[2]}},$$

where [1] and [2] mean one point source and another point source. Consequently;

$$N = N^{[1]} + N^{[2]} = T^{[1]} + T^{[2]} + \frac{A_1^{[1]} \times A_2^{[1]}}{A_{12}^{[1]}} + \frac{A_1^{[2]} \times A_2^{[2]}}{A_{12}^{[2]}}$$

$$N_c = T^{[1]} + T^{[2]} + \frac{(A_1^{[1]} + A_1^{[2]}) \times (A_2^{[1]} + A_2^{[2]})}{(A_{12}^{[1]} + A_{12}^{[2]})}$$

hence

$$N - N_c = \left(\frac{A_1^{[1]} \times A_2^{[1]}}{A_{12}^{[1]}} + \frac{A_1^{[2]} \times A_2^{[2]}}{A_{12}^{[2]}} \right) - \left(\frac{(A_1^{[1]} + A_1^{[2]}) \times (A_2^{[1]} + A_2^{[2]})}{(A_{12}^{[1]} + A_{12}^{[2]})} \right)$$

$$= \frac{A_{12}^{[2]} A_1^{[1]} A_2^{[1]} + A_{12}^{[1]} A_1^{[2]} A_2^{[2]}}{A_{12}^{[1]} A_{12}^{[2]}}$$

$$- \frac{(A_1^{[1]} A_2^{[1]} + A_1^{[2]} A_2^{[1]}) + (A_1^{[1]} A_2^{[2]} + A_1^{[2]} A_2^{[2]})}{(A_{12}^{[1]} + A_{12}^{[2]})}$$

$$= \frac{1}{A_{12}^{[1]} A_{12}^{[2]} (A_{12}^{[1]} + A_{12}^{[2]})}$$

$$\times \Big\{ A_{12}^{[2]} A_1^{[1]} A_2^{[1]} (A_{12}^{[1]} + A_{12}^{[2]})$$

$$+ A_{12}^{[1]} A_1^{[2]} A_2^{[2]} (A_{12}^{[1]} + A_{12}^{[2]})$$

$$- A_{12}^{[1]} A_{12}^{[2]} (A_1^{[1]} A_2^{[1]} + A_1^{[2]} A_2^{[1]})$$

$$- A_{12}^{[1]} A_{12}^{[2]} (A_1^{[1]} A_2^{[2]} + A_1^{[2]} A_2^{[2]}) \Big\}$$

$$= \frac{1}{A_{12}^{[1]} A_{12}^{[2]} (A_{12}^{[1]} + A_{12}^{[2]})}$$

$$\times \Big\{ \underline{A_{12}^{[2]} A_1^{[1]} A_2^{[1]} A_{12}^{[1]}} + A_{12}^{[2]} A_1^{[1]} A_2^{[1]} A_{12}^{[2]}$$

$$+ A_{12}^{[1]} A_1^{[2]} A_2^{[2]} A_{12}^{[1]} + \underline{A_{12}^{[1]} A_1^{[2]} A_2^{[2]} A_{12}^{[2]}}$$

$$- \underline{A_{12}^{[1]} A_{12}^{[2]} A_1^{[1]} A_2^{[1]}} - A_{12}^{[1]} A_{12}^{[2]} A_1^{[2]} A_2^{[1]}$$

$$- A_{12}^{[1]} A_{12}^{[2]} A_1^{[1]} A_2^{[2]} - \underline{A_{12}^{[1]} A_{12}^{[2]} A_1^{[2]} A_2^{[2]}} \Big\}$$

$$= \frac{1}{A_{12}^{[1]} A_{12}^{[2]} (A_{12}^{[1]} + A_{12}^{[2]})}$$

$$\times \Big\{ A_{12}^{[2]} A_1^{[1]} A_2^{[1]} A_{12}^{[2]} + A_{12}^{[1]} A_1^{[2]} A_2^{[2]} A_{12}^{[1]}$$

$$- A_{12}^{[1]} A_{12}^{[2]} A_1^{[2]} A_2^{[1]} - A_{12}^{[1]} A_{12}^{[2]} A_1^{[1]} A_2^{[2]} \Big\}$$

$$= \frac{A_{12}^{[1]} A_{12}^{[2]}}{(A_{12}^{[1]} + A_{12}^{[2]})}$$

$$\times \left(\frac{A_{12}^{[2]} A_1^{[1]} A_2^{[1]} A_{12}^{[2]}}{(A_{12}^{[1]} A_{12}^{[2]})^2} + \frac{A_{12}^{[1]} A_1^{[2]} A_2^{[2]} A_{12}^{[1]}}{(A_{12}^{[1]} A_{12}^{[2]})^2} \right.$$

$$\left. - \frac{A_{12}^{[1]} A_{12}^{[2]} A_1^{[2]} A_2^{[1]}}{(A_{12}^{[1]} A_{12}^{[2]})^2} - \frac{A_{12}^{[1]} A_{12}^{[2]} A_1^{[1]} A_2^{[2]}}{(A_{12}^{[1]} A_{12}^{[2]})^2} \right)$$

$$= \frac{A_{12}^{[1]} A_{12}^{[2]}}{(A_{12}^{[1]} + A_{12}^{[2]})}$$

$$\times \left(\frac{A_1^{[1]} A_2^{[1]}}{A_{12}^{[1]} A_{12}^{[1]}} + \frac{A_1^{[2]} A_2^{[2]}}{A_{12}^{[2]} A_{12}^{[2]}} \right.$$

$$\left. - \frac{A_1^{[2]} A_2^{[1]}}{A_{12}^{[1]} A_{12}^{[2]}} - \frac{A_1^{[1]} A_2^{[2]}}{A_{12}^{[1]} A_{12}^{[2]}} \right)$$

$$= \frac{A_{12}^{[1]} A_{12}^{[2]}}{(A_{12}^{[1]} + A_{12}^{[2]})}$$

$$\times \left(\frac{A_1^{[1]}}{A_{12}^{[1]}} \frac{A_2^{[1]}}{A_{12}^{[1]}} + \frac{A_1^{[2]}}{A_{12}^{[2]}} \frac{A_2^{[2]}}{A_{12}^{[2]}} \right.$$

$$\left. - \frac{A_1^{[2]}}{A_{12}^{[1]}} \frac{A_2^{[1]}}{A_{12}^{[2]}} - \frac{A_1^{[1]}}{A_{12}^{[1]}} \frac{A_2^{[2]}}{A_{12}^{[2]}} \right)$$

$$= \frac{A_{12}^{[1]} A_{12}^{[2]}}{(A_{12}^{[1]} + A_{12}^{[2]})}$$

$$\times \left(\frac{A_1^{[1]}}{A_{12}^{[1]}} \left(\frac{A_2^{[1]}}{A_{12}^{[1]}} - \frac{A_2^{[2]}}{A_{12}^{[2]}} \right) \right.$$

$$\left. + \frac{A_1^{[2]}}{A_{12}^{[2]}} \left(\frac{A_2^{[2]}}{A_{12}^{[2]}} - \frac{A_2^{[1]}}{A_{12}^{[1]}} \right) \right)$$

$$= \frac{A_{12}^{[1]} A_{12}^{[2]}}{(A_{12}^{[1]} + A_{12}^{[2]})}$$

$$\times \left(\frac{A_2^{[1]}}{A_{12}^{[1]}} - \frac{A_2^{[2]}}{A_{12}^{[2]}} \right) \left(\frac{A_1^{[1]}}{A_{12}^{[1]}} - \frac{A_1^{[2]}}{A_{12}^{[2]}} \right)$$

Defining $\chi_1^{[1]}$, $\chi_2^{[1]}$, $\chi_2^{[2]}$ and $\chi_1^{[2]}$ as follows;

$$\frac{A_2^{[1]}}{A_{12}^{[1]}} = \chi_1^{[1]}, \qquad \frac{A_1^{[1]}}{A_{12}^{[1]}} = \chi_2^{[1]},$$

$$\frac{A_2^{[2]}}{A_{12}^{[2]}} = \chi_1^{[2]}, \quad \text{and} \quad \frac{A_1^{[2]}}{A_{12}^{[2]}} = \chi_2^{[2]},$$

then,

$$N - N_c = \frac{A_{12}^{[1]} A_{12}^{[2]}}{(A_{12}^{[1]} + A_{12}^{[2]})} (\chi_1^{[1]} - \chi_1^{[2]})(\chi_2^{[1]} - \chi_2^{[2]}).$$

In the case of ^{60}Co,

$$N - N_c = \frac{A_{12}^{[1]} A_{12}^{[2]}}{(A_{12}^{[1]} + A_{12}^{[2]})} (\chi_1^{[1]} - \chi_1^{[2]})^2.$$

This is equation (45).

[Appendix-4]

$$N - N_c = \frac{1}{2A_{12}} \sum_{i}^{(k,m)} \sum_{j} A_{12}{}^{i} \, A_{12}{}^{j} \, (\chi_1{}^{i} - \chi_1{}^{j}) \, (\chi_2{}^{i} - \chi_2{}^{j})$$

$$= \frac{1}{2A_{12}} \sum_{i}^{(k,m)} A_{12}{}^{i} \left\{ A_{12}{}^{[k]} (\chi_1{}^{i} - \chi_1{}^{[k]}) (\chi_2{}^{i} - \chi_2{}^{[k]}) + A_{12}{}^{[m]} (\chi_1{}^{i} - \chi_1{}^{[m]}) (\chi_2{}^{i} - \chi_2{}^{[m]}) \right\}$$

$$= \frac{1}{2A_{12}} \left\{ A_{12}{}^{[k]} A_{12}{}^{[k]} \underbrace{(\chi_1{}^{[k]} - \chi_1{}^{[k]})}_{=0} \underbrace{(\chi_2{}^{[k]} - \chi_2{}^{[k]})}_{=0} + A_{12}{}^{[k]} A_{12}{}^{[m]} (\chi_1{}^{[k]} - \chi_1{}^{[m]}) (\chi_2{}^{[k]} - \chi_2{}^{[m]}) + A_{12}{}^{[m]} A_{12}{}^{[k]} (\chi_1{}^{[m]} - \chi_1{}^{[k]}) (\chi_2{}^{[m]} - \chi_2{}^{[k]}) + A_{12}{}^{[m]} A_{12}{}^{[m]} \underbrace{(\chi_1{}^{[m]} - \chi_1{}^{[m]})}_{=0} \underbrace{(\chi_2{}^{[m]} - \chi_2{}^{[m]})}_{=0} \right\}$$

$$= \frac{A_{12}{}^{[k]} A_{12}{}^{[m]}}{A_{12}} (\chi_1{}^{[k]} - \chi_1{}^{[m]}) (\chi_2{}^{[k]} - \chi_2{}^{[m]}).$$

This lead to equation (53).

[Appendix-5]

$$(N - N_c)^{[k,m]} = \frac{A_{12}{}^k A_{12}{}^m}{A_{12}{}^k + A_{12}{}^m}(\chi_1{}^k - \chi_1{}^m)(\chi_2{}^k - \chi_2{}^m)$$

$$= \frac{2A_{12}{}^k A_{12}{}^m}{2(A_{12}{}^k + A_{12}{}^m)}(\chi_1{}^k - \chi_1{}^m)(\chi_2{}^k - \chi_2{}^m)$$

$$< \frac{2A_{12}{}^k A_{12}{}^m + (A_{12}{}^k)^2 + (A_{12}{}^m)^2}{2(A_{12}{}^k + A_{12}{}^m)}(\chi_1{}^k - \chi_1{}^m)(\chi_2{}^k - \chi_2{}^m)$$

$$< \frac{(A_{12}{}^k + A_{12}{}^m)^2}{2(A_{12}{}^k + A_{12}{}^m)}(\chi_1{}^k - \chi_1{}^m)(\chi_2{}^k - \chi_2{}^m)$$

$$< \frac{A_{12}{}^k + A_{12}{}^m}{2}(\chi_1{}^k - \chi_1{}^m)(\chi_2{}^k - \chi_2{}^m).$$

And

$$\mathrm{Max}(N - N_c)^{[k,m]} = \frac{A_{12}{}^k + A_{12}{}^m}{2}(\chi_1{}^k - \chi_1{}^m)(\chi_2{}^k - \chi_2{}^m).$$

This is equation (54).

[Appendix-6]

$$F_R(N - N_c)^{[k,m]} = \frac{\mathrm{Max}(N - N_c)^{[k,m]}}{(N - N_c)^{[k,m]}}$$

$$= \frac{[A_{12}{}^k + A_{12}{}^m]^2}{2A_{12}{}^k A_{12}{}^m}$$

$$= \frac{2A_{12}{}^k A_{12}{}^m + [A_{12}{}^k]^2 + [A_{12}{}^m]^2}{2A_{12}{}^k A_{12}{}^m}$$

$$= \frac{4A_{12}{}^k A_{12}{}^m + [A_{12}{}^k]^2 + [A_{12}{}^m]^2 - 2A_{12}{}^k A_{12}{}^m}{2A_{12}{}^k A_{12}{}^m}$$

$$= 2 + \frac{[A_{12}{}^k - A_{12}{}^m]^2}{2A_{12}{}^k A_{12}{}^m} > 2.$$

[Appendix-7]

Practical determination of values of "a"

[A1] In the case of a ^{60}Co point source

Figures 30 (A) ∿ (D) show the spectrum of a ^{60}Co point source, the background spectrum for the ^{60}Co spectrum, the spectrum of a ^{22}Na point source and the background spectrum for the ^{22}Na spectrum. Figures 30 (B) and (D) are actually the same each other. In experiments, all the spectra in Fig. 30 were obtained under an equal measuring condition referring to a source-to-detector geometry and absorbers between a source and a detector, however, a little channel drift probably occurred because those spectra were obtained by a NaI(Tl) scintillation detector. The drift was corrected by use of the peak channels of ^{40}K which was one of naturally occurring radionuclides and emitted 1461 keV γ-rays.

[A1.1] Meaning of symbols used in the ^{60}Co spectrum of Fig. 30 (A) is as shown under;

I_1, I_2 : the areas under the photopeaks of the 1173 keV γ-ray and the 1332 keV γ-ray,

P_1, P_2 : the peak channel numbers of the photopeaks of the 1173 keV γ-ray and the 1332 keV γ-ray,

CHL(1): the starting channel number of the photopeak of the 1173 keV γ-ray,

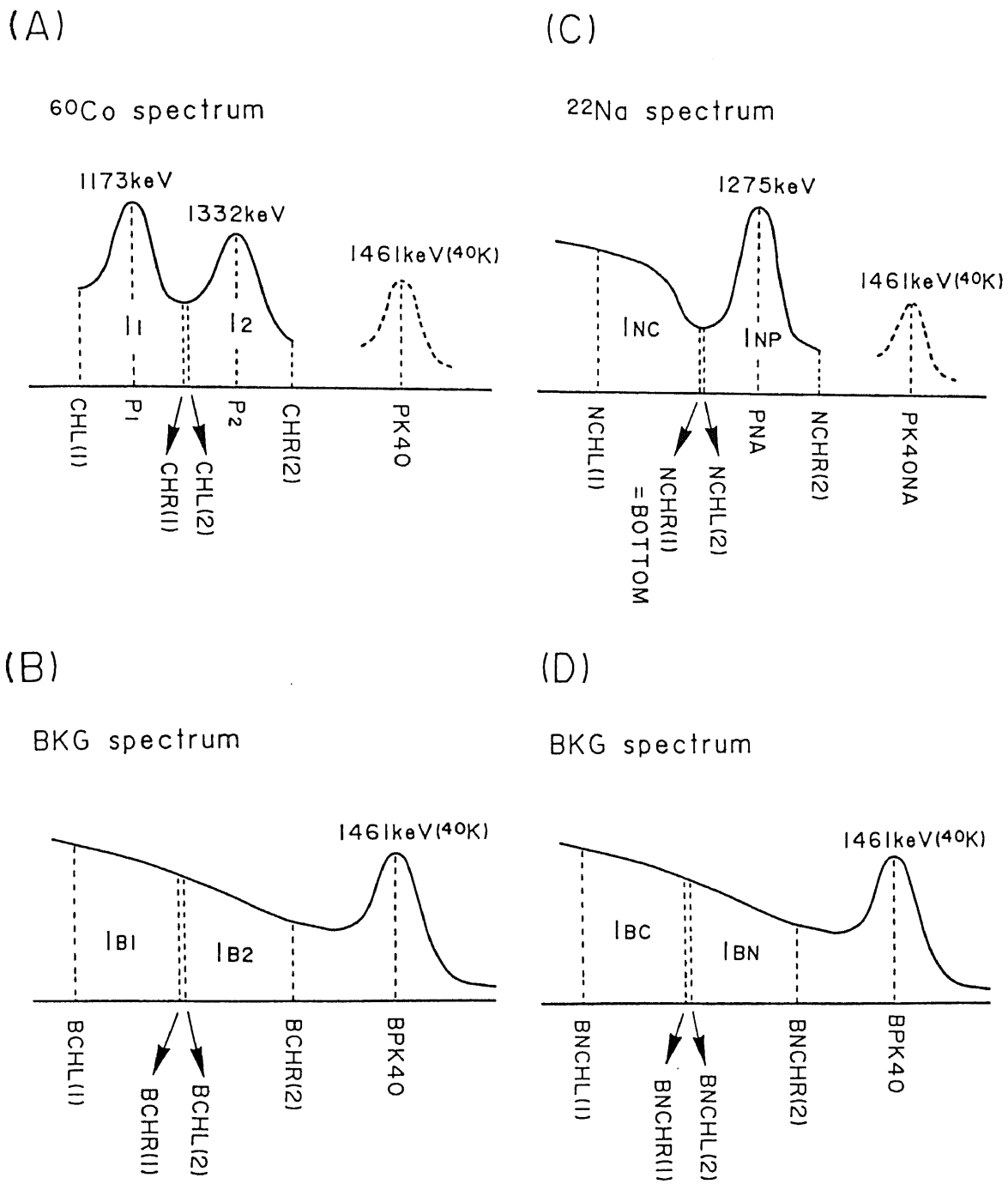

Fig. 30 Relationship among spectra of ^{60}Co, ^{22}Na and background.

CHR(1): the last channel number of the photopeak of the 1173 keV γ-ray,

CHL(2): the starting channel number of the photopeak of the 1332 keV γ-ray,

CHR(2): the last channel number of the photopeak of the 1332 keV γ-ray,

and

PK40 : the peak channel number of the photopeak of the 1461 keV γ-ray emitted from ^{40}K,

in which all values of the symbols can be usually read off from the ^{60}Co spectrum except for that of PK40, because the photopeak of ^{40}K is too small to recognize in the spectrum of ^{60}Co. Consequently a numerical value of PK40 was calculated by a following equation;

$$PK40 = P_2 + \frac{1461 - 1332}{1332 - 1173} \times (P_2 - P_1),$$

in which, the numerical numbers of 1173, 1332 and 1461 are the values of energies (keV) of the two γ-rays emitted from ^{60}Co and that from ^{40}K, respectively.

[A1.2] Meaning of symbols used in the background spectrum of Fig. 30 (B) is as shown under;

BCHL(1): the channel number corresponding to the starting channel number (CHL(1)) of the photopeak of the 1173 keV γ-ray of the ^{60}Co spectrum,

BCHR(1): the channel number corresponding to the last channel number (CHR(1)) of the photopeak of the 1173 keV γ-ray of the ^{60}Co spectrum,

BCHL(2): the channel number corresponding to the starting channel number (CHL(2)) of the photopeak of the 1332 keV γ-ray of the ^{60}Co spectrum,

BCHR(2): the channel number corresponding to the last channel number (CHR(2)) of the photopeak of the 1332 keV γ-ray of the ^{60}Co spectrum,

I_{B1} : the background area between BCHL(1) and BCHR(1),

I_{B2} : the background area between BCHL(2) and BCHR(2),

and

BPK40 : the peak channel number of the photopeak of 1461 keV γ-ray emitted from ^{40}K,

in which the numerical value of BPK40 can be directly read off from the background (BKG) spectrum, and the others were calculated by following equations;

$$BCHL(1) = BPK40 - (PK40 - CHL(1)),$$

$$BCHR(1) = BPK40 - (PK40 - CHR(1)),$$

$$BCHL(2) = BPK40 - (PK40 - CHL(2)),$$

and

$$BCHR(2) = BPK40 - (PK40 - CHR(2)),$$

therefore, in case that the channel drift does not occur as compared the background spectrum with the ^{60}Co spectrum, BCHL(1) = CHL(1), BCHR(1) = CHR(1), BCHL(2) = CHL(2) and BCHR(2) = CHR(2) because PK40 = BPK40.

[A1.3] Meaning of the symbols used in the ^{22}Na spectrum of Fig. 30 (C) is as shown under;

PNA : the channel number of the peak of the 1275 keV γ-ray of ^{22}Na,

BOTTOM : the channel number of the border of Compton scattering region and the peak region,

NCHL(1): the channel number corresponding to the starting channel number (CHL(1)) of the photopeak of the 1173 keV γ-ray of the ^{60}Co spectrum in (A),

NCHR(1): = BOTTOM,

NCHL(2): = BOTTOM + 1,

NCHR(2): the channel number corresponding to the last channel number (CHR(2)) of the photopeak of the 1332 keV γ-ray of the ^{60}Co spectrum in (A),

I_{NC} : the area attributed to Compton scattering of the 1275 keV γ-ray emitted from ^{22}Na, which is assumed to be equivalent to that of the 1332 kev γ-ray under the area of the photopeak of the 1173 keV γ-ray from ^{60}Co,

I_{NP} : the area under the photopeak of the 1275 keV γ-ray

emitted from ^{22}Na, which is assumed to be equivalent to that of the 1332 keV γ-ray from ^{60}Co,

and

PK40NA : the peak channel number of the photopeak of the 1461 keV γ-ray emitted from ^{40}K,

in which the numerical values of PNA and BOTTOM can be directly read off from the ^{22}Na spectrum, and the others were determined by the following calculations.

$$NCHL(1) = PNA - (P_2 - CHL(1)),$$

$$NCHR(2) = PNA + (CHR(2) - P_2),$$

and

$$PK40NA = PNA + \frac{(1461 - 1275)}{(1332 - 1173)} \times (P_2 - P_1),$$

in which, P_2 and P_1 are from the ^{60}Co spectrum in (A). The numerical values of I_{NC} and I_{NP} can be read off from the ^{22}Na spectrum by use of NCHL(1), NCHR(1), NCHL(2) and NCHR(2) determined above.

[A1.4] Meaning of the symbols used in the background spectrum of Fig. 30 (D) is as shown under;

BNCHL(1): the channel number equivalent to the left channel number (NCHL(1)) of Compton region of the 1275 keV γ-ray, corresponding to the starting channel number of the 1173 keV γ-ray in the ^{60}Co spectrum in (A),

BNCHR(1): the channel number equivalent to the right channel number (NCHR(1) = BOTTOM) of Compton region of the 1275 keV γ-ray in (C),

BNCHL(2): the channel number equivalent to the starting channel number (NCHL(2) = BOTTOM + 1) of the photopeak of the 1275 keV γ-ray in (C),

BNCHR(2): the channel number equivalent to the last channel of the photopeak of the 1275 keV γ-ray, corresponding to the last channel number of the 1332 keV γ-ray in the ^{60}Co spectrum in (A),

I_{BC} : the background area between BNCHL(1) and BNCHR(1), which is a part of I_{Nc} in (C),

I_{BN} : the background area between BNCHL(2) and BNCHR(2), which is a part of I_{Np} in (C),

and

BPK40 : the peak channel number of the photopeak of the 1461 keV γ-ray emitted from ^{40}K,

in which the numerical value of BPK40 can be directly read off from the spectrum, and the others were calculated by following equations;

$$BNCHL(1) = BPK40 - (PK40NA - NCHL(1)),$$

$$BNCHR(1) = BPK40 - (PK40NA - NCHR(1)),$$

$$BNCHL(2) = BNCHL(1) + 1,$$

and

BNCHR(2) = BPK40 - (PK40NA - NCHR(2)),

therefore, in case that the channel drift does not occur as compared the background spectrum with the ^{22}Na spectrum, BNCHL(1) = NCHL(1), BNCHR(1) = NCHR(1), BNCHL(2) = NCHL(2) and BNCHR(2) = NCHR(2) because BPK40 = PK40NA. The areas of I_{BC} and I_{BN} can be determined from the spectrum of Fig. 30 (D) by use of the channel numbers of BNCHL(1), BNCHR(1), BNCHL(2) and BNCHR(2).

Consequently, the value of "α" is calculated by equation (73);

$$\alpha = \frac{I_{NC} - I_{BC}}{I_{Np} - I_{BN}}, \tag{73}$$

in which the numerical values of I_{NC} and I_{Np} were determined in *[A1.3]*, then I_{BC} and I_{BN}, in *[A1.4]*. Therefore, the photopeak areas of A_1 and A_2 are calculated by equation (74);

$$A_1 = A_2 = \frac{(I_{1+2} - B_S)}{2 + \alpha} = \frac{(I_1 + I_2) - (I_{B1} + I_{B2})}{2 + \dfrac{I_{NC} - I_{BC}}{I_{Np} - I_{BN}}}. \tag{74}$$

We could practically determine the photopeak areas for ^{60}Co point sources by calculation of equation (74), and those for ^{60}Co bulky sources, through the same process by use of the spectra of ^{22}Na bulky sources with the same dimension as those of the ^{60}Co bulky sources in the present studies.

[A2] In the case of an extended source composed of two ^{60}Co point sources

The method for determination of value of "α" in the case of a ^{60}Co point source was shown in *[A1]*. Following shows how to determine values of "α" in the case of an extended source composed of two ^{60}Co point sources. In explanation shown under, effects of "background counting" of measuring system used are abridged for convenience sake.

Four measuring arrangements are shown in Fig. 31. In Fig. 31 (A)

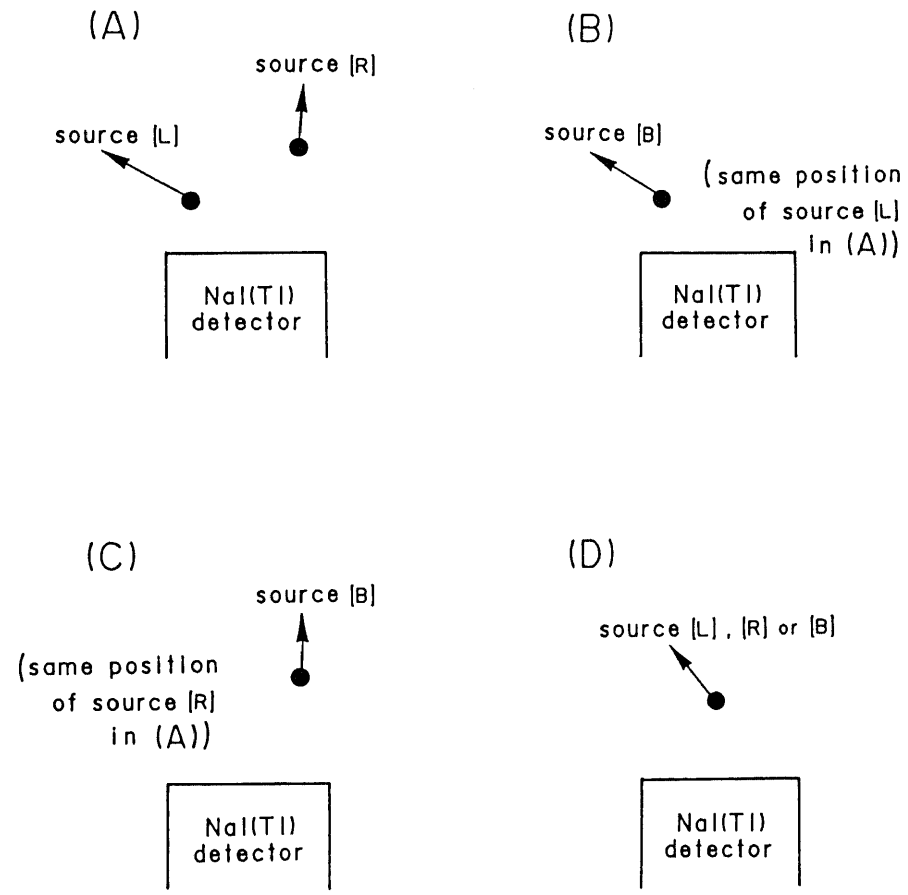

Fig. 31 Four measuring arrangements used for determination of value of "α" in the case of an extended source composed of two ^{60}Co point sources.

two ^{60}Co point sources (a source [L] and a source [R]) are located, in (B) a source [B] at the same position of the source [L] in (A), in (C) a source [B] at the same position of the source [R] in (A), and in (D) one of sources [L], [R] and [B] at a definite position.

On condition that the two point sources of Fig. 31 (A) form an extended source, if a measuring arrangement equivalent to that of Fig. 31 (A) can be realized by using two ^{22}Na point sources, in which the ratio of both radioactivities is equal to those of both the ^{60}Co sources, the value of "α" can be determined through the same process shown in *[A1]*. However it is usually difficult to provide such pair of ^{22}Na point sources. Therefore, we determined indirectly the value of "α" as follows.

Assuming that $I^{[L+R]}$ stands for the area under the two photopeaks (1173 and 1332 kev γ-rays) of a ^{60}Co spectrum obtained by the measuring arrangement (A) in Fig. 31,

$$I^{[L+R]} = I^{[L]} + I^{[R]},$$

$$I^{[L]} = A_1{}^{[L]} + A_2{}^{[L]}(1 + \alpha^{[L]}),$$

and

$$I^{[R]} = A_1{}^{[R]} + A_2{}^{[R]}(1 + \alpha^{[R]}),$$

where

$I^{[L]or[R]}$: the total area under both the photopeaks of the 1173 and 1332 keV γ-rays attributed to the sources [L] or [R] in (A),

$A_1^{[L]or[R]}$, $A_2^{[L]or[R]}$: the areas under the photopeaks of the 1173 and 1332 keV γ-rays attributed to the sources [L] or [R], which can not be determined directly through the measurement (A),

and

$\alpha^{[L]or[R]}$: the ratio of the area attributed to Compton scattering of the 1332 keV γ-ray under the photopeak of the 1173 keV γ-ray to the area under the 1332 keV γ-ray with respect to the sources [L] or [R].

Consequently,

$$I^{[L+R]} = A_1^{[L]} + A_2^{[L]}(1 + \alpha^{[L]}) + A_1^{[R]} + A_2^{[R]}(1 + \alpha^{[R]})$$

$$= (A_1^{[L]} + A_1^{[R]}) + (A_2^{[L]} + A_2^{[R]})(1 + \alpha^{[L+R]}),$$

where

$$\alpha^{[L+R]} = \frac{(A_2^{[L]} \times \alpha^{[L]}) + (A_2^{[R]} \times \alpha^{[R]})}{(A_2^{[L]} + A_2^{[R]})}. \qquad (75)$$

Since $(A_1^{[L]} + A_1^{[R]})$ and $(A_2^{[L]} + A_2^{[R]})$ are the areas under the photopeaks the 1173 keV and the 1332 keV γ-rays, $\alpha^{[L+R]}$ means the ratio of the area attributed to Compton scattering of the 1332 keV γ-ray under the photopeak of the 1173 keV γ-ray to the area under the 1332 keV γ-ray in the spectrum of an extended source composed of the two ^{60}Co sources [L] and [R]. If the values of $A_1^{[L]}$, $A_1^{[R]}$, $A_2^{[L]}$, $A_2^{[R]}$, $\alpha^{[L]}$ and $\alpha^{[R]}$ are obtained, the value of $\alpha^{[L+R]}$ can be

calculated by equation (75).

Considering that the value of $(A_1^{[L]} + A_1^{[R]})$ is equal to that of $(A_2^{[L]} + A_2^{[R]})$ in the case of the ^{60}Co spectrum,

$$(A_1^{[L]} + A_1^{[R]}) = (A_2^{[L]} + A_2^{[R]}) = \frac{I^{[L+R]}}{(2 + \alpha^{[L+R]})}, \qquad (76)$$

which gives the areas under the photopeaks (the 1173 and 1332 keV γ-rays) in the spectrum of the extended source. However, except for $I^{[L+R]}$, none of the values ($A_1^{[L]}$, $A_1^{[R]}$, $A_2^{[L]}$, $A_2^{[R]}$, $\alpha^{[L]}$ and $\alpha^{[R]}$) can be directly determined from the spectrum, therefore the values of $\alpha^{[L+R]}$, $(A_1^{[L]} + A_1^{[R]})$ and $(A_2^{[L]} + A_2^{[R]})$ are also unknown. Those values can be obtained based on the measurements of Figs. 31 (B), (C) and (D).

Assuming that $I^{[BL]}$ and $I^{[BR]}$ are the total areas under both the photopeaks of spectra obtained by the measurements (B) and (C), respectively,

$$I^{[BL]} = A_1^{[BL]} + A_2^{[BL]}(1 + \alpha^{[BL]}),$$

and

$$I^{[BR]} = A_1^{[BR]} + A_2^{[BR]}(1 + \alpha^{[BR]}),$$

$A_1^{[BL]}$, $A_2^{[BL]}$: the areas under the photopeaks (the 1173 and 1332 keV γ-rays) of the spectrum obtained by the measurement (B),

$A_1^{[BR]}$, $A_2^{[BR]}$: the areas under the photopeaks (the 1173 and 1332 keV γ-rays) of the spectrum obtained by the measurement (C),

$\alpha^{[BL]}$: the ratio of the area attributed to Compton scattering of the 1332 keV γ-ray under the photopeak of the 1173 keV γ-ray to $A_2^{[BL]}$ in the spectrum obtained by the measurement (B),

and

$\alpha^{[BR]}$: the ratio of the area attributed to Compton scattering of the 1332 keV γ-ray under the photopeak of the 1173 keV γ-ray to $A_2^{[BR]}$ in the spectrum obtained by the measurement (C),

therefore,

$$A_1^{[BL]} = A_2^{[BL]} = \frac{I^{[BL]}}{(2 + \alpha^{[BL]})},$$

and

$$A_1^{[BR]} = A_2^{[BR]} = \frac{I^{[BR]}}{(2 + \alpha^{[BR]})}.$$

Since only one point source is treated at the measurements (B) and (C), the values of $\alpha^{[BL]}$ and $\alpha^{[BR]}$ can be determined by the same procedure with a ^{22}Na source as shown in *[A1]*. Besides the values of $I^{[BL]}$ and $I^{[BR]}$ are read off from the spectra obtained by the measurements (B) and (C). Consequently, all the photopeak areas can be determined. The source [B] in the measurement (B) is located at the same position of that of the source [L] in the measurement (A), and the source [B] in the measurement (C), that of the source [R] in the measurement (A), therefore,

$$\alpha^{[BL]} = \alpha^{[L]}, \quad \text{and} \quad \alpha^{[BR]} = \alpha^{[R]}.$$

The values of $\alpha^{[L]}$ and $\alpha^{[R]}$ can be determined through the measurements (B) and (C).

Assuming that $I^{[LD]}$, $I^{[RD]}$ and $I^{[BD]}$ are the total areas under both the photopeaks of spectra of the sources [L], [R] and [B] obtained by the measurement (D), respectively,

$$I^{[LD]} = A_1^{[LD]} + A_2^{[LD]}(1 + \alpha^{[LD]}),$$

$$I^{[RD]} = A_1^{[RD]} + A_2^{[RD]}(1 + \alpha^{[RD]}),$$

and

$$I^{[BD]} = A_1^{[BD]} + A_2^{[BD]}(1 + \alpha^{[BD]}),$$

$A_1^{[LD]}$, $A_2^{[LD]}$: the areas under the photopeaks (the 1173 and 1332 keV γ-rays) of the spectrum of the source [L] in the measurement (D),

$A_1^{[RD]}$, $A_2^{[RD]}$: the areas under the photopeaks (the 1173 and 1332 keV γ-rays) of the spectrum of the source [R] in the measurement (D),

$A_1^{[BD]}$, $A_2^{[RD]}$: the areas under the photopeaks (the 1173 and 1332 keV γ-rays) of the spectrum of the source [B] in the measurement (D),

$\alpha^{[LD]}$: the ratio of the area attributed to Compton scattering of the 1332 keV γ-ray under the photopeak of the 1173 keV γ-ray to $A_2^{[LD]}$ in the spectrum obtained by the measurement (D),

$\alpha^{[RD]}$: the ratio of the area attributed to Compton scattering of the 1332 keV γ-ray under the

photopeak of the 1173 keV γ-ray to $A_2^{[RD]}$ in the spectrum obtained by the measurement (D),

and

$\alpha^{[BD]}$: the ratio of the area attributed to Compton scattering of the 1332 keV γ-ray under the photopeak of the 1173 keV γ-ray to $A_2^{[BD]}$ in the spectrum obtained by the measurement (D),

therefore,

$$A_1^{[LD]} = A_2^{[LD]} = \frac{I^{[LD]}}{(2 + \alpha^{[LD]})},$$

$$A_1^{[RD]} = A_2^{[RD]} = \frac{I^{[RD]}}{(2 + \alpha^{[RD]})},$$

and

$$A_1^{[BD]} = A_2^{[BD]} = \frac{I^{[BD]}}{(2 + \alpha^{[BD]})}.$$

Since the spectrum is obtained for each of the sources [L], [R] and [B] placed at the definite position in (D),

$$\alpha^{[LD]} = \alpha^{[RD]} = \alpha^{[BD]}.$$

The ratios of the radioactivities of the sources [L] and [R] to that of the source [B] were;

$$r^{[L]} = \frac{A_1^{[LD]}}{A_1^{[BD]}} = \frac{A_2^{[LD]}}{A_2^{[BD]}} = \frac{I^{[LD]}}{I^{[BD]}}$$

and

$$r^{[R]} = \frac{A_1^{[RD]}}{A_1^{[BD]}} = \frac{A_2^{[RD]}}{A_2^{[BD]}} = \frac{I^{[RD]}}{I^{[BD]}} .$$

Consequently

$$A_1^{[L]} = A_2^{[L]} = r^{[L]} \times A_1^{[BL]} = r^{[L]} \times A_2^{[BL]} ,$$

and

$$A_1^{[R]} = A_2^{[R]} = r^{[R]} \times A_1^{[BR]} = r^{[R]} \times A_2^{[BR]} .$$

In consequence, equations (75) can be rewritten as follows;

$$\alpha^{[L+R]} = \frac{(r^{[L]} \times A_2^{[BL]} \times \alpha^{[L]}) + (r^{[R]} \times A_2^{[BR]} \times \alpha^{[R]})}{(r^{[L]} \times A_2^{[BL]}) + (r^{[R]} \times A_2^{[BR]})} . \qquad (77)$$

Referring to equations (76) and (77), the numerical value of $I^{[L+R]}$ can be determined by the measurement (A), those of $A_2^{[BL]}$, $A_2^{[BR]}$, $\alpha^{[L]}$ and $\alpha^{[R]}$, by the measurements (B) and (C), and those of $r^{[L]}$ and $r^{[R]}$, by the measurement (D). As results, the photopeak areas of the extended source in Fig. 31 (A), which are denoted by $(A_1^{[L]} + A_1^{[R]})$ and $(A_2^{[L]} + A_2^{[R]})$, can be calculated by equations (76) and (77). Practical calculation in experiments was performed taking account of effects of "background counting" on the photopeak areas.